

**RODRIGO CUPERTINO BERNARDES**

**ETHOFLOW: AN ARTIFICIAL INTELLIGENCE-BASED SOFTWARE THAT  
FACILITATES BEHAVIORAL MEASUREMENTS AND THEIR APPLICATION FOR  
TOXICOLOGICAL ASSESSMENTS IN INSECTS**

Tese apresentada à Universidade Federal de Viçosa,  
como parte das exigências do Programa de Pós-  
Graduação em Entomologia, para obtenção do título  
de *Doctor Scientiae*.

Orientador: Gustavo Ferreira Martins

Coorientadora: Maria Augusta Lima Siqueira

**VIÇOSA - MINAS GERAIS  
2021**

**Ficha catalográfica elaborada pela Biblioteca Central da Universidade  
Federal de Viçosa - Campus Viçosa**

T

B522e  
2021  
Bernardes, Rodrigo Cupertino, 1991-  
Ethoflow : an artificial intelligence-based software that  
facilitates behavioral measurements and their application for  
toxicological assessments in insects / Rodrigo Cupertino  
Bernardes. – Viçosa, MG, 2021.  
129 f. : il. (algumas color.) ; 29 cm.

Texto em inglês.

Inclui apêndices.

Orientador: Gustavo Ferreira Martins.

Tese (doutorado) - Universidade Federal de Viçosa.

Inclui bibliografia.

1. Abelhas - Comportamento. 2. Ethoflow (Software).  
3. Visão por computador. 4. Inteligência artificial.  
I. Universidade Federal de Viçosa. Departamento de  
Entomologia. Programa de Pós-Graduação em Entomologia.  
II. Título.

CDD 22. ed. 595.799

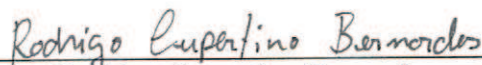
**RODRIGO CUPERTINO BERNARDES**

**ETHOFLOW: AN ARTIFICIAL INTELLIGENCE-BASED SOFTWARE THAT  
FACILITATES BEHAVIORAL MEASUREMENTS AND THEIR APPLICATION FOR  
TOXICOLOGICAL ASSESSMENTS IN INSECTS**

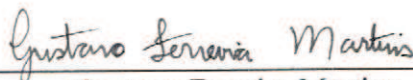
Tese apresentada à Universidade Federal de Viçosa,  
como parte das exigências do Programa de Pós-  
Graduação em Entomologia, para obtenção do título  
de *Doctor Scientiae*.

APROVADA: 16 de julho de 2021.

Assentimento:



Rodrigo Cupertino Bernardes  
Autor



Gustavo Ferreira Martins  
Orientador

## **AGRADECIMENTOS**

À Universidade Federal de Viçosa, por meio do Programa de Pós-graduação em Entomologia, pela oportunidade de realizar a pós-graduação.

Ao Conselho Nacional de Desenvolvimento Científico e Tecnológico (CNPQ), pela concessão da bolsa de estudos e a Fundação de Amparo à Pesquisa do Estado de Minas Gerais (FAPEMIG) pelos recursos fornecidos. O presente trabalho foi realizado com apoio da Coordenação de Aperfeiçoamento de Pessoal de Nível Superior – Brasil (CAPES) – Código de Financiamento 001.

Agradeço ao meu orientador, Prof. Dr. Gustavo Ferreira Martins que sempre esteve disponível para atender as minhas demandas. Agradeço pela confiança, os conselhos sinceros, críticas construtivas e o bom convívio durante toda a orientação.

A minha coorientadora, Prof. Dra. Maria Augusta Lima Siqueira por ter me dado a oportunidade de estágio no início da graduação e me inserido na academia. Agradeço pelo bom convívio, confiança e incentivo para arriscar nos conhecimentos dos problemas computacionais.

Aos integrantes do Laboratório de Biologia Molecular de Insetos (DBG) e Laboratório de Abelhas e Vespas (DBA) da UFV pela contribuição e parceria que geraram muitos trabalhos importantes para minha formação.

Agradeço à minha família pelo carinho, apoio e reconhecimento. À minha esposa Karina que foi fundamental para eu iniciar minha jornada acadêmica, sempre me incentivando e apoiando. Obrigado por compartilhar sua vida com a minha. A família está aumentando com a chegada da nossa filha Helena que vem nos trazer ainda mais alegria. Amo vocês!

## ABSTRACT

BERNARDES, Rodrigo Cupertino, D.Sc., Universidade Federal de Viçosa, July, 2021.  
**Ethoflow: an artificial intelligence-based software that facilitates behavioral measurements and their application for toxicological assessments in insects.** Adviser: Gustavo Ferreira Martins. Co-adviser: Maria Augusta Lima Siqueira.

The application of artificial intelligence (AI) techniques has demonstrated outstanding performance for automating complex tasks in many areas. Thus, software with AI implementation can be sufficiently robust to meet the demand for studies on animal behavior (e.g., evaluating behavior under field conditions). Studies on risk assessment in bees have focused on the possible causes of loss of their colonies worldwide, which is attributed to different factors, including agricultural practices with the use of agrochemicals. In toxicological studies of agrochemicals in bees, behavioral assessment is an important sublethal parameter. Thus, the development and application of AI tools can considerably contribute to the understanding of how agrochemicals and other factors are affecting the bees' health. The present work aimed to develop an AI-based software (Ethoflow) to automatically assess animal behavior. In addition, Ethoflow was applied to evaluate sublethal behavioral changes in toxicological studies of agrochemicals in forages of two stingless bee species, including *Melipona quadrifasciata* and *Partamona helleri* (Hymenoptera, Apidae, Meliponini). The results obtained demonstrate that: (1) Ethoflow is robust for multivariate behavioral assessments, behavioral assessments in heterogeneous environments, tracking individuals in groups maintaining their identities and can be trained to learn behaviors specific to animals; (2) it is possible to classify agrochemical contamination in bees with high accuracy by integrating multivariate behavioral data with AI algorithms and the agrochemicals glyphosate and imidacloprid differentially impact the midgut physiology of *M. quadrifasciata*; (3) the foliar fertilizer copper sulfate (CuSO<sub>4</sub>) causes sublethal effects on the behavior and structure and physiology of the midgut epithelium of *P. helleri*; (4) the mixture of mesotrione and atrazine herbicides interfered in food intake and behavioral parameters, caused damage to the midgut epithelium and altered the pattern of proteins related to the cell proliferation and differentiation in midgut of *P. helleri*. In general, Ethoflow is a useful support tool for technical-scientific applications in the animal behavior field and has significant potential in risk assessments of non-target organisms for modeling the multiple factors affecting bees' health, including the

adverse effects of agrochemicals. Besides, AI algorithms trained with multivariate behavioral data predict bees' agrochemical contamination with high accuracy. Finally, the analyzes enabled holistic assessments of sublethal effects of different agrochemicals on the behavior and physiology of bees.

Keywords: Bee. Computer vision. Machine learning. Meliponini. Pollinators.

## RESUMO

BERNARDES, Rodrigo Cupertino, D.Sc., Universidade Federal de Viçosa, julho de 2021. **Ethoflow: software baseado em inteligência artificial para medições comportamentais e suas aplicações em avaliações toxicológicas em insetos.** Orientador: Gustavo Ferreira Martins. Coorientadora: Maria Augusta Lima Siqueira.

A aplicação de técnicas de inteligência artificial (IA) tem demonstrado desempenho excepcional para automatizar tarefas complexas em muitas áreas. Um software com implementação de IA pode ser robusto atender a demanda de estudos sobre comportamento animal (por exemplo, para avaliar comportamentos em condições de campo). Estudos sobre avaliação de risco em abelhas têm se concentrado nas possíveis causas de perda de suas colônias em todo o mundo, o que é atribuído a diferentes fatores incluindo práticas agrícolas com uso de agroquímicos. Em estudos toxicológicos de agroquímicos em abelhas, avaliação comportamental é um importante parâmetro subletal. Dessa forma, o desenvolvimento e aplicação de ferramentas com IA pode contribuir substancialmente para o entendimento de como os agroquímicos e outros fatores estão afetando a saúde das abelhas. O presente trabalho objetivou desenvolver um software (Ethoflow) baseado em IA para avaliar comportamento animal automaticamente. Além disso, o Ethoflow foi aplicado em avaliações comportamentais em forrageiras de duas espécies de abelha sem ferrão, *Melipona quadrifasciata* e *Partamona helleri* (Hymenoptera, Apidae, Meliponini) expostas a diferentes agroquímicos. Os resultados obtidos demonstram que: (1) o Ethoflow é robusto para avaliações comportamentais multivariadas, avaliações comportamentais em ambientes heterogêneos, rastreamento de indivíduos em grupos mantendo suas identidades e pode ser treinado para aprender comportamentos específicos dos animais; (2) é possível classificar contaminação por agroquímicos em abelhas com alta acurácia, integrando dados comportamentais multivariados com algoritmos de IA e os agroquímicos glifosato e imidaclopride, diferencialmente, impactam a fisiologia do intestino médio de *M. quadrifasciata*; (3) o fertilizante foliar sulfato de cobre causa efeitos subletais no comportamento e na estrutura e fisiologia do epitélio do intestino médio de *P. helleri*; (4) a mistura dos herbicidas mesotriona e atrazina interferiu no consumo alimentar e parâmetros comportamentais, causou danos ao epitélio do intestino médio e alterou o padrão de proteínas relacionadas à proliferação e diferenciação de células-tronco do intestino médio de *P. helleri*. Em resumo, o Ethoflow é uma ferramenta de suporte útil para aplicações

técnico-científicas em comportamento animal e tem potencial significativo em avaliações de risco de organismos não-alvo para modelar os múltiplos fatores que afetam a saúde das abelhas, incluindo os efeitos adversos dos agroquímicos. Além disso, algoritmos de IA, treinados com dados comportamentais multivariados, preveem a contaminação por agroquímicos em abelhas com alta acurácia. Finalmente, as análises permitiram avaliações holísticas dos efeitos subletais de diferentes agroquímicos no comportamento e fisiologia das abelhas.

Palavras-chave: Abelha. Aprendizado de máquina. Meliponini. Polinizadores. Visão computacional.

## SUMMARY

INTRODUCTION .....	9
AIMS .....	11
REFERENCES .....	11
CHAPTER 1. Ethoflow: computer vision and artificial intelligence-based software for automatic behavior analysis .....	15
CHAPTER 2. Machine learning algorithms and sublethal features applied to the toxicological assessment of agrochemicals in bees .....	40
CHAPTER 3. Impact of copper sulfate on survival, behavior, midgut morphology, and antioxidant activity of <i>Partamona helleri</i> (Apidae: Meliponini) .....	82
CHAPTER 4. A mixture containing the herbicides Mesotrione and Atrazine imposes toxicological risks on workers of <i>Partamona helleri</i> .....	117
CONCLUSIONS .....	128

## INTRODUCTION

The increase in the availability of computational resources, especially the graphic units for processing in parallel, has contributed to the outstanding performance of artificial intelligence (AI) in many areas. Using AI approaches it is possible to train algorithms on a representative dataset to perform classification predictions on other independent datasets (Ghahramani, 2015). Thus, a properly trained AI algorithm can generalize to new situations and automate tasks.

Due to subjectivity and non-parametrization, evaluating animal behavior manually is a limited method (Noldus et al., 2002) and the implementation of AI for automatic behavior analysis has great potential (Dell et al., 2014). AI applications in animal behavior science seem to be an active topic nowadays and tools have been developed, for example, software for animal tracking (it gets the animal's position in each frame of a digital video and record the Cartesian or polar coordinates of the movement) (Rodriguez et al., 2018; Romero-Ferrero et al., 2019; Sridhar et al., 2019; Walter and Couzin, 2020) and software for animal pose estimation (it measures the geometrical configuration of animal body parts) (Graving et al., 2019; Mathis et al., 2018; Pereira et al., 2019).

In general, the available software for animal behavior analyses detect the animals by background subtraction or thresholding (Dell et al., 2014; Yilmaz et al., 2006). These computer vision approaches require videos with good contrast between the object and the background, and homogeneous background (i.e., with slight variation in color, luminosity, and texture). Nonetheless, sufficiently robust systems are needed to assess multiple individuals, maintaining individual identities in heterogeneous environments (i.e., complex environmental landscapes such as in the field or multi-scenes with variation in color, luminosity, texture, and different objects) (Dell et al., 2014).

By tracking animals, it is possible to calculate important kinematic measurements (from animals' Cartesian or polar coordinates over time) (Yilmaz et al., 2006) of their behavior, such as speed and walked distance. Additionally, evaluating complex behaviors of animals can bring important insights, for example, in ecotoxicity assessments. In the case of social insects, evaluation of complex behaviors such as changes in trophallaxis (i.e., a complex social behavior of food exchange among social insect nestmates) is of great importance under pesticide exposure (Boff et al., 2018; Gandra et al., 2016). Without accessible tools, many of these

assessments are done manually and subjectively, limiting the detection of complex behavioral changes.

A suitable tool to automatically assess animal behavior has great potential for risk assessment in bees. Efforts for risk assessment in bees are crucial to understanding the different factors that have led to the decline of these pollinators. The decline of bees worldwide is attributed to different factors, including agricultural practices with increased agrochemicals (Barbosa et al., 2015; Freitas et al., 2009; Lima et al., 2016). Studies showed that the harmful effects in bees by exposure to agrochemicals resulting from the adverse sublethal impacts on behavior and gut physiology and morphology, such as damage to the midgut cells (Farder-Gomes et al., 2021b, 2021a; Lima et al., 2016; Sgolastra et al., 2019). Assessing these sublethal effects are essentials to understand the factors associated with the long-term success of bee colonies because changes that compromise the individual, without leading to death, can affect the entire dynamics of colonies (Johnson, 2015; Lima et al., 2016).

This work aimed to develop an AI-based software (Ethoflow) to improve animal behavior analyzes. The developed software was applied to assess behavioral changes in agrochemical-exposed bees in toxicological studies. The software developed in this work has achieved substantial contribution in the animal behavior field being successfully applied in other studies (Araújo et al., 2021; Farder-Gomes et al., 2021b; Viana et al., 2021). With Ethoflow it was possible to obtain multivariate behavioral data to train AI algorithms that predicted the contamination by agrochemicals in bees with high accuracy. Moreover, the analyzes enabled holistic assessments of the agrochemical sublethal effects in stingless bee species, including behavioral disorders and morphology, protein quantification, and antioxidant activity in bees' midgut.

The first chapter reports the development, algorithm, and performance of the Ethoflow software, which was trained to recognize trophallaxis and applied in bioassays with two species of eusocial bees to compute kinematic behavioral variables. In the second chapter, the software Ethoflow was used to measure multivariate behavior data of foragers of *Melipona quadrifasciata* exposed to agrochemicals (glyphosate, and imidacloprid), and AI algorithms were applied to predicting bees' agrochemical contamination. Besides, changes in the detection pattern of different proteins related to bee gut physiology after exposure to the two types of agrochemicals were quantified. The third chapter assesses the sublethal effects of copper sulfate ( $\text{CuSO}_4$ ; used in crops primarily as foliar fertilizer) in the behavior and midgut physiology of

the stingless bee *Partamona helleri*. The fourth and last chapter evaluates the harmful effects of a mixture containing the herbicides mesotrione and atrazine on *P. helleri*.

## AIMS

- Develop and validate an open-source desktop software (Ethoflow) using AI tools to assessing animal behavior in heterogeneous environments, tracking individuals in groups, maintaining their identities, and assessing specific behavior.
- Apply AI algorithms to predicting bees' agrochemical contamination (glyphosate, and imidacloprid) from behavior data and assess the detection pattern of different proteins related to bee gut physiology after exposure to the agrochemicals in foragers of *M. quadrifasciata*.
- Estimate the lethal concentration at 50% of CuSO<sub>4</sub> (LC<sub>50</sub>; the concentration that led to the deaths of 50% of the exposed population) in foragers of *P. helleri* and assess the walking behavior, morphologies of midgut and peritrophic matrix (PM), midgut oxidative stress, and immunofluorescence detection of proteins related to midgut physiology after exposure to CuSO<sub>4</sub>.
- Estimate lethal concentrations at 50% and 10% (LC<sub>50</sub> and LC<sub>10</sub>) for acute oral exposure to a mix of herbicides (mesotrione and atrazine), and assess food consumption, behavior, midgut epithelium and PM, and the pattern of cells positive for proteins related to the proliferation and differentiation of midgut stem cells in forages of *P. helleri*.

## REFERENCES

- Araújo, R.D.S., Bernardes, R.C., Martins, G.F., 2021. A mixture containing the herbicides Mesotrione and Atrazine imposes toxicological risks on workers of *Partamona helleri*. Sci. Total Environ. 763. <https://doi.org/10.1016/j.scitotenv.2020.142980>
- Barbosa, W.F., Smagghe, G., Guedes, R.N.C., 2015. Pesticides and reduced-risk insecticides, native bees and pantropical stingless bees: pitfalls and perspectives. Pest Manag. Sci. 71, 1049–1053. <https://doi.org/10.1002/ps.4025>
- Boff, S., Friedel, A., Mussury, R.M., Lenis, P.R., Raizer, J., 2018. Changes in social behavior are induced by pesticide ingestion in a Neotropical stingless bee. Ecotoxicol. Environ. Saf. 164, 548–553. <https://doi.org/https://doi.org/10.1016/j.ecoenv.2018.08.061>

- Dell, A.I., Bender, J.A., Branson, K., Couzin, I.D., de Polavieja, G.G., Noldus, L.P.J.J., Pérez-Escudero, A., Perona, P., Straw, A.D., Wikelski, M., Brose, U., 2014. Automated image-based tracking and its application in ecology. *Trends Ecol. Evol.* 29, 417–428.  
<https://doi.org/10.1016/J.TREE.2014.05.004>
- Farder-Gomes, C.F., Fernandes, K.M., Bernardes, R.C., Bastos, D.S.S., Martins, G.F., Serrão, J.E., 2021a. Acute exposure to fipronil induces oxidative stress, apoptosis and impairs epithelial homeostasis in the midgut of the stingless bee *Partamona helleri* Friese (Hymenoptera: Apidae). *Sci. Total Environ.* 774, 145679.  
<https://doi.org/10.1016/j.scitotenv.2021.145679>
- Farder-Gomes, C.F., Fernandes, K.M., Bernardes, R.C., Bastos, D.S.S., Oliveira, L.L. de, Martins, G.F., Serrão, J.E., 2021b. Harmful effects of fipronil exposure on the behavior and brain of the stingless bee *Partamona helleri* Friese (Hymenoptera: Meliponini). *Sci. Total Environ.* 794, 148678. <https://doi.org/10.1016/J.SCITOTENV.2021.148678>
- Freitas, B.M., Imperatriz-Fonseca, V.L., Medina, L.M., de Matos Peixoto Kleinert, A., Galetto, L., Nates-Parra, G., Quezada-Euán, J.J.G., 2009. Diversity, threats and conservation of native bees in the Neotropics. *Apidologie* 40, 332–346.  
<https://doi.org/10.1051/apido/2009012>
- Gandra, L.C., Amaral, K.D., Couceiro, J.C., Della Lucia, T.M., Guedes, R.N., 2016. Mechanism of leaf-cutting ant colony suppression by fipronil used in attractive toxic baits. *Pest Manag. Sci.* 72, 1475–1481. <https://doi.org/10.1002/ps.4239>
- Ghahramani, Z., 2015. Probabilistic machine learning and artificial intelligence. *Nature* 521, 452–459. <https://doi.org/10.1038/nature14541>
- Graving, J.M., Chae, D., Naik, H., Li, L., Koger, B., Costelloe, B.R., Couzin, I.D., 2019. DeepPoseKit, a software toolkit for fast and robust animal pose estimation using deep learning. *Elife* 8, e47994. <https://doi.org/10.7554/eLife.47994>
- Johnson, R.M., 2015. Honey bee toxicology. *Annu. Rev. Entomol.* 60, 415–434.  
<https://doi.org/10.1146/annurev-ento-011613-162005>
- Lima, M.A.P., Martins, G.F., Oliveira, E.E., Guedes, R.N.C., 2016. Agrochemical-induced stress in stingless bees: peculiarities, underlying basis, and challenges. *J. Comp. Physiol.*

- A 202, 733–747. <https://doi.org/10.1007/s00359-016-1110-3>
- Mathis, A., Mamidanna, P., Cury, K.M., Abe, T., Murthy, V.N., Mathis, M.W., Bethge, M., 2018. DeepLabCut: markerless pose estimation of user-defined body parts with deep learning. *Nat. Neurosci.* 21, 1281–1289. <https://doi.org/10.1038/s41593-018-0209-y>
- Noldus, L.P.J., Spink, A.J., Tegelenbosch, R.A., 2002. Computerised video tracking, movement analysis and behaviour recognition in insects. *Comput. Electron. Agric.* 35, 201–227. [https://doi.org/10.1016/S0168-1699\(02\)00019-4](https://doi.org/10.1016/S0168-1699(02)00019-4)
- Pereira, T.D., Aldarondo, D.E., Willmore, L., Kislin, M., Wang, S.S.H., Murthy, M., Shaevitz, J.W., 2019. Fast animal pose estimation using deep neural networks. *Nat. Methods* 16, 117–125. <https://doi.org/10.1038/s41592-018-0234-5>
- Rodriguez, A., Zhang, H., Klaminder, J., Brodin, T., Andersson, P.L., Andersson, M., 2018. ToxTrac: A fast and robust software for tracking organisms. *Methods Ecol. Evol.* 9, 460–464. <https://doi.org/10.1111/2041-210X.12874>
- Romero-Ferrero, F., Bergomi, M.G., Hinz, R.C., Heras, F.J.H., de Polavieja, G.G., 2019. idtracker.ai: tracking all individuals in small or large collectives of unmarked animals. *Nat. Methods* 16, 179–182. <https://doi.org/10.1038/s41592-018-0295-5>
- Sgolastra, F., Hinarejos, S., Pitts-Singer, T.L., Boyle, N.K., Joseph, T., Lückmann, J., Raine, N.E., Singh, R., Williams, N.M., Bosch, J., 2019. Pesticide exposure assessment paradigm for solitary bees. *Environ. Entomol.* 48, 22–35. <https://doi.org/10.1093/ee/nvy105>
- Sridhar, V.H., Roche, D.G., Giggins, S., 2019. Tracktor: Image-based automated tracking of animal movement and behaviour. *Methods Ecol. Evol.* 10, 815–820. <https://doi.org/10.1111/2041-210X.13166>
- Viana, T.A., Barbosa, W.F., Jojoa, L.L.B., Bernardes, R.C., Silva, J.S. da, Jacobs-Lorena, M., Martins, G.F., 2021. A genetically modified anti-plasmodium bacterium is harmless to the foragers of the stingless bee *Partamona helleri*. *Microb. Ecol.* 2021 1, 1–10. <https://doi.org/10.1007/S00248-021-01805-9>
- Walter, T., Couzin, I.D., 2020. TRex, a fast multi-animal tracking system with markerless identification, and 2D estimation of posture and visual fields. *bioRxiv*.

<https://doi.org/10.1101/2020.10.14.338996>

Yilmaz, A., Javed, O., Shah, M., 2006. Object tracking: A survey. *ACM Comput. Surv.* 38, 13--es.

**CHAPTER 1. Ethoflow: computer vision and artificial intelligence-based software for automatic behavior analysis**

## Article

# Ethoflow: Computer Vision and Artificial Intelligence-Based Software for Automatic Behavior Analysis

Rodrigo Cupertino Bernardes <sup>1,\*</sup>, Maria Augusta Pereira Lima <sup>2</sup>, Raul Narciso Carvalho Guedes <sup>1</sup>, Clíssia Barboza da Silva <sup>3</sup> and Gustavo Ferreira Martins <sup>4</sup>

<sup>1</sup> Department of Entomology, Federal University of Viçosa, Viçosa 36570-900, MG, Brazil; guedes@ufv.br

<sup>2</sup> Department of Animal Biology, Federal University of Viçosa, Viçosa 36570-900, MG, Brazil; maugusta@ufv.br

<sup>3</sup> Laboratory of Radiobiology and Environment, University of São Paulo-Center for Nuclear Energy in Agriculture, 303 Centenário Avenue, Piracicaba 13416-000, SP, Brazil; clissia@usp.br

<sup>4</sup> Department of General Biology, Federal University of Viçosa, Viçosa 36570-900, MG, Brazil; gmartins@ufv.br

\* Correspondence: bernardesrodrigoc@gmail.com; Tel.: +55-3199-516-9902

**Abstract:** Manual monitoring of animal behavior is time-consuming and prone to bias. An alternative to such limitations is using computational resources in behavioral assessments, such as tracking systems, to facilitate accurate and long-term evaluations. There is a demand for robust software that addresses analysis in heterogeneous environments (such as in field conditions) and evaluates multiple individuals in groups while maintaining their identities. The Ethoflow software was developed using computer vision and artificial intelligence (AI) tools to monitor various behavioral parameters automatically. An object detection algorithm based on instance segmentation was implemented, allowing behavior monitoring in the field under heterogeneous environments. Moreover, a convolutional neural network was implemented to assess complex behaviors expanding behavior analyses' possibilities. The heuristics used to generate training data for the AI models automatically are described, and the models trained with these datasets exhibited high accuracy in detecting individuals in heterogeneous environments and assessing complex behavior. Ethoflow was employed for kinematic assessments and to detect trophallaxis in social bees. The software was developed in desktop applications and had a graphical user interface. In the Ethoflow algorithm, the processing with AI is separate from the other modules, facilitating measurements on an ordinary computer and complex behavior assessing on machines with graphics processing units. Ethoflow is a useful support tool for applications in biology and related fields.

**Keywords:** animal monitoring; convolutional neural networks; deep learning; machine learning; object detection; tracking



**Citation:** Bernardes, R.C.; Lima, M.A.P.; Guedes, R.N.C.; da Silva, C.B.; Martins, G.F. Ethoflow: Computer Vision and Artificial Intelligence-Based Software for Automatic Behavior Analysis. *Sensors* **2021**, *21*, 3237. <https://doi.org/10.3390/s21093237>

Academic Editor: Alexander Wong

Received: 7 April 2021

Accepted: 3 May 2021

Published: 7 May 2021

**Publisher's Note:** MDPI stays neutral with regard to jurisdictional claims in published maps and institutional affiliations.



**Copyright:** © 2021 by the authors. Licensee MDPI, Basel, Switzerland. This article is an open access article distributed under the terms and conditions of the Creative Commons Attribution (CC BY) license (<https://creativecommons.org/licenses/by/4.0/>).

## 1. Introduction

Behavioral studies are critical to understanding the fundamental aspects of animal ecology [1,2]. The assessment of animal behavior by visual inspection is limited and subjective and does not allow observations over long periods [3]. The use of computational tools in behavioral assessments allows accurate and long-term evaluations of animals [2,4]. For instance, automatic tracking systems obtain the animal's position in each frame of a digital video and record the Cartesian or polar coordinates of the movement [5].

From animals' coordinates over time is possible to calculate important kinematic measurements (e.g., the animal walked distance and meandering). Furthermore, evaluating complex behaviors (measurements based on characteristics extracted from specific animal behaviors) can provide relevant insights into animal biology. For example, the evaluation of complex behaviors among social insects, such as changes in trophallaxis (the complex social behavior of food exchange among nestmates), is important for understanding their response to stress agents such as pesticides [6,7].

Robust systems are needed for animal monitoring in heterogeneous environments (i.e., complex environmental landscapes such as in the field or multi-scenes with variation in color, luminosity, texture, and different objects) [2]. The greatest challenge in heterogeneous environments involves extracting target objects from the background (segmentation) [8]. Background subtraction or thresholding are well-established in digital image processing for object segmentation [5]. However, these approaches require video recordings of homogeneous environments (i.e., with similar pixel values or slight variation in color, luminosity, and texture) and are not applicable in heterogeneous environments.

Using artificial intelligence (AI) technics such as machine and deep learning can be sufficiently robust for animal behavior assessments in heterogeneous environments [9]. Convolutional neural networks (CNNs) are deep learning models widely used in computer vision [10]. These models are organized into layers composed of several neurons and convolutional kernels/filters with learnable weights. The CNNs comprise two basic parts: a convolutional base and a densely connected classifier. In the convolutional base, operations (convolutions) decompose the input in abstract and useful information (feature extraction) for classification in dense layers. Thus, the convolutional base's function is finding appropriate representations (feature map) for the classification in the dense layers, where the feature map undergoes successive nonlinear operations to obtain the predictions. The learning process of neural networks consists of updating the network parameters in the opposite direction of the cost function gradient, reducing the loss, until finding optimal parameters that result in a minimal loss (i.e., minimal difference between the expected value and the predicted value) [10].

Given the potential application of AI and the demand for studying animal behavior in natural conditions [2], we developed the open-source desktop software Ethoflow. In the software algorithm, (i) we used unsupervised machine learning to provides an optimal identity assignment and maintain the identity among individuals in animal group tracking. Using deep learning, (ii) we implemented instance segmentation for animal monitoring in heterogeneous environments. Moreover, (iii) deep learning was applied to recognize animal complex behaviors. Besides, (iv) we performed bioassays with two species of eusocial bees to validate Ethoflow. Finally, (v) we evaluated parameters associated with Ethoflow's performance. Thus, the proposed software:

- has a graphical user interface (GUI) and has already been successfully applied in other studies [11,12];
- performs animal tracking in homogeneous or heterogeneous environments;
- can maintain the identity among individuals in animal group tracking;
- evaluates various kinematic variables (e.g., mean speed, turning angle, and group interaction);
- supports complex behavior assessment (e.g., mating, grooming, and trophallaxis).

A brief overview of recent tools involving tracking methods and AI techniques for animal behavioral assessments is presented in Section 2. The methods and results of the Ethoflow algorithm, applications in different setups and bioassays, and performance in processing speed and accuracy are described in Sections 3 and 4. Finally, the discussion and conclusions are presented in Sections 5 and 6, respectively.

## 2. Related Work

The tracking software Tracktor uses unsupervised machine learning to track animal groups maintaining individuals' identities [13]. This software exhibited advantages in processing speed and robustness compared to the software IdTracker [14] and the ToxTrac [15]. Some other tracking software exhibit outstanding performance using deep learning algorithms [16], including the idtracker.ai [17] and the TRex [18]. These two software also apply CNNs to track many animals simultaneously with high accuracy in maintaining individuals' identities.

In addition to tracking software, there are also tools for measuring the geometrical configuration of body parts denoted as pose estimation [16]. Deep learning approaches have also led to notable improvements in pose estimation software (e.g., DeepPoseKit,

DeepLabCut, and LEAP) [19–21]. For instance, the DeepLabCut uses transfer learning with a pre-trained network in large datasets (e.g., ImageNet). This approach can improve performance and reduce the number of required training examples [19]. However, it may come with the cost of slow inference due to excessive parameterization in large networks. The LEAP framework uses a relatively simple 15 layers CNN to limit model complexity and maximize inference speed [20]. However, the LEAP achieved limited accuracy compared to the DeepPoseKit and DeepLabCut [21]. To improve the speed-accuracy tradeoff in DeepLabCut and LEAP, the DeepPoseKit toolkit was developed using Stacked DenseNet, a deep learning architecture that provides fast and accurate detection even at low spatial resolutions [21].

The unfolding of behavioral assessments in tools without graphical user interface (GUI) (e.g., Tractor) [13] requires familiarity with programming, which can limit the general public use. In this context, the Ethoflow software looks user-friendly due to the GUI. The available tracking software measure large collectively animal groups with high accuracy, especially those using deep learning. However, these tracking software operate by background subtraction or thresholding [13–15,17,18]. These approaches require video recordings of homogeneous environments and are not applicable in the field. In Ethoflow, we implemented thresholding by Otsu's method [22] (Section 3.1.3) to handle assessments in a homogeneous environment. In addition, we also implemented instance segmentation by Mask R-CNN [9] for evaluation in heterogeneous environments (Section 3.1.4).

With pose estimation toolkits, variables can be measured to predict complex animal behavior after some posterior machine learning analysis [23]. Although our goal with the Ethoflow software is tracking analysis, Ethoflow also directly measures complex behaviors. After hyperparameter optimization, we defined a parsimonious CNN architecture to assess complex binary behavior (Section 3.1.8). Deep learning software is computationally costly and requires graphics processing unit (GPU) hardware. Accordingly, they are not feasible to use on an ordinary computer. An interesting feature in our proposal is that the deep learning algorithms (used for analysis in a heterogeneous environment and measurement of complex behaviors) are separate from the other modules in Ethoflow. Wherefore, Ethoflow covers kinematic measurements on an ordinary computer and assesses more complex behavior with a GPU.

### 3. Materials and Methods

#### 3.1. Software Features and Algorithm

The Ethoflow software was developed in modality desktop application with Python language, including the image library OpenCV [24] and the framework TensorFlow [25] with Keras for AI models. Other libraries, such as SciPy [26], Numpy [27], Pandas [28], and SciKit Learn [29], were also used. We recommended Python version 3.6.8 and Microsoft Windows 10 when running the Ethoflow. The main input and output files, formats, descriptions, and quick examples of using these Ethoflow files are described in Supplementary materials (Table S1). The following subsections will provide further details on the Ethoflow algorithm steps (Figure 1).

##### 3.1.1. Input Video

Multi-threaded processing was implemented in the algorithm. In this procedure, the video is read in a thread independent of the processing thread, and the frames are stored in a stack (Figure 1; step 1.1; Appendix A). This avoids the delay between frame reading and other processing steps of the algorithm, whereby frames are always available to obtain better rates in frames per second (fps).

##### 3.1.2. Preprocessing

In preprocessing (Figure 1; step 1.2), the video is processed to eliminate the regions that are not of interest to the user and transformed into a virtual primary color system (color space XYZ). In this color space, the chromaticity (XZ) and luminance (Y) are coded sepa-

rately, resulting in a more uniform response to the luminosity variation. Then, grayscale transformation and normalization are applied to increase homogeneity between the frames. Smoothing is also applied through a transformation based on the median of neighborhood pixels to eliminate noise.

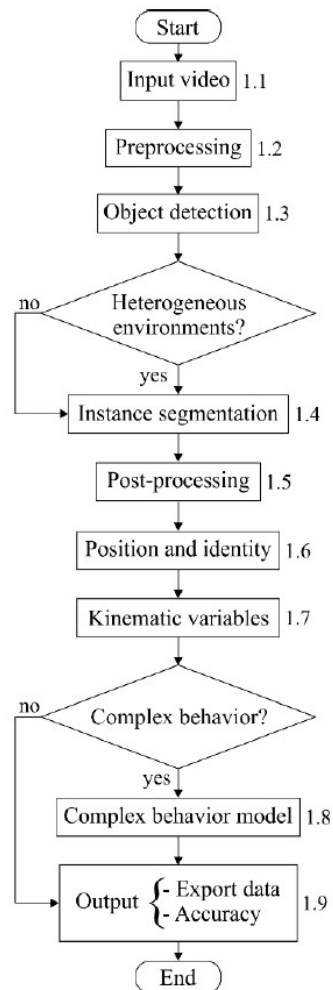


**Figure 1.** Flowchart of the Ethoflow algorithm. The numbers on the right side of the rectangles indicate the steps in the algorithm process. These steps are described in the subsequent sections from Sections 3.1.1–3.1.9. Diamond symbols indicate the option of using the deep learning algorithms (for analysis in a heterogeneous environment or measurement of complex behaviors) according to the need. Thus, the Ethoflow performs kinematic measurements on an ordinary computer and assesses more complex behavior with a graphics processing unit hardware.

### 3.1.3. Object Detection

After preprocessing, manual and automatic image thresholds are applied to detect individuals (Figure 1; step 1.3). In manual thresholding, the classification of pixel  $(x, y)$  is performed according to a global threshold defined by the user ( $g$ ):

$$f(x, y) = \begin{cases} 1 & \text{if } (x, y) > g \\ 0 & \text{if } (x, y) \leq g \end{cases}. \quad (1)$$

One of the automatic thresholding options is based on Otsu's method [22], wherein the optimal threshold minimizes the within-class variance. This algorithm attempts to find

a threshold value ( $k$ ) that minimizes the within-class variances  $c_0$  and  $c_1$  (background and objects, respectively). If the set of gray levels of an image  $L = \{1, 2, \dots, l\}$  and the total number of pixels  $N = \{n_1, n_2, \dots, n_l\}$ , then the probability of occurrence of a gray level ( $p_i$ ) is given by

$$p_i = \frac{n_l}{N}. \quad (2)$$

As the method is based on the normalized histogram,

$$\sum_{i=1}^L p_i = 1. \quad (3)$$

Thus, the probability of occurrence ( $\omega_i$ ), means ( $\mu_i$ ), and variances ( $\sigma_i$ ) of each class, are given by

$$\omega_0 = \sum_{i=1}^k p_i \text{ and } \omega_1 = \sum_{i=k+1}^L p_i, \quad (4)$$

$$\mu_0 = \frac{\sum_{i=1}^k i * p_i}{\omega_0} \text{ and } \mu_1 = \frac{\sum_{i=k+1}^L i * p_i}{\omega_1}, \quad (5)$$

$$\sigma_0^2 = \frac{\sum_{i=1}^k (i - \mu_0)^2 p_i}{\omega_0} \text{ and } \sigma_1^2 = \frac{\sum_{i=k+1}^L (i - \mu_1)^2 p_i}{\omega_1}. \quad (6)$$

The within-class ( $\sigma_w$ ) and between-class ( $\sigma_b$ ) variances are

$$\sigma_w^2 = \omega_0 \sigma_0^2 + \omega_1 \sigma_1^2, \quad (7)$$

$$\sigma_b^2 = \omega_0 \omega_1 (\mu_1 - \mu_0)^2. \quad (8)$$

The total variance is  $\sigma_t^2 = \sigma_w^2 + \sigma_b^2$ , and calculating the between-class variance improves the computational time because the variance between classes is based on first-order statistics (class means) [22].

### 3.1.4. Instance Segmentation

Instance segmentation (IS) [9] is another type of automatic segmentation available in Ethoflow for animal behavior assessments in heterogeneous environments (Figure 1; step 1.4). ResNet-101 [30] was the convolutional base used in this model, following a Mask R-CNN implementation [31]. In this model, the video frames pass through a convolutional base for feature extraction, leading to feature map generation. The region proposal network (RPN) is then applied, which provides several candidate boxes (ROI proposals). As several ROIs are generated, the model classifies these boxes into foreground proposals (animals) and backgrounds. ROI pooling is applied to standardize the foreground proposals' size, slicing each foreground into a fixed number of parts, and max pooling is applied to standardize the size. Finally, the boxes labeled as real animals are instantiated using a pixel-wise sigmoid function (Figure 2).

### 3.1.5. Post-Processing

In post-processing (Figure 1; step 1.5), morphological operations are applied to eliminate residues. First, dilation is used to fill parts that belong to the same individual but are detected separately. Second, the gradient is calculated and subtracted from the expanded frame to eliminate undesirable edges. Finally, erosion is applied to eliminate any noise erroneously detected as individuals.

### 3.1.6. Position and Identity

In step 1.6 of the algorithm, the animal contours (the pixels contained in the animal body) are identified. The contours are identified without establishing hierarchies while retaining only the extreme points of the contour line segments. The contour measurements,

such as the area, length, and the ratio between the area and length, are calculated to restrict the contours that are identified based on the user's inputs.

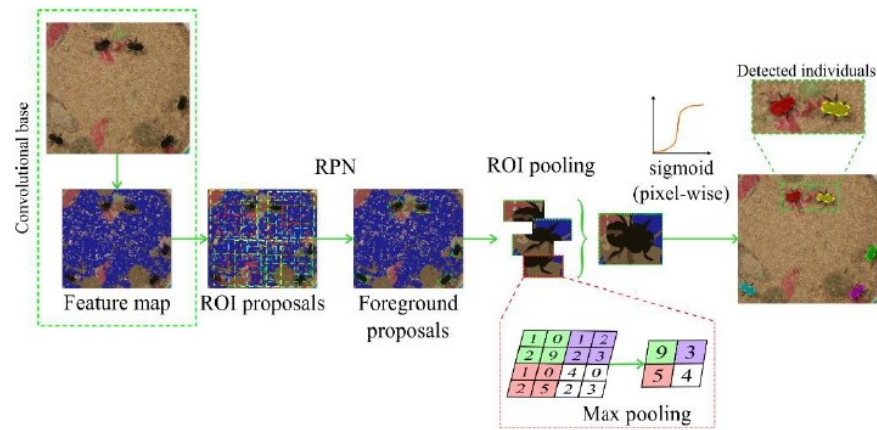


**Figure 2.** Diagram depicting the operations involved in instance segmentation used in Ethoflow for animal behavior assessments in heterogeneous environments. RPN: region proposal network; ROI: box surrounding the object of interest.

When the number of contours identified is smaller than the number of individuals specified by the user, the nonhierarchical clustering k-means algorithm is applied to separate merged individuals. In this unsupervised machine learning algorithm, the number of groups ( $k$ ) in which the set of pixels will be grouped is equal to the number of individuals specified by the user. The initial  $k$  centroids are randomly defined among the set of data points. Then, the next set of centroids are chosen according to the probability of spreading between the centers [32]. The contour points are compared with each centroid and are allocated to the group where the Euclidean distance is minimal. Considering the inputs for the algorithm  $X = \{x_1, \dots, x_n\}$  of  $n$  data points, this algorithm runs interactively to find a set  $C = \{c_1, \dots, c_k\}$  that minimizes the function  $\varphi_x(C)$  as follows:

$$\varphi_x(C) = \sum_{x \in X} d(x, C)^2, \quad (9)$$

where  $d(x, C)^2$  is the distance from  $x$  to the closest center in  $C$ . To choose centroids in the k-means algorithm, the first set of centers  $C_0$  are randomly selected from the dataset. Then, this step is repeated for  $2 \leq i \leq k$ :  $c_i$  is chosen to be equal to a data point  $x_n$  according to the probability [32]:

$$\frac{d(x_0, C)^2}{\varphi_x(C)}. \quad (10)$$

A combinatorial optimization algorithm [33] is applied to maintain the identity of individuals, which provides the optimal identity assignment among the centroids of animal contours. This is based on the Euclidean distance between the set of centroids of the objects in the  $frame_{i+1} = \{a_1, a_2, \dots, a_n\}$  and the set of centroids in the  $frame_i = \{b_1, b_2, \dots, b_n\}$ . Considering that each  $a_n$  is assigned to only one  $b_n$ , the goal is to minimize the total cost of assignments about the distance matrix ( $D$ ) between each  $a_n$  and  $b_n$ :

$$D = \begin{bmatrix} d_{1,1}d_{1,2} \cdots d_{1,n} \\ d_{2,1}d_{2,2} \cdots d_{2,n} \\ \vdots \\ d_{n,1}d_{n,2} \cdots d_{n,n} \end{bmatrix}. \quad (11)$$

The mathematical model [33] for the assignments is given as  $Minimum : \sum_{x=1}^n \sum_{j=1}^n d_{ij}$ , where  $d_{ij}$  is the cost (Euclidean distance) from centroid  $a_n$  to centroid  $b_n$ . There are  $n!$  ways to assign  $a_n$  to  $b_n$  and achieve the optimal assignment, interactively, with the following steps:

1. The minimum of each row is subtracted from the entire row.
2. The minimum of each column is subtracted from the entire column.
3. All zeros in the matrix are crossed with the minimum possible lines.

If crossing lines =  $n$ , then the optimal assignment is found.

Else:

To determine the smallest entry not crossed by any line,

Subtract this entry from each uncrossed row and add it to each crossed column.

Proceed to step 3.

### 3.1.7. Kinematic Variables

Among the identified and assigned animal contours, each individual's centroid (Cartesian position) is determined. Based on this Cartesian position  $x, y$  of individuals over time (video frames;  $f$ ), various kinematic variables are computed in algorithm step 1.7. The distance that an animal walks during the video is tracked distance ( $td$ ) (Equation (12)). Dividing  $td$  by the total time of the video, the mean velocity can be calculated. Ethoflow also calculates the maximum velocity achieved by the animal.

$$td = \sum_{i=1}^f \sqrt{(x_{i+1} - x_i)^2 + (y_{i+1} - y_i)^2}. \quad (12)$$

The average angle that the individual rotated in each frame (turning angle;  $ta$ ) is computed by the absolute sum of the angles ( $^\circ$ ) of the movement divided by the video frames ( $f$ ) (Equation (13)), while the meandering (the average angle that the individual rotated during the video;  $M$ ) is divided by tracked distance ( $td$ ) (Equation (14)); the angle of the movement is the arctangent of the locomotion in planes  $y$  ( $\Delta y_i$ ) and  $x$  ( $\Delta x_i$ ).

$$ta = \frac{1}{n} \sum_{i=1}^f \left| \left( \frac{\arctan\left(\frac{\Delta y_i}{\Delta x_i}\right) 180}{\pi} \right) \right|. \quad (13)$$

$$M = \frac{1}{td} \sum_{i=1}^f \left| \left( \frac{\arctan\left(\frac{\Delta y_i}{\Delta x_i}\right) 180}{\pi} \right) \right|. \quad (14)$$

The movement of individuals is categorized based on the user-defined values. When defining the analysis protocol, the user defines the thresholds for low ( $tl$ ) and high movement ( $th$ ). Thus, considering the movement of individuals in each frame as  $mf$ :  $mf \leq tl$  is counted as resting (the time associated with no activity of the individual);  $tl < mf \leq th$  is counted as mean movement (the time in intermediated activity);  $mf > th$  is counted as fast movement (the time in high activity). The sum of these counts is divided by the frames per second ( $fps$ ) used to sample the video to obtain these values in time.

The user also sets a threshold for interaction ( $ti$ ). The interaction is considered when the individuals approach a distance  $\leq ti$ . The sum of all interactions of an individual is defined as centrality. The network density ( $nd$ ) is a measurement associated with group interaction (Equation (15)). A network is a set of items in which the vertices are defined as nodes ( $n$ ), and the connections among them are defined as edges ( $m$ ) [34]. Here, the nodes are the individuals, and the edges represent the number of interactions among them.

$$nd = \frac{2m}{n(n-1)}. \quad (15)$$

If the user defines a region of interest ( $ri$ ), Ethoflow computes how long the individuals stayed inside this region, considering the position (coordinates  $x, y$ ) of each individual in the video frames ( $f$ ):

$$\sum_{i=1}^f (x_i, y_i) \in ri. \quad (16)$$

Considering the direction unit ( $u$ ) of the individuals ( $i$ ), the proportion of the group polarized ( $p$ ) at each frame is calculated as

$$p = \frac{1}{i} \left| \sum_{j=1}^i u_j \right|. \quad (17)$$

The angular momentum (rotate;  $r$ ) for each frame is a cross product (or vector product;  $\times$ ) between the distance ( $d$ ) of an individual to the center of mass of the group and the direction of movement ( $u$ ):

$$r = \frac{1}{i} \left| \sum_{j=1}^i u_j \times d_j \right|. \quad (18)$$

These parameters provide information on the global structure of the group [35], such as how much individuals are aligned in a group (polarization;  $gp$ ), how much the group displays low directional alignment between neighboring individuals (swarming;  $gs$ ), and how much the group moves around its center of mass (milling;  $gm$ ). The sum of these counts is divided by the  $fps$  to obtain these values in time:

$$gp = \frac{\sum p > 0.65 \text{ and } r < 0.35}{fps}, \quad (19)$$

$$gs = \frac{\sum p < 0.35 \text{ and } r < 0.35}{fps}, \quad (20)$$

$$gm = \frac{\sum p < 0.35 \text{ and } r > 0.65}{fps}, \quad (21)$$

### 3.1.8. Complex Behavior Model

Ethoflow also measures complex behaviors using a CNN model (step 1.8). Different hyperparameter configurations were tested to define the CNN model (Figure 3) (Appendix B). In this step, the bounding box computed from animal contours passes through the convolutional base (convolutional and max-pooling layers) for feature extraction. The activation function is applied to the output of each layer to introduce nonlinearity. Then, behavior classification is performed in the dense layers. When the complex behavior that the user is evaluating occurs, the network output will be equal to behavior 1; otherwise, behavior 0. The behavior occurrence sum is divided by the video frames to generate the percentage of occurrence of the behavior. Thus, we are interested in determining the occurrence of binary behaviors that are detectable through spatial information.

### 3.1.9. Output

In step 1.8, the behavioral parameters are automatically saved in a comma-separated values (csv) file in the path defined by the user. This file also contains the raw data, the coordinates ( $x, y$ ) of movement in each frame. Thus, the user is free to calculate other kinematic parameters, in addition to those automatically computed by the software. At the end of the video processing, Ethoflow exhibits the detection rate ( $dr$ ), which is the proportion that the individual was detected during the entire video minus false detection. False detection is considered when an individual has between frames velocity greater than

the percentile at 95% of group velocity across all frames. Given the instantaneous speed vector  $IS = (is_1, \dots, is_n)$  and  $f$  frames in the video,  $dr$  is defined as:

$$dr = 1 - \left( \left( \frac{\sum_{i=1}^f is_i > 2 * P_{95}(IS)}{is_i} \right) \left( \frac{1}{f} \right) \right), \quad (22)$$

where  $P_{.95}$  is the percentile at 95% of the  $IS$  vector.

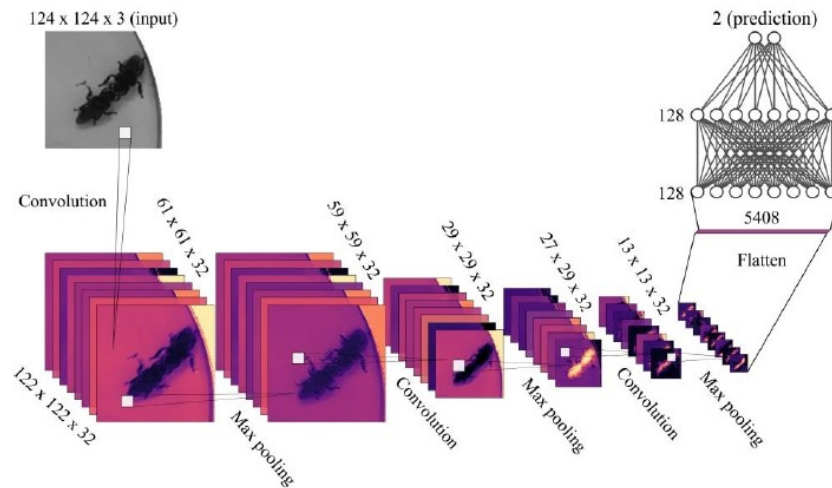


**Figure 3.** Convolutional neural network architecture defined after hyperparameter optimization (Appendix B) to recognize animal complex behavior on Ethoflow. This model was configured with stochastic gradient descent (learning rate at 0.0001 and momentum at 0.9) as an optimizer and binary cross-entropy as a loss function. Batch normalization was applied before max-pooling layers. Dropout was also applied after dense inner layers. In the inner layers (convolutional or dense), the function activation was Elu. The dimensions (width × height × depth) of feature map are given in each layer; the output dimensions of a layer are the same as the input dimensions of the next layer. In the flatten process, the data are transformed into a vector to enter the dense layers. In the last dense layer, a sigmoid function is applied, which gives the binary output.

### 3.2. Applications and Performance

#### 3.2.1. Application in Heterogeneous Environments

The Ethoflow was run on a machine with Intel i7-9750H CPU 2.60 GHz × 12, 8 GB RAM and GPU NVIDIA® GeForce® GTX 1660 (6 GB) Ti Max-Q. To apply Ethoflow in a heterogeneous environment experiment, we trained the IS model to detect the bee *Melipona quadrifasciata* through the 1325 images in various heterogeneous backgrounds (Figure 4). In addition to these image data, the inputs with bounding box positions, classes, and masks (pixel-wise positions of the animals) are required to train the IS model [9]. The manual generation of these inputs is a laborious task. Then, we developed a heuristic to automatically generate these inputs based on several random backgrounds and a video in homogeneous conditions to detect objects using manual segmentation or Otsu's method. Frames are randomly sampled in the video and pass through the algorithm's preprocessing and object detection stages (Figure 5A). Then, the animals are "copied," and the contours are "pasted" into random backgrounds (Figure 5B). Concomitantly, the bounding box, class, and mask of each animals are saved in a dictionary with the following structure: Dictionary {image: {object: {box: {center: {x,y}, width, height}; class:{target}; mask:{all points (x,y)}}}}.

Of all the data generated with the heuristic, 976 (74%) were used for training, 249 (19%) for validation, and 100 (7%) to evaluate the classification using the average precision (AP) [36]. To obtain AP, we calculated the intersection over union (IoU) of the predicted

bounding boxes (i.e., the  $x, y$  coordinates in the upper-left corner and width and height of the rectangular box around the object of interest) and target bounding boxes. Based on the  $IoU$ , the precision (Equation (23)) and recall (Equation (24)) can be calculated using the true positives ( $TP$ ), false positives ( $FP$ ), and false negatives ( $FN$ ) for the detected objects ( $DO$ ) in a determined threshold ( $x$ ) (Equation (25)).

$$\text{precision} = \frac{TP}{TP + FP}. \quad (23)$$

$$\text{recall} = \frac{TP}{TP + FN}. \quad (24)$$

$$\left\{ \begin{array}{l} \text{if } IoU \geq x, DO = TP \\ \text{if } IoU < x, DO = FP \\ \text{if the model fails to detect a target object, } DO = FN \end{array} \right\} \quad (25)$$

There is a tradeoff between the precision and recall, wherein the higher the recall, the more the model tends to find all the target objects, i.e., a low  $FN$  value. However, an increase in the recall tends to decrease the precision, as it increases  $FP$ . Considering equally spaced recall levels  $n = (0, 0.1, \dots, 1.0)$ , interpolation is performed using the highest precision value for a given recall. Then, the  $AP$  is obtained from the interpolated values of the precision ( $P_{interp}(r)$ ):

$$AP = \frac{1}{n} \sum_{i=0}^n P_{interp}(r_i). \quad (26)$$

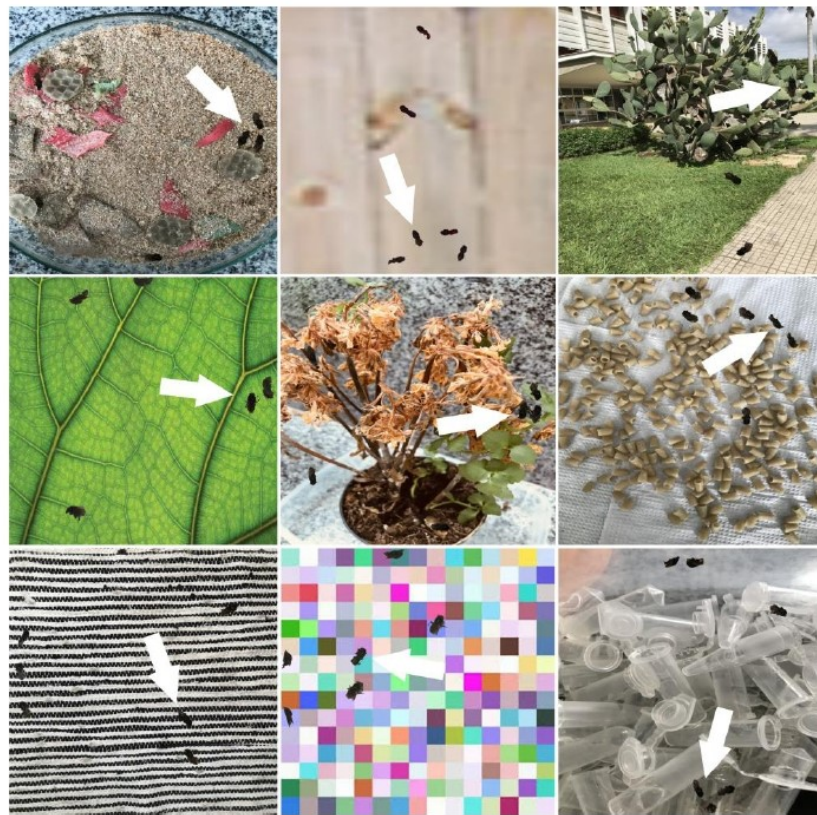


**Figure 4.** Examples of some images that were generated automatically to train the model for tracking the stingless bee *Melipona quadrifasciata* in different conditions of a heterogeneous background. The white arrows indicate some bee contours pasted in the backgrounds.

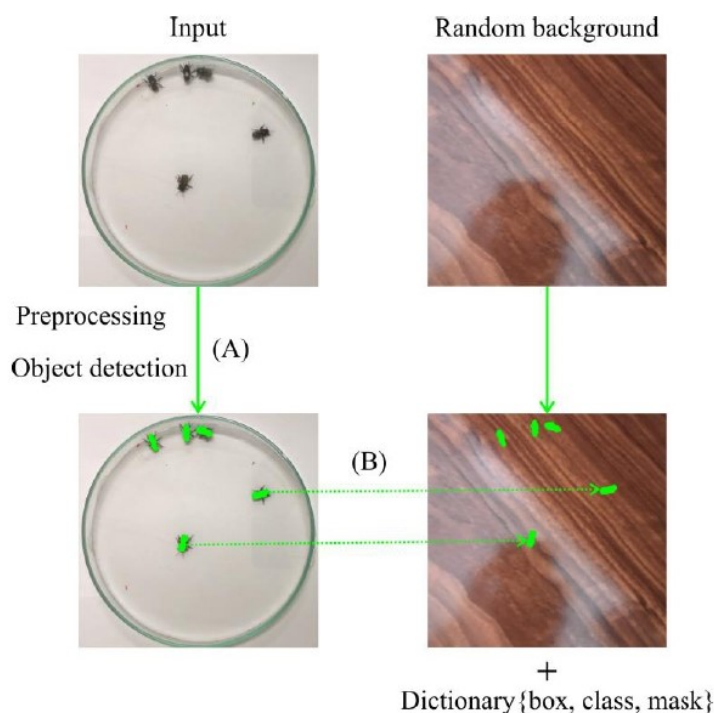


**Figure 5.** Schematic representation of the heuristic used to generate labeled images for the IS model automatically. The segmented objects (indicated by green masks) on a homogeneous background (A) are glued to random backgrounds (B).

### 3.2.2. Application in Complex Behavior

Ethoflow was also applied to learn the detection of trophallaxis, the complex social behavior of food exchange among nestmates, in *M. quadrifasciata*. Thus, 1270 labeled images were generated (724 for non-trophallaxis and 546 for trophallaxis) (Figure 6). In this dataset, 70% of the data was used for training, while 20% was used for validation. Another sample dataset (10%) was used to assess the classifier's performance based on the global accuracy from the confusion matrix, Kappa index, and Z-test (5%).



**Figure 6.** Examples of images that were automatically labeled with our heuristic to train the CNN model to recognize trophallaxis in the stingless bee *Melipona quadrifasciata*. The images with green outlines (**top**) are examples of trophallaxis. The images with dashed purple outlines (**bottom**) are examples of non-trophallaxis.

The labeled images used to train the CNN model for recognizing trophallaxis were also generated through a heuristic automatically. When bees perform trophallaxis, they position themselves in front of each other and exchange food. Based on this predictable positioning, the heuristic was based on the individuals' area and body length. Initially, the program estimates the median ( $M$ ) and standard deviation ( $sd$ ) of the body area ( $a$ ) and length ( $l$ ) in frames where there is no crossing (no meeting between individuals). Subsequently, the software obtains the images ( $b$ ) from the video and labels them as trophallaxis if:

$$\left\{ \begin{array}{l} area(b) \geq 2 * (M(a) - sd(a)) \text{ and} \\ area(b) \leq 2 * (M(a) + sd(a)) \text{ and} \\ length(b) \geq 2 * (M(l) - sd(l)) \text{ and} \\ length(b) \leq 2 * (M(l) + sd(l)) \end{array} \right\}, Else : b \text{ is not trophallaxis.} \quad (27)$$

### 3.2.3. Application in Behavioral Bioassays

A behavioral assay was performed with the two stingless bee species. Bees of both species were collected from four colonies each of *M. quadrifasciata* and *Partamona helleri* in Viçosa, State of Minas Gerais, Brazil (20°45' S and 42°52' W). The collected bees were kept for 1 h in the laboratory under conditions similar to those found in their colonies (28 °C and 80% relative humidity in total darkness) [37]. Subsequently, bee behavior was recorded in the arenas (Petri dish, 9 cm diameter, 2 cm height) for 15 min with a digital video camera (HDR-XR520V, Sony Corporation) at 30 fps and high definition (1920 × 1080 pixels). Behavioral bioassays were performed in a room with artificial fluorescent light at 25 ± 3 °C and 70 ± 5% relative humidity. Bioassays were performed with 37 replicates, with each replicate corresponding to a group of five bees of each of the two species. The kinematic variables measured with EthoFlow included centrality, polarization, milling, resting, meandering, and tracked distance. In the centrality response, the interaction was considered when the individuals approached a distance ≤1.41 cm. An instantaneous tracked distance ≤0.046 cm frame<sup>-1</sup> was counted as resting. Centrality was the response variable in the model with interaction between polarization and bee species, or model with interaction between milling and bee species. Meandering was the response variable in the model with interaction between resting and bee species. Besides, the tracked distance between the bee species was compared. These models were fitted with generalized linear models (GLM) with a gamma distribution, displaying adequate distribution for continuous data in which the variance increases with the square of the mean [38]. When an explanatory variable had no significant effect, the model was simplified, and the results were plotted as a function of the significant variable.

A toxicological bioassay was also performed with *M. quadrifasciata* to demonstrate trophallaxis recognition under pesticide stress conditions. The acclimated bees were orally exposed to the commercial formulation (cf) (water-dispersible granules at 700 g a.i. Kg<sup>-1</sup>, Bayer CropScience, São Paulo, SP, Brazil) of the neonicotinoid imidacloprid in a sublethal concentration (0.2 mg cf L<sup>-1</sup>). This concentration is 300× smaller than that recommended for controlling the whitefly *Bemisia tabaci* (60 mg cf L<sup>-1</sup>) [39]. The pesticide imidacloprid is commonly associated with bee decline and causes motor impairments in bees [40]. After 3 h of exposure, the bees were filmed as previously described, and trophallaxis behavior was quantified using EthoFlow. Trophallaxis response ( $n = 60$ ) to the pesticide was assessed using a GLM with a Poisson distribution, a suitable distribution for count data [38].

### 3.2.4. Performance

Using videos with variations in resolution, the number of individuals, animals, and backgrounds (Supplementary Materials; Figure S1), we evaluated some parameters associated with EthoFlow's performance and also compared it with other tracking software that has a satisfactory processing rate, based on the processing speed obtained by Sridhar et al. (2019) [13]. A multiple regression model was applied to assess whether the fps rate responds to the interaction between the resolution and the number of individuals.

The effect of centrality and the number of individuals in fps was assessed using a GLM with a gamma distribution. Analysis of covariance (ANCOVA) was performed to assess whether the detection rate varied with the interaction between the number of individuals and background (homogeneous and heterogeneous).

#### 4. Results

##### 4.1. Heterogeneous Environment and Complex Behavior

Ethoflow was efficient in detecting the tested bees with high precision and low false positives in heterogeneous environments (average precision  $\pm$  standard error =  $0.916 \pm 0.02$ ; Figure 7A). In addition, in complex behavior assessment, the CNN model exhibited high accuracy in the validation process (global accuracy = 92.13%, Kappa index = 0.84,  $Z = 24.74$ , Figure 7B).

##### 4.2. Behavioral Bioassays

The results of the bioassays demonstrated significant differences between behaviors, bee species, and response to pesticide stress. In both species, the centrality increased with the polarization of the group ( $F_{1,35} = 25.1$ ,  $p < 0.0001$ ) and decreased with milling ( $F_{1,35} = 46.2$ ,  $p < 0.0001$ ) (Figure 8A). Meandering was influenced by the statistical interaction between the variables resting and bee species ( $F_{1,33} = 4.71$ ,  $p = 0.037$ ; Figure 8B). Moreover, a difference between species was observed in the tracked distance ( $F_{1,35} = 13.6$ ,  $p = 0.0008$ ; Figure 8C), and bees exposed to the pesticide exhibited significantly reduced trophallaxis ( $\chi^2 = 94.9$ ,  $df = 58$ ,  $p < 0.0001$ ; Figure 8D).

##### 4.3. Performance

In homogeneous backgrounds, Ethoflow achieved a median rate of 32.5 fps. This rate is a satisfactory processing speed compared to other tracking software that does not use AI in their algorithms (e.g., idTracker = 5.5 fps; ToxTrac = 28.6 fps; Tracktor = 25.7 fps) (Figure 9).

Statistical interaction was observed between the variables video resolution and group size in fps rate ( $F_{1,130} = 12.81$ ,  $p = 0.0005$ , Figure 10A). The heterogeneous environment quantification was not influenced by the video resolution or number of individuals ( $F_{1,28} = 0.81$ ,  $p = 0.37$ , Figure 10B), and the fps rate in a heterogeneous environment (0.386) was lower than in homogeneous backgrounds. The fps decreased with an increase in the centrality of individuals ( $F_{1,38} = 81.24$ ,  $p < 0.0001$ , Figure 10C). There was no significant effect on the number of individuals ( $F_{1,37} = 0.009$ ,  $p = 0.93$ ), and no interaction was observed between the centrality and individuals ( $F_{1,36} = 1.62$ ,  $p = 0.21$ ). Besides, the software exhibited high detection rates with significant interaction between the number of individuals and type of background ( $F_{1,94} = 137.85$ ,  $p < 0.0001$ , Figure 10D), where an increase in the number of individuals had a greater influence on the heterogeneous environments.

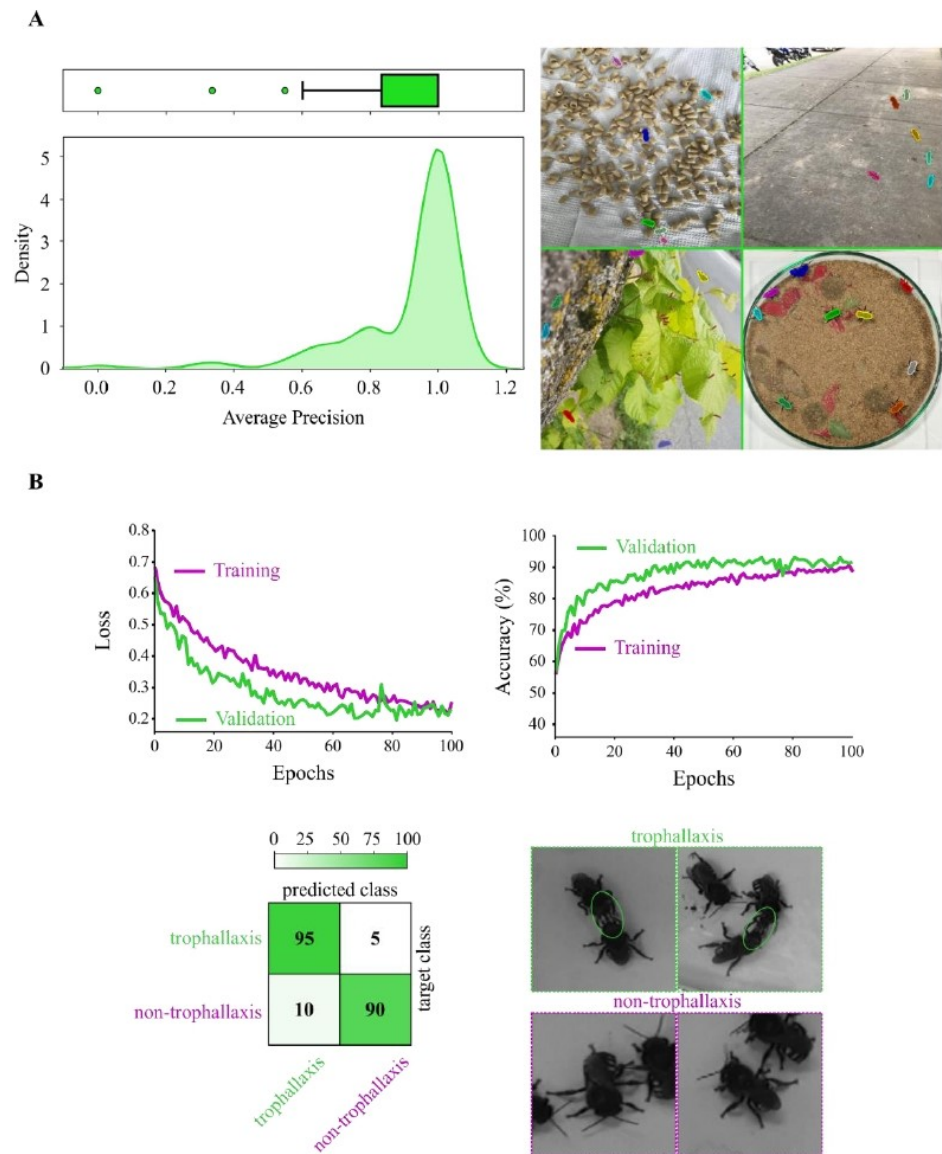


**Figure 7.** Performance of the AI models used in Ethoflow. **(A)** Animals' detection in heterogeneous environments based on instance segmentation (IS). The high average precision (left panel;  $n = 100$ ) implies that the model precisely detects real animals in the scenes with no false positives, as demonstrated by (right panel) the detected animals (marked *Melipona quadrifasciata* bees with masks in random colors) in different heterogeneous backgrounds. **(B)** The training process of the CNN model (top panel) and validation (percentage confusion matrix; bottom left panel) ( $n = 127$ ) for the monitoring of trophallaxis (green circles) in bees (bottom right panel).

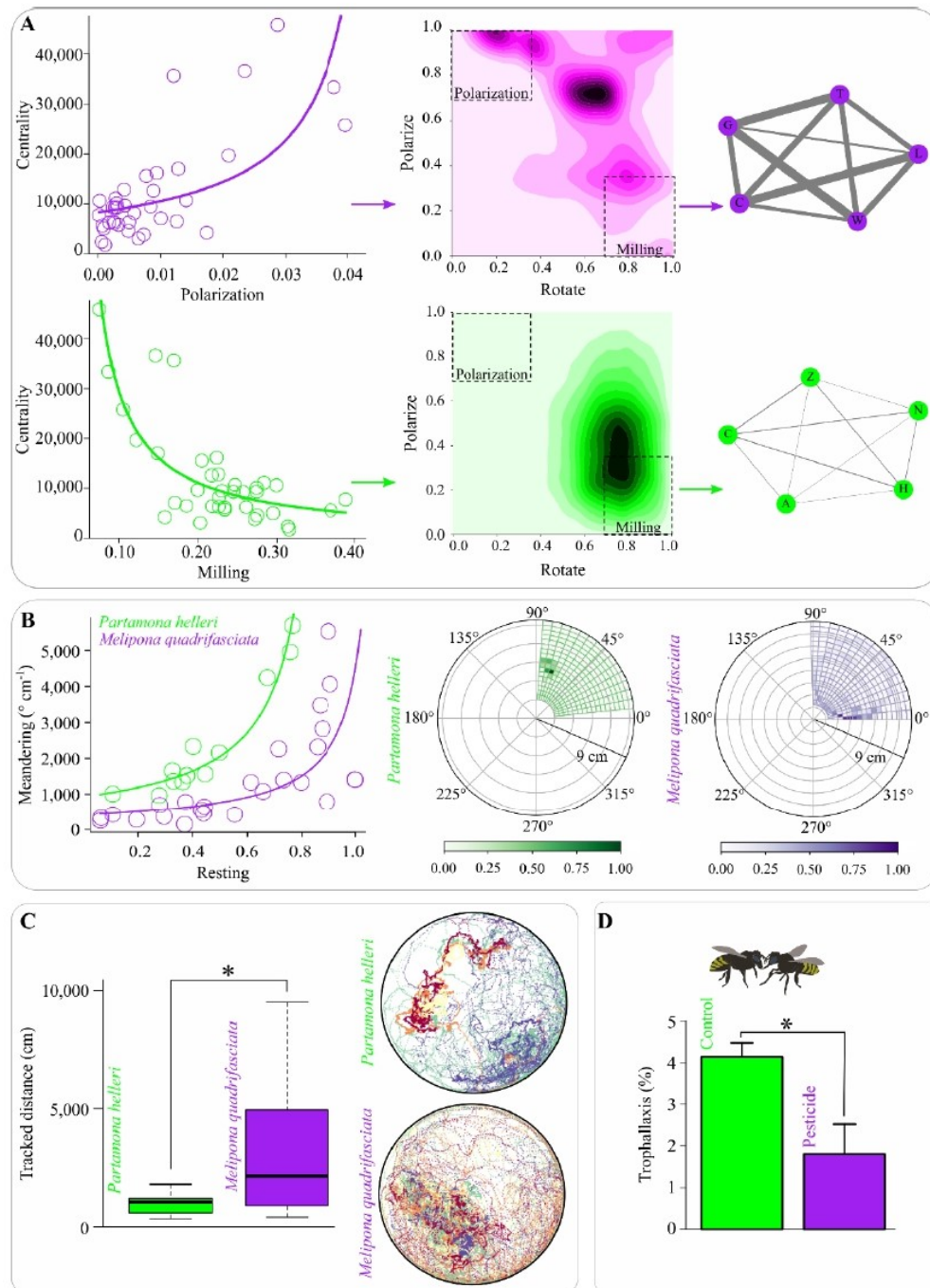


**Figure 8.** Behavioral assessments conducted using the Ethoflow software. **(A)** Association between centrality and group dynamics polarization (top panel) and milling (bottom panel) ( $n = 37$ ). The 2D density plots and network diagrams showed that a higher interaction exists among individuals in more polarized bee groups, while this interaction is reduced in the milling groups. In the networks, the circles represent individuals, and connections correspond to the edges, where their widths are proportional to the frequency of interactions. **(B)** Meandering behavior is associated with resting proportions (left panel) ( $n = 37$ ) and histograms of polar coordinates (rays and azimuth angles) for the two bee species (right panel). **(C)** The tracked distance of the assessed bee species ( $n = 37$ ). In group representative tracks, the track color reflects the individual identity (right panel). **(D)** Trophallaxis alteration in *Melipona quadrifasciata* after pesticide exposure ( $n = 60$ ). \*  $p < 0.05$  in the generalized linear model.

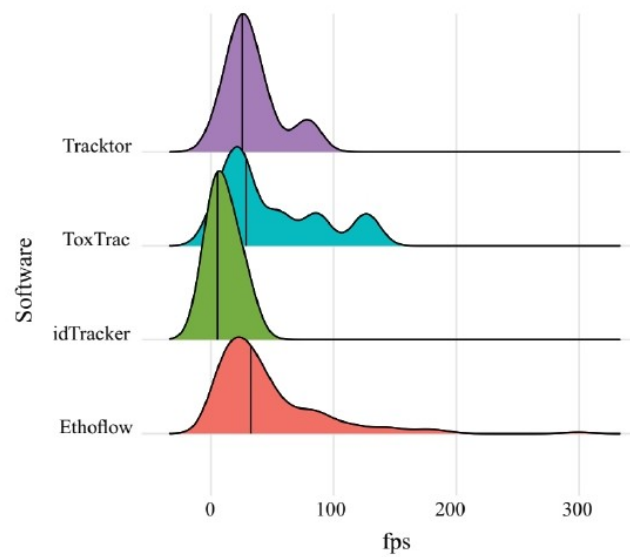


**Figure 9.** Distribution of frames per second rate exhibited for tracking software. The vertical lines within the density curves show the median.

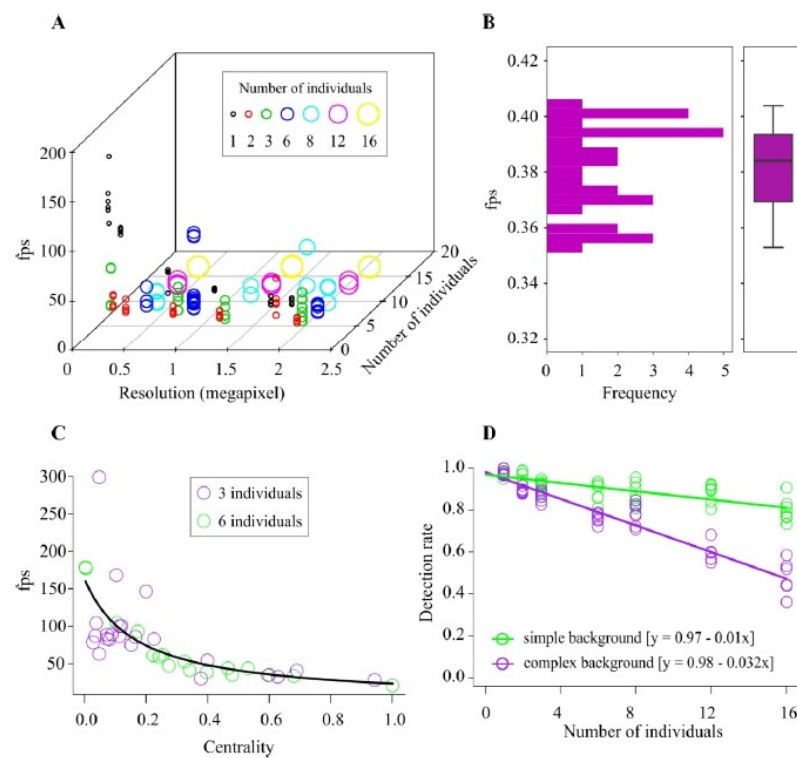


**Figure 10.** Quantification of the performance of EthoFlow. (A) Frames per seconds (fps) response to the video resolution (in pixels) and the number of individuals in homogeneous backgrounds; the dots ( $n = 134$ ) represent the raw data. (B) Histogram of the fps in heterogeneous environments ( $n = 30$ ). The box plot indicates the median and range of dispersion (lower and upper quartiles and outliers). (C) Fps in response to centrality. The proportion of group interaction per frame was used to quantify the centrality ( $n = 40$ ). (D) Accuracy of the software as a function of the interaction between the number of individuals and type of environment (homogeneous and heterogeneous); the symbols represent the raw data (circles;  $n = 98$ ).

## 5. Discussion

We developed Ethoflow software using computer vision, machine learning and deep learning techniques. This program had consistent speed rates and accuracy on processing. In addition to the possibility to study complex behaviors, Ethoflow allows multivariate assessment of kinematic behaviors. Multivariate assessment of behavioral traits can bring important insights into animals' ecological aspects, for instance, in studies of toxicological assessments and animal behavior [41–43]. Some modern software programs that use deep learning to evaluate behaviors demand powerful machines with GPU [17,18,44], which makes the analysis of laboratory routines in ordinary computers difficult. In the Ethoflow algorithm, the AI processing is separate from the other modules, enabling kinematic measurements on an ordinary computer and assessing more complex behavior using a GPU. Wherefore, to perform kinematic measurements in homogeneous environments, an ordinary computer is sufficient (e.g., a central process unit of the 3.60 GHz) to run Ethoflow. In complex behavior assessments and heterogeneous environments, a GPU computer is interesting for optimizing speed-up computational processes.

Unraveling complex behaviors can be limited by software without adequate tools or software that are complex to set up or does not have a GUI, requiring familiarity with their tools [13,17,45], limiting their usage in the general public. Thus, there is a demand in research for powerful software with simplified-interface that, at the same time, increase the ability to study more complex behaviors. In this context, the Ethoflow software looks friendly and does not require line commands to be used due to the GUI. Additionally, Ethoflow does not require a great familiarity with computational tools and has multidisciplinary applications.

During the processing in homogeneous backgrounds, the effects of resolution and number of individuals in the fps demonstrated that the frame reading step (higher resolution, higher reading time) and calculating identities (more individuals, more combinations) could decrease the processing speed. Nonetheless, the implementation of multi-threaded reading [46] in Ethoflow solves these problems. This type of reading avoids the delay between calculating the identity and reading the frames, whereby there will always be frames available in the queue for immediate calculation of the identity. This procedure possibility satisfactory fps rates compared to other software available for the same purpose [13–15]. The identity calculation algorithm step occurs when at least two individuals interact. Thus, fps showed a negative correlation with centrality because the greater the interaction, the greater the identity calculations. The number of individuals (mainly in groups > 3) had no binding effect on the fps, probably, because the amount of interaction between individuals depends on the density of the group (i.e., number of individuals per space) and not only on the size (i.e., the number of individuals) [35].

In heterogeneous environments, there is no influence of the video resolution or number of individuals on the processing, and the fps rate is lower than in homogeneous backgrounds. This shows that the main bottleneck in processing occurs in the detection of animals by Ethoflow through the instance segmentation model. With instance segmentation, real-time processing (~30 fps) has not been achieved; processing around 5 fps was reported using a robust GPU [9]. Even though it is not possible to achieve real-time processing with instance segmentation, this functionality in the Ethoflow imposes great advantages given the various possibilities of analysis in heterogeneous environments. Furthermore, video acquisition by Ethoflow is independent of processing, which enables real-time video records.

The reliable detection rates obtained with Ethoflow demonstrated that this software is sufficiently robust for applications in different assays. Moreover, using the heuristic to generate training data automatically made it possible to obtain a high average precision model. Such in heterogeneous environments, there was a more pronounced decrease in the detection rate of objects; therefore, increasing the amount of data for training can improve the detection [47]. With the use of our heuristic, increasing the amount of data does not take much time from the user, but it could increase the time of computational training and

inference. Another alternative would be to increase the quality of the data with images annotated manually. One tool that can be used to label images manually is VGG Image Annotator (VIA) [48].

## 6. Conclusions

This study provides information about the development of e-applications of computer vision and the artificial intelligence-based software Ethoflow. This software is suitable for multivariate kinematic evaluations, behavioral assessments in heterogeneous environments, tracking individuals in groups maintaining their identities, and can be trained to learn complex behaviors. Ethoflow was applied to biological assessments and was efficient to detect significant differences between different bee species and pesticide stress. Some possibilities of data analysis and representation were demonstrated with Ethoflow's output. The deep learning models were implemented to expand the possibilities of animal behavior analyses to other fields, including the behavioral monitoring of domestic animals in precision livestock farming. According to demand, Ethoflow will be constantly updated for future improvements and new functions, such as tracking three dimensions. Therefore, Ethoflow is a helpful support tool for technical and scientific applications in biology and related fields.

## 7. Patents

This software is registered with the Brazilian National Institute of Intellectual Property (INPI, Ministério da Economia, Brazil, reg. no. BR 51 2020 000737-6).

**Supplementary Materials:** The following are available online at <https://www.mdpi.com/article/10.3390/s21093237/s1>, Figure S1 and Table S1.

**Author Contributions:** Conceptualization, R.C.B., G.F.M., R.N.C.G. and M.A.P.L.; methodology, R.C.B.; software, R.C.B.; validation, R.C.B.; formal analysis, R.C.B.; resources, G.F.M., R.N.C.G. and M.A.P.L.; data curation, R.C.B.; writing—original draft preparation, R.C.B., G.F.M., R.N.C.G. and M.A.P.L.; writing—review and editing, R.C.B., G.F.M., R.N.C.G., M.A.P.L. and C.B.d.S.; visualization, R.C.B.; funding acquisition, C.B.d.S. and G.F.M. All authors have read and agreed to the published version of the manuscript.

**Funding:** This research was funded by the São Paulo Research Foundation (FAPESP; Grant#2017/15220-7), the National Council of Scientific and Technological Development (CNPq; 142206/2017-2 and 301725/2019-5), and the Coordination for the Improvement of Higher Education Personnel (CAPES; Financial Code 001).

**Institutional Review Board Statement:** Not applicable.

**Informed Consent Statement:** Not applicable.

**Data Availability Statement:** Ethoflow-related files, including source code and video tutorials, are available at <https://sites.google.com/view/ethoflow> (accessed on 6 May 2021). The datasets generated for this study are available at <https://github.com/bernardesrodrigoc/Ethoflow> (accessed on 6 May 2021).

**Conflicts of Interest:** The authors declare no conflict of interest.

## Appendix A

The video is read by a thread that is independent of the processing thread, and the frames are stored in a stack (queue). This queue is a linear data structure that stores items in a “FIFO” (First In, First Out) manner (Figure A1). Frames are exchanged between the reading and processing threads. This increases the processing speed, as frames are always present in the queue and ready for processing, and no time is spent waiting for the next frame to be read.

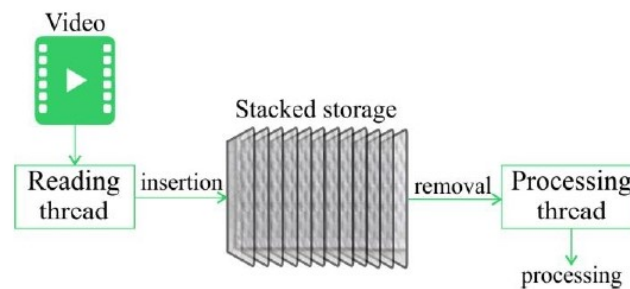


Figure A1. Representation of the processing steps in the multi-threading feature of Ethoflow.

## Appendix B

Different hyperparameters were tested to find a suitable convolutional neural network (CNN) model. This model was trained to recognize trophallaxis in the stingless bees, *Melipona quadrifasciata*, and can be used to recognize many binary behaviors. Using the validation accuracy of such a variable response, the interaction between the dropout and the activation function of the network output was evaluated (Figure A2A). Dropout is a regularization technique that randomly zeros out the input units of a layer, breaking fixed patterns to avoid overfitting [49]. Here, a better response was obtained, deactivating neurons with a probability of 0.2 (dropout = 0.2) (Figure A2A). The higher rates, despite reducing overfitting, decreased the accuracy. The activation function of the network output that presented the best response was the sigmoid function (Equation (A1)) (Figure A2A). This function binarizes the network output (0 or 1). As it involves a binary behavior classification, the sigmoid function is expected to generate better output.

$$\left\{ f(x) = \frac{1}{1 + e^{-x}}, \text{ where } x \text{ is the output from the previously hidden layer} \right\}. \quad (\text{A1})$$

The activation function of the inner layers and the optimization method were also evaluated. The best result was obtained with the exponential linear unit (Elu) function, along with mini-batch stochastic gradient descent (mini-batch SGD) as the optimizer (Figure A2B). The Elu function (Equation (A2)) is an identity function for positive values, and it tends smoothly to  $-\alpha$  for negative values. This function saturates for very small (extremely negative) values, resulting in the activation average being close to zero. Thus, ELUs tend to normalize the layer's output, accelerate learning, and increase accuracy [50].

$$f(x) = \begin{pmatrix} x, & \text{if } x > 0 \\ \alpha * (e^x - 1), & \text{if } x \leq 0 \end{pmatrix}. \quad (\text{A2})$$

In the mini-batch SGD, the term stochastic refers to a random sampling of batches in the data. Based on the loss value, the optimizer plays the role of updating the network's trainable parameters (weights). This is executed by calculating the loss gradient concerning the parameters (current weights) of the network. Mathematically, this process is performed by deriving the cost function and finding the gradient of the current weights. Then, the weights are updated in the gradient's opposite direction, reducing the loss slightly with each batch. Since the classification is binary (the output from the network is a probability), binary cross-entropy (Equation (A3)) was used as the cost function. Cross-entropy is a measure of the distance between the expected result  $y$  and the predictions  $p(y)$ .

$$H_p(q) = \frac{-1}{n} \sum_{i=1}^n y_i * \log(p(y_i)) + (1 - y_i) * \log(1 - p(y_i)), \quad (\text{A3})$$

where  $n$  is the number of network outputs.

As an increase in the learning rate tended to decrease the accuracy (Figure A2C), the lowest rate tested (0.0005) was maintained. The learning rate determines the magnitude of gradient descent. At high learning rates, network updates can result in great randomness.

The network interacts with the data in mini-batches, i.e., it does not process an entire dataset simultaneously; rather, the data is divided into small batches. Although this hyperparameter is important in CNN models [51], it does not play an important role in our model (Figure A2D). Therefore, one of the smallest values (batch size = 5) was selected to accelerate the network's training time.

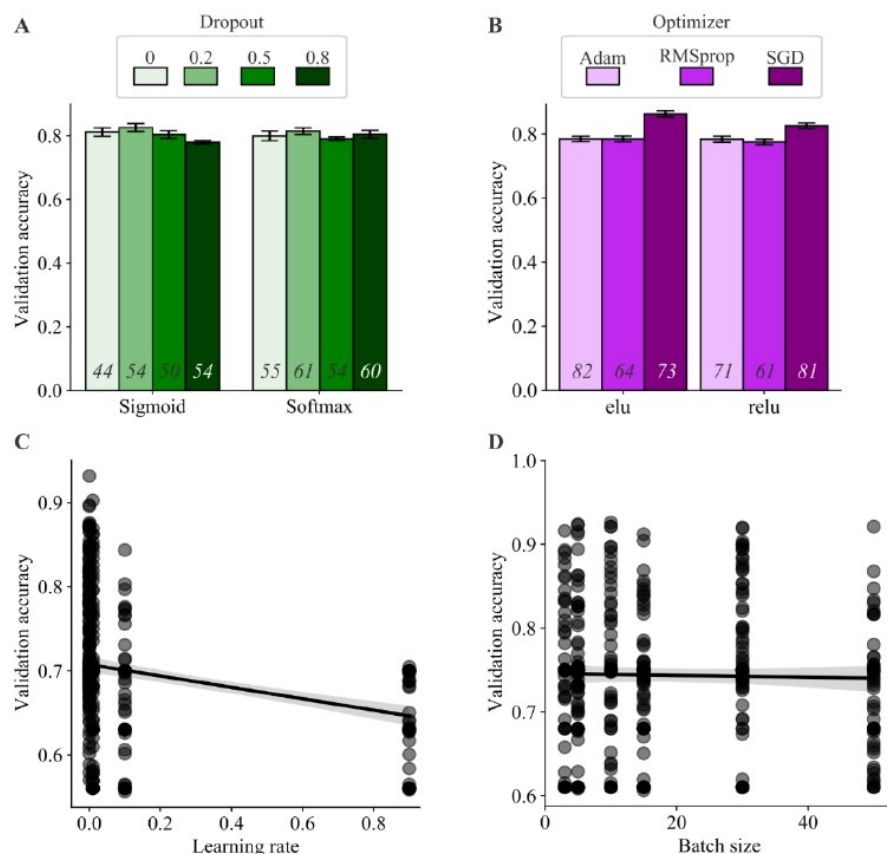


**Figure A2.** Hyperparameter optimization of the CNN model used in Ethoflow. (A) Compilation of the validation accuracy in response to the dropout and the activation function of the network output. (B) Validation accuracy in response to the optimizer and activation function of the inner layers. (A,B) The bars represent the mean  $\pm$  standard error. The values at the base of each bar represent the number of times a given configuration was tested. Scatterplot of the accuracy as a function of the (C) learning rate and (D) batch size. The translucent band around the line of regression represents the confidence interval ( $n = 432$ ).

In many statistical models, the normalization of variables is important (e.g., to avoid the predominance of some variables due to different scales). To this end, batch normalization layers were used in the CNN model. This layer can adaptively normalize the data as the mean and variance change during training [52].

Using the hyperparameters defined above, the network's size (number of layers) was also evaluated, and better accuracy was obtained with smaller architectures (Table A1). While more layers (a higher-dimensional representation space) allow the network to learn more complex representations, this increases the network's computational cost; accordingly, model L7 was employed.

**Table A1.** Different architectures tested to ascertain the ideal number of layers in the CNN model ( $n = 28$ ).

Validation Accuracy (Mean $\pm$ sd)	Number of Layers		Model
	Convolutional	Dense	
0.63 $\pm$ 0.028	5	4	L1
78 $\pm$ 0.036	5	3	L2
0.83 $\pm$ 0.042	5	2	L3
0.81 $\pm$ 0.063	4	4	L4
0.8 $\pm$ 0.121	4	2	L5
0.8 $\pm$ 0.020	3	4	L6
0.91 $\pm$ 0.031	3	3	L7

Data augmentation is a powerful technique for mitigating overfitting. Using the defined architecture (model L7 in Table A1), different data augmentation configurations were tested (Table A2). Excessive data augmentation reduces the accuracy, while sets with little augmentation increase overfitting. Thus, set 3 was deemed the best option to address the problem of overfitting.

**Table A2.** Sets tested for data augmentation. In all the tests, the horizontal flip and fill mode = the “nearest” was used. Model L7 in Table A1 was used for these tests.

Parameters	Set 1	Set 2	Set 3	Set 4
Rotation range	20	16	14	11
Width shift range	0.1	0.08	0.06	0.01
Height shift range	0.1	0.08	0.06	0.01
Shear range	0.05	0.02	0.01	0.008
Zoom range	0.1	0.08	0.06	0.01

## References

- Anderson, D.J.; Perona, P. Toward a Science of Computational Ethology. *Neuron* **2014**, *84*, 18–31. [\[CrossRef\]](#)
- Dell, A.I.; Bender, J.A.; Branson, K.; Couzin, I.D.; de Polavieja, G.G.; Noldus, L.P.J.J.; Pérez-Escudero, A.; Perona, P.; Straw, A.D.; Wikelski, M.; et al. Automated image-based tracking and its application in ecology. *Trends Ecol. Evol.* **2014**, *29*, 417–428. [\[CrossRef\]](#)
- Noldus, L.P.J.J.; Spink, A.J.; Tegelenbosch, R.A. Computerised video tracking, movement analysis and behaviour recognition in insects. *Comput. Electron. Agric.* **2002**, *35*, 201–227. [\[CrossRef\]](#)
- Valletta, J.J.; Torney, C.; Kings, M.; Thornton, A.; Madden, J. Applications of machine learning in animal behaviour studies. *Anim. Behav.* **2017**, *124*, 203–220. [\[CrossRef\]](#)
- Yilmaz, A.; Javed, O.; Shah, M. Object tracking: A survey. *ACM Comput. Surv.* **2006**, *38*. [\[CrossRef\]](#)
- Gandra, L.C.; Amaral, K.D.; Couceiro, J.C.; Della Lucia, T.M.; Guedes, R.N. Mechanism of leaf-cutting ant colony suppression by fipronil used in attractive toxic baits. *Pest Manag. Sci.* **2016**, *72*, 1475–1481. [\[CrossRef\]](#) [\[PubMed\]](#)
- Boff, S.; Friedel, A.; Mussury, R.M.; Lenis, P.R.; Raizer, J. Changes in social behavior are induced by pesticide ingestion in a Neotropical stingless bee. *Ecotoxicol. Environ. Saf.* **2018**, *164*, 548–553. [\[CrossRef\]](#) [\[PubMed\]](#)
- Zou, Z.; Shi, Z.; Guo, Y.; Ye, J. Object Detection in 20 Years: A Survey. *arXiv* **2019**, arXiv:1905.05055.
- He, K.; Gkioxari, G.; Dollár, P.; Girshick, R. Mask R-CNN. *IEEE Trans. Pattern Anal. Mach. Intell.* **2018**, *42*, 386–397. [\[CrossRef\]](#)
- Khan, A.; Sohail, A.; Zahoor, U.; Qureshi, A.S. A survey of the recent architectures of deep convolutional neural networks. *Artif. Intell. Rev.* **2020**, *53*, 5455–5516. [\[CrossRef\]](#)
- dos Santos Araújo, R.; Bernardes, R.C.; Martins, G.F. A mixture containing the herbicides Mesotrione and Atrazine imposes toxicological risks on workers of *Partamona helleri*. *Sci. Total Environ.* **2021**, *763*, 142980. [\[CrossRef\]](#) [\[PubMed\]](#)
- Viana, T.A.; Barbosa, W.F.; Botina, L.L.; Bernardes, R.C.; Soares, J.; Jacobs-Lorena, M.; Martins, G.F. A genetically modified anti-plasmodium bacterium is harmless to the stingless bee *Partamona helleri*. *Res. Sq.* **2021**. [\[CrossRef\]](#)
- Sridhar, V.H.; Roche, D.G.; Gingins, S. Tracktor: Image-based automated tracking of animal movement and behaviour. *Methods Ecol. Evol.* **2019**, *10*, 815–820. [\[CrossRef\]](#)
- Pérez-Escudero, A.; Vicente-Page, J.; Hinz, R.C.; Arganda, S.; De Polavieja, G.G. IdTracker: Tracking individuals in a group by automatic identification of unmarked animals. *Nat. Methods* **2014**, *11*, 743–748. [\[CrossRef\]](#)
- Rodríguez, A.; Zhang, H.; Klaminder, J.; Brodin, T.; Andersson, P.L.; Andersson, M. ToxTrac: A fast and robust software for tracking organisms. *Methods Ecol. Evol.* **2018**, *9*, 460–464. [\[CrossRef\]](#)

16. Mathis, M.W.; Mathis, A. Deep learning tools for the measurement of animal behavior in neuroscience. *Curr. Opin. Neurobiol.* **2020**, *60*, 1–11. [\[CrossRef\]](#)
17. Romero-Ferrero, F.; Bergomi, M.G.; Hinz, R.C.; Heras, F.J.H.; de Polavieja, G.G. idtracker.ai: Tracking all individuals in small or large collectives of unmarked animals. *Nat. Methods* **2019**, *16*, 179–182. [\[CrossRef\]](#)
18. Walter, T.; Couzin, I.D. TRex, a fast multi-animal tracking system with markerless identification, and 2D estimation of posture and visual fields. *Elife* **2021**, *10*, e64000. [\[CrossRef\]](#)
19. Mathis, A.; Mamidanna, P.; Cury, K.M.; Abe, T.; Murthy, V.N.; Mathis, M.W.; Bethge, M. DeepLabCut: Markerless pose estimation of user-defined body parts with deep learning. *Nat. Neurosci.* **2018**, *21*, 1281–1289. [\[CrossRef\]](#)
20. Pereira, T.D.; Aldarondo, D.E.; Willmore, L.; Kislin, M.; Wang, S.S.H.; Murthy, M.; Shaevitz, J.W. Fast animal pose estimation using deep neural networks. *Nat. Methods* **2019**, *16*, 117–125. [\[CrossRef\]](#)
21. Graving, J.M.; Chae, D.; Naik, H.; Li, L.; Koger, B.; Costelloe, B.R.; Couzin, I.D. DeepPoseKit, a software toolkit for fast and robust animal pose estimation using deep learning. *eLife* **2019**, *8*, e47994. [\[CrossRef\]](#) [\[PubMed\]](#)
22. Otsu, N. A threshold selection method from gray-level histograms. *IEEE Trans. Syst. Man. Cybern.* **1979**, *9*, 62–66. [\[CrossRef\]](#)
23. Fang, C.; Zhang, T.; Zheng, H.; Huang, J.; Cuan, K. Pose estimation and behavior classification of broiler chickens based on deep neural networks. *Comput. Electron. Agric.* **2021**, *180*, 105863. [\[CrossRef\]](#)
24. OpenCV–OpenCV. Available online: <https://opencv.org/> (accessed on 16 April 2021).
25. Abadi, M.; Agarwal, A.; Barham, P.; Brevdo, E.; Chen, Z.; Citro, C.; Corrado, G.S.; Davis, A.; Dean, J.; Devin, M.; et al. TensorFlow: Large-Scale Machine Learning on Heterogeneous Systems. *arXiv* **2015**, arXiv:1603.04467.
26. Virtanen, P.; Gommers, R.; Oliphant, T.E.; Haberland, M.; Reddy, T.; Cournapeau, D.; Burovski, E.; Peterson, P.; Weckesser, W.; Bright, J.; et al. SciPy 1.0: Fundamental Algorithms for Scientific Computing in Python. *Nat. Methods* **2020**, *17*, 261–272. [\[CrossRef\]](#)
27. Harris, C.R.; Millman, K.J.; van der Walt, S.J.; Gommers, R.; Virtanen, P.; Cournapeau, D.; Wieser, E.; Taylor, J.; Berg, S.; Smith, N.J.; et al. Array programming with NumPy. *Nature* **2020**, *585*, 357–362. [\[CrossRef\]](#)
28. Pandas Development Team. Pandas-Dev/Pandas: Pandas 2020. Available online: <https://zenodo.org/record/3715232#.YJTcRaERVPy> (accessed on 16 April 2021).
29. Pedregosa, F.; Varoquaux, G.; Gramfort, A.; Michel, V.; Thirion, B.; Grisel, O.; Blondel, M.; Prettenhofer, P.; Weiss, R.; Dubourg, V.; et al. Scikit-learn: Machine Learning in Python. *J. Mach. Learn. Res.* **2011**, *12*, 2825–2830.
30. He, K.; Zhang, X.; Ren, S.; Sun, J. Deep residual learning for image recognition. In Proceedings of the IEEE Computer Society Conference on Computer Vision and Pattern Recognition, IEEE Computer Society, Las Vegas, NV, USA, 27–30 June 2016; Volume 2016, pp. 770–778.
31. Abdulla, W. Mask R-CNN for Object Detection and Instance Segmentation on Keras and TensorFlow. 2017. Available online: [https://github.com/matterport/Mask\\_RCNN](https://github.com/matterport/Mask_RCNN) (accessed on 16 April 2021).
32. Arthur, D.; Vassilvitskii, S. *k-Means++: The Advantages of Careful Seeding*; Stanford University: Stanford, CA, USA, 2006.
33. Kuhn, H.W. The Hungarian method for the assignment problem. *Nav. Res. Logist. Q.* **1955**, *2*, 83–97. [\[CrossRef\]](#)
34. Newman, M.E.J. The structure and function of complex networks. *SIAM Rev.* **2003**, *45*, 167–256. [\[CrossRef\]](#)
35. Tunström, K.; Katz, Y.; Ioannou, C.C.; Huepe, C.; Lutz, M.J.; Couzin, I.D. Collective states, multistability and transitional behavior in schooling fish. *PLoS Comput. Biol.* **2013**, *9*, e1002915. [\[CrossRef\]](#)
36. Everingham, M.; Van Gool, L.; Williams, C.K.I.; Winn, J.; Zisserman, A. The pascal visual object classes (VOC) challenge. *Int. J. Comput. Vis.* **2010**, *88*, 303–338. [\[CrossRef\]](#)
37. Botina, L.L.; Bernardes, R.C.; Barbosa, W.F.; Lima, M.A.P.; Guedes, R.N.C.; Martins, G.F. Toxicological assessments of agrochemical effects on stingless bees (Apidae, Meliponini). *MethodsX* **2020**, 100906. [\[CrossRef\]](#)
38. Crawley, M.J. *The R book*, 2nd ed.; Wiley: Chichester, UK, 2012; ISBN 9780470973929.
39. MAPA Ministério da Agricultura, Pecuária e Abastecimento (MAPA). Available online: [http://agrofit.agricultura.gov.br/agrofit\\_cons/principal\\_agrofit\\_cons](http://agrofit.agricultura.gov.br/agrofit_cons/principal_agrofit_cons) (accessed on 24 November 2020).
40. Lima, M.A.P.; Martins, G.F.; Oliveira, E.E.; Guedes, R.N.C. Agrochemical-induced stress in stingless bees: Peculiarities, underlying basis, and challenges. *J. Comp. Physiol. A Neuroethol. Sens. Neural Behav. Physiol.* **2016**, *202*, 733–747. [\[CrossRef\]](#) [\[PubMed\]](#)
41. Turchen, L.; Cosme, L.; Guedes, R. Bidirectional selection of walking velocity, associated behavioral syndrome and reproductive output in the maize weevil *Sitophilus zeamais*. *J. Pest Sci.* **2018**, *91*, 1063–1071. [\[CrossRef\]](#)
42. Rodrigues, A.S.; Botina, L.; Nascimento, C.P.; Gontijo, L.M.; Torres, J.B.; Guedes, R.N.C. Ontogenic behavioral consistency, individual variation and fitness consequences among lady beetles. *Behav. Process.* **2016**, *131*, 32–39. [\[CrossRef\]](#)
43. Vélez, M.; Bernardes, R.C.; Barbosa, W.F.; Santos, J.C.; Guedes, R.N.C. Walking activity and dispersal on deltamethrin- and spinosad-treated grains by the maize weevil *Sitophilus Zeamais*. *Crop Prot.* **2019**, *118*, 50–56. [\[CrossRef\]](#)
44. Steinkraus, D.; Buck, I.; Simard, P.Y. Using GPUs for machine learning algorithms. In Proceedings of the Eighth International Conference on Document Analysis and Recognition (ICDAR'05), Seoul, Korea, 31 August–1 September 2005; Volume 2, pp. 1115–1120.
45. Pennekamp, F.; Schtickzelle, N.; Petchey, O.L. BEMOVI, software for extracting behavior and morphology from videos, illustrated with analyses of microbes. *Ecol. Evol.* **2015**, *5*, 2584–2595. [\[CrossRef\]](#)
46. Malakhov, A. Composable multi-threading for python libraries. In Proceedings of the 15th Python in Science Conference, Austin, TX, USA, 11–17 July 2016; pp. 15–19.

- 
47. Kavzoglu, T. Increasing the accuracy of neural network classification using refined training data. *Environ. Model. Softw.* **2009**, *24*, 850–858. [\[CrossRef\]](#)
  48. Dutta, A.; Zisserman, A. The VIA Annotation Software for Images, Audio and Video. In Proceedings of the 27th ACM International Conference on Multimedia, Nice, France, 21–25 October 2019; pp. 2276–2279. [\[CrossRef\]](#)
  49. Srivastava, N.; Hinton, G.; Krizhevsky, A.; Sutskever, I.; Salakhutdinov, R. Dropout: A simple way to prevent neural networks from overfitting. *J. Mach. Learn. Res.* **2014**, *15*, 1929–1958.
  50. Clevert, D.-A.; Unterthiner, T.; Hochreiter, S. Fast and accurate deep network learning by exponential linear units (ELUs). *arXiv* **2015**, arXiv:1511.07289.
  51. Radiuk, P.M. Impact of training set batch size on the performance of convolutional neural networks for diverse datasets. *Inf. Technol. Manag. Sci.* **2017**, *20*, 20–24. [\[CrossRef\]](#)
  52. Ioffe, S.; Szegedy, C. Batch normalization: Accelerating deep network training by reducing internal covariate shift. *arXiv* **2015**, arXiv:1502.03167.

## Patent



Assinado  
Digitalmente

REPÚBLICA FEDERATIVA DO BRASIL  
MINISTÉRIO DA ECONOMIA  
INSTITUTO NACIONAL DA PROPRIEDADE INDUSTRIAL  
DIRETORIA DE PATENTES, PROGRAMAS DE COMPUTADOR E TOPOGRAFIAS DE CIRCUITOS INTEGRADOS

## Certificado de Registro de Programa de Computador

Processo Nº: **BR512020000737-6**

O Instituto Nacional da Propriedade Industrial expede o presente certificado de registro de programa de computador, válido por 50 anos a partir de 1º de janeiro subsequente à data de 02/10/2019, em conformidade com o §2º, art. 2º da Lei 9.609, de 19 de Fevereiro de 1998.

**Título:** Ethoflow

**Data de criação:** 02/10/2019

**Titular(es):** UNIVERSIDADE FEDERAL DE VIÇOSA

**Autor(es):** RODRIGO CUPERTINO BERNARDES; GUSTAVO FERREIRA MARTINS; MARIA AUGUSTA LIMA SIQUEIRA; RAUL NARCISO CARVALHO GUEDES

**Linguagem:** PYTHON

**Campo de aplicação:** BL-01; EL-05

**Tipo de programa:** FA-01; TC-01; TC-04

**Algoritmo hash:** SHA-512

**Resumo digital hash:**

5c6e17cf1bc87fbfc65768b0ce23ef0ed889d65b76d6b866c3e9f20fcd4a4fb1aab499c581b3c35c8943fcf9ead924d2dc15d44156734316d798be933711d44

**Expedido em:** 28/04/2020

**Aprovado por:**

Helmar Alvares

Chefe da DIPTO - Portaria/INPI/DIRPA Nº 09, de 01 de julho de 2019

**CHAPTER 2. Machine learning algorithms and sublethal features applied to the  
toxicological assessment of agrochemicals in bees**

*Submitted to Journal of Hazardous Materials*

## Machine learning algorithms and sublethal features applied to the toxicological assessment of agrochemicals in bees

Rodrigo Cupertino Bernardes<sup>1\*</sup>; Lorena Lisbetd Botina<sup>2</sup>; Fernanda Pereira da Silva<sup>3</sup>; Kenner Morais Fernandes<sup>4</sup>; Maria Augusta Pereira Lima<sup>5</sup>; Gustavo Ferreira Martins<sup>6</sup>

<sup>1</sup>Departamento de Entomologia. Universidade Federal de Viçosa. Viçosa, Minas Gerais, Brazil. bernardesrodrigoc@gmail.com - <https://orcid.org/0000-0001-9481-036X>

<sup>2</sup>Departamento de Entomologia. Universidade Federal de Viçosa. Viçosa, Minas Gerais, Brazil.

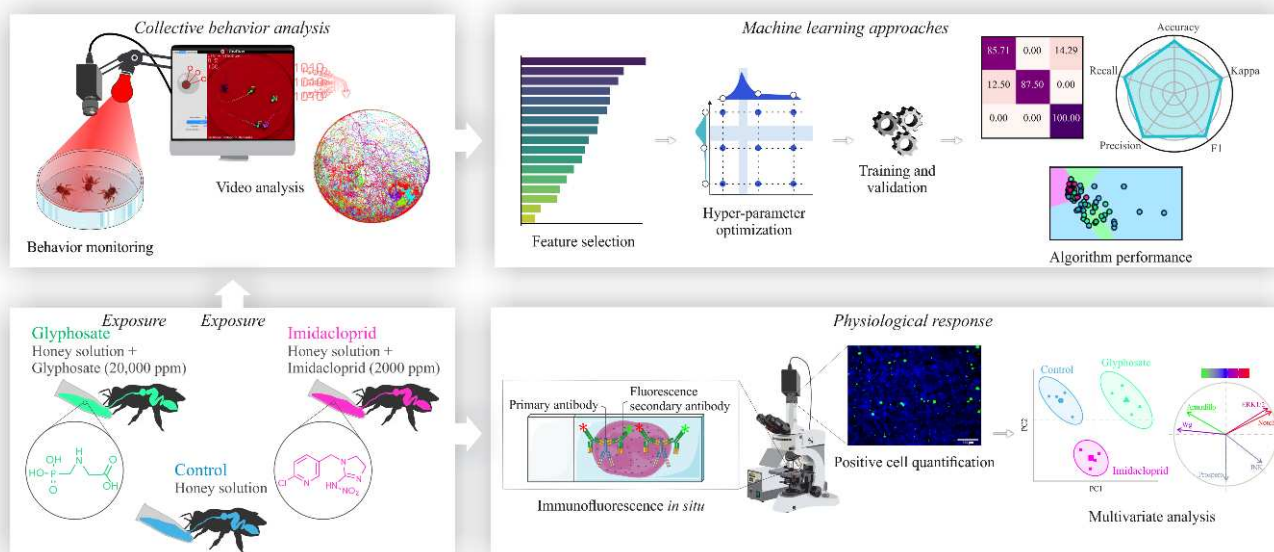
<sup>3</sup>Departamento de Agronomia; Universidade Federal do Espírito Santo. Alegre, Espírito Santo, Brazil.

<sup>4</sup>Departamento de Biologia Geral. Universidade Federal de Viçosa. Viçosa, Minas Gerais, Brazil.

<sup>5</sup>Departamento de Biologia Animal. Universidade Federal de Viçosa. Viçosa, Minas Gerais, Brazil.

<sup>6</sup>Departamento de Biologia Geral. Universidade Federal de Viçosa. Viçosa, Minas Gerais, Brazil.

### Graphical abstract



## Abstract<sup>1</sup>

Machine learning (ML) is a branch of artificial intelligence (AI) that enables the analysis of complex multivariate data. ML has significant potential in risk assessments of non-target insects for modeling the multiple factors affecting insect health, including the adverse effects of agrochemicals. Here, the potential of ML for risk assessments of glyphosate (herbicide; formulation) and imidacloprid (insecticide, neonicotinoid; formulation) on the stingless bee *Melipona quadrifasciata* was explored. The collective behavior of forager bees was analyzed after *in vitro* exposure to agrochemicals. ML algorithms were applied to identify the agrochemicals that the bees have been exposed to based on multivariate behavioral features. Changes in the *in situ* detection of different proteins in the midgut were also studied. Imidacloprid exposure leads to the greatest changes in behavior. The ML algorithms achieved a higher accuracy (up to 91%) in identifying agrochemical contamination. The two agrochemicals altered the detection of cells positive for different proteins, which can be detrimental to midgut physiology. This study provides a holistic assessment of the sublethal effects of glyphosate and imidacloprid on a key pollinator. The procedures used here can be applied in future studies to monitor and predict multiple environmental factors affecting insect health in the field.

**Keywords:** Artificial intelligence, Ecotoxicology, Modelling, Physiological response, Pollinators, Risk assessment

---

<sup>1</sup> List of abbreviations: ML, machine learning; AI, artificial intelligence; ERK1/2, extracellular signal-regulated kinase; JNK, c-Jun NH2-terminal kinase; MAPK, mitogen-activated protein kinase; cf, commercial formulation; GLM, generalized linear model; ANOVA, analysis of variance; RFE, recursive feature elimination; RF, random forest; LDA, linear discriminant analysis; QDA, quadratic discriminant analysis; KNN, k-nearest neighbors; NB, naive Bayes; SVM, support vector machine; GB, gradient boosting; MLP, multilayer perceptron; PCA, principal component analysis; PERMANOVA, permutational multivariate analysis of variance; AChE, acetylcholinesterase enzyme; ACh, acetylcholine.

## 1. Introduction

Artificial intelligence (AI) based approaches are used to find and predict answers from different unknowns in nature with high efficiency and precision in cause-effect relationships (Ghahramani, 2015). Machine learning (ML) is a branch of AI that learns complex structures (linear or non-linear) in multivariate data without the assumption of a statistical distribution (Crisci et al., 2012). Once trained, ML algorithms can accurately predict new independent datasets. AI-based tools also enable accurate automatic behavioral measurements in insects (Bernardes et al., 2021; Graving et al., 2019). Recent studies have shown the use of these tools for toxicological assessment in bees, such as the use of ML to characterize the foraging activity of bees in the field (Gomes et al., 2020) and to measure the effect of exposure to insecticides (neonicotinoids) on the behavior of honey bees within colonies (Siefert et al., 2020). Therefore, ML approaches can also be applied to predict exposure to different agrochemicals in bees through automatically measured behavioral features.

The risk assessment in bees has focused on the possible causes of their colony losses worldwide, which has been attributed to different factors, such as climate change, loss of habitat, pathogens, parasites, and agricultural practices with increased agrochemical usage (Cham et al., 2018; Freitas et al., 2009). The harmful effects of agrochemicals on bees include adverse sublethal impacts on behavior and gut physiology and morphology, such as damage to the midgut cells, which can impair the survival, nutrient absorption, and long-term success of bee colonies (Araújo et al., 2021; Farder-Gomes et al., 2021; Johnson, 2015; Lima et al., 2016; Sgolastra et al., 2019).

Oral exposure to agrochemicals can change the detection pattern of proteins related to cell signaling pathways in the midgut of the stingless bee *Partamona helleri* (Araújo et al., 2021; Farder-Gomes et al., 2021), including variations in extracellular signal-regulated kinase (ERK1/2) and c-Jun NH2-terminal kinase (JNK) proteins, which belong to the mitogen-activated protein kinase (MAPK) family. This protein family is involved in modulating proliferation, differentiation, and programmed cell death in response to a wide range of stimuli, including oxidative stress (Biteau and Jasper, 2011; Kockel et al., 2001; Simon et al., 2009). Similarly, the Notch protein with the homeodomain transcription factor Prospero and Wingless (Wg) protein and the crucial mediator Armadillo protein are involved in vital processes of proliferation, differentiation, and death in the insect midgut (Guruharsha et al., 2012; Liu et al.,

2010; Swarup and Verheyen, 2012; Tian et al., 2018). Nonetheless, these proteins related to cell signaling pathways have been poorly studied in bees.

Glyphosate is a systemic herbicide used to prevent weed growth (Brookes et al., 2017). This herbicide acts on the cycle of shikimic acid, inhibiting the biosynthesis of essential aromatic amino acids (e.g., tyrosine, phenylalanine, and tryptophan) for plant growth and microorganisms (Dill et al., 2010; Herrmann and Weaver, 1999; Maeda and Dudareva, 2012). Although this biochemical pathway is not found in animals, the detrimental effects of glyphosate on vertebrates and invertebrates, including bees, have already been reported (Battisti et al., 2021; Helmer et al., 2015; Luo et al., 2021; Straw et al., 2021; Tomé et al., 2020). The potentially harmful effects of glyphosate on honey bees include impaired foraging behavior and cognitive ability (Balbuena et al., 2015; Herbert et al., 2014; Luo et al., 2021).

Neonicotinoid imidacloprid, an agonist of nicotinic acetylcholine receptors (nAChR), is one of the most widely used agrochemicals for pest control in crops (Liu et al., 2006), and acts on the central nervous system of insects on cholinergic synaptic transmissions, causing alterations in sensory and motor systems (Matsuda et al., 2001). In addition to causing high mortality, bees treated with imidacloprid showed disturbances in behavior, development of mushroom bodies, and learning (Brito et al., 2020; Carrillo et al., 2013; Jacob et al., 2019; Tomé et al., 2012). In 2013, the European Commission adopted certain strategies to maintain healthy bee colonies and restrict the use of three neonicotinoids, including imidacloprid, in crops in open fields owing to high toxicity in bees according to the guidelines on a risk assessment of plant protection products on bees (EFSA, 2013).

Stingless bees (Hymenoptera, Apidae, Meliponini) are important pollinators and are more sensitive to agrochemical exposure than honey bees (Arena and Sgolastra, 2014; Cham et al., 2018; Tomé et al., 2017) owing to peculiar characteristics, such as small colony size, longer development time, and mass provisioning of the larval diet (Boyle et al., 2018; Lima et al., 2016). Among stingless bees, the genus *Melipona* stands out because it represents the largest group of eusocial bees, including many species of economic importance, which can compete with the exotic and Africanized honey bees for pollination sites (Pires et al., 2018; Ramírez et al., 2018; Slaa et al., 2006). Furthermore, in recent years, some species of *Melipona* have been endangered in Brazil, which has led to the creation of risk assessment programs by government agencies that help preserve these species owing to their important role in ecosystem services (ICMBio, 2018; Pires et al., 2018).

In this study, the potential of applying ML for agrochemical risk assessment was explored in stingless bees. ML algorithms have been proposed to predict agrochemical effects in bees based on multivariate behavioral features. Our study included the treatment of the stingless bee *Melipona quadrifasciata* to glyphosate (herbicide, formulation) and imidacloprid (insecticide, formulation) using an established protocol for the exposure of caged bees (Botina et al., 2020). The collective behavior of bees treated with these two agrochemicals using AI-based software for an automatic behavior analysis was assessed. Then, feature selection and optimization of the hyper-parameters were conducted to improve the predictive performance of several ML algorithms. In addition, different metrics associated with the predictive performance were evaluated, and the decision boundaries of the trained ML algorithms were checked. In addition, the physiological response to agrochemicals was evaluated through the *in situ* detection of different proteins that play a role in the immune response (i.e., ERK1/2 and JNK), and in the cell proliferation and differentiation (i.e., Nocht, Prospero, Wg, and Armadillo) in the midgut of bees. To the best of our knowledge, this is the first effort to predict the contamination of a stingless bee by agrochemicals using ML approaches based on multivariate behavioral features and an assessment of cellular protein responses related to gut physiology.

## 2. Materials and methods

### 2.1. Exposure bioassay

The herbicide glyphosate (commercial formulation (cf); Roundup Original DI<sup>®</sup>, Monsanto do Brasil Ltd., São José dos Campos, SP, Brazil) was used at the concentration of 20  $\mu\text{L}$  cf  $\text{mL}^{-1}$  (20,000 ppm), based on the recommendation applied for managing different weeds in crops (MAPA, 2021). The insecticide imidacloprid (cf; Evidence<sup>®</sup>, Bayer CropScience, São Paulo, SP, Brazil) was used at the concentration of 2  $\mu\text{g}$  cf  $\text{mL}^{-1}$  (2000 ppm). Because imidacloprid is highly toxic to bees, a concentration 300-times less than recommended for controlling the whitefly *Bemisia tabaci* (MAPA, 2021) was used, based on the sublethal concentration previously reported for *M. quadrifasciata* (Tomé et al., 2015b). The agrochemicals were diluted in a honey solution (50% distilled water, 50% honey) to prepare the contaminated diets (i.e., honey solution + agrochemical) at the concentrations mentioned above. An uncontaminated diet (i.e., a honey solution without agrochemicals) was offered to the control.

Foragers of *M. quadrifasciata* were collected from six unrelated colonies (SISBIO, ID 46746-1, Chico Mendes Institute for Biodiversity Conservation) and maintained at the Experimental Apiary at UFV (Minas Gerais, Brazil; 20° 45' S and 42° 52' W). The foragers were collected at the hive entrance using glass jars, transferred to plastic pots kept in an incubator, and fasted under conditions similar to those found in their colonies (28 °C and 80% relative humidity in total darkness) for 1 h before exposure (Botina et al., 2020). The bees were approximately 20–30 days old when workers conducted the foraging activities (Giannini, 1997; Kerr and dos Santos Neto, 1956). Bees from different colonies were not mixed, that is, bees from the same colony were kept in the same pot. The bees had access to contaminated diets for 3 h *ad libitum*. The exposure occurred orally through feeders (2 mL microcentrifuge tubes) inserted laterally in holes in the walls of the cages (500 mL plastic pots), where 13 bees were kept per cage. After the exposure period, the contaminated diets were replaced with feeders with a non-contaminated diet (i.e., honey in water). In the control group, the non-contaminated diet was replaced with a new diet (Botina et al., 2020). The mortality of the bees was checked 24 h after the exposure period, and bees were counted as dead if they were unable to move or stand upright. A total of 468 bees were exposed, considering all treatments (13 bees per cage × 2 cages × 3 treatments × 6 hives).

To assess the mortality, a generalized linear model (GLM) was fitted with a binomial error distribution, considering the treatment with agrochemicals as the explanatory variable and the proportion of bees that died as the response variable. The differences among levels of the explanatory variable (agrochemical treatments) were determined by gradual simplification of the GLM ( $p < 0.05$ ) (Crawley, 2012). These analyses were conducted in R software using the stats package (R Core Team, 2020).

## 2.2. Collective behavior analysis

The collective behavior of bees was assessed immediately after exposure (at 0 h) and 24 h after exposure. Different bees were used at 0 and 24 h after exposure to avoid temporal pseudo-replication and increase the robustness of the predictive capacity of the ML algorithms (Hendriksma et al., 2011). The bees were recorded within an arena (Petri dish, 15 cm diameter, 2 cm height) for 15 min with a digital video camera (HDR-XR520V, Sony Corporation) at 30 fps and high definition (pixel resolution of  $1920 \times 1080$ ). A microcentrifuge tube cap with honey solution was added to each arena to feed the bees during the recording period.. The

recordings were conducted in a room at  $25 \pm 3$  °C and  $70 \pm 5\%$  relative humidity with three red LED lights (6 W) placed 50 cm above the arena to avoid phototactic influence on behavior monitoring. A group of six bees from the same hive was filmed in each arena. The average response of the group was considered a replicate to avoid pseudo-replication owing to the non-independence of errors among individuals from the same hive (Hendriksma et al., 2011). A total of 72 replicates ( $2 \text{ arenas} \times 6 \text{ hives} \times 3 \text{ treatments} \times 2 \text{ times}$ ), totaling 432 sampled bees ( $6 \text{ bees} \times 72 \text{ replicates}$ ) were considered.

The videos were analyzed using Ethoflow<sup>®</sup> software, an AI-based software for automatic behavior analysis (Bernardes et al., 2021) (Supplementary videos). With this tool, the multivariate behavioral data containing the following 17 features were extracted: tracked distance (centimeter), max speed (centimeter per second), turn angle (degree, the average angle that the individual rotated in each video frame), meandering (degree, the average angle that the individual rotated during the video), number of stops, number of mean movements (count associated with intermediated activity), number of fast movements, resting, mean movement (proportion of time the insects stayed during intermediated activity, tracked distance of  $> 0.046$  and  $\leq 0.53 \text{ cm frame}^{-1}$ ), fast movement, degree (all interactions of an individual with others of the group), network density (the proportion of interaction in the insect group), feeding, polarization (the proportion of individuals aligned in a group), milling (the proportion of individuals in rotation about the center of mass), swarm (the proportion of individuals having disordered movements), and transition (the proportion of individuals not among the states of polarization, milling, or swarming). A detailed description of these features is provided in Appendix A.

Behavioral features were extracted as difference of the mean of each feature separately divided by the standard deviation to obtain a standard range (a distribution with mean = 0 and standard deviation = 1) to avoid the effect of a scale that may generate predominance of a specific feature (Singh and Singh, 2020). Behavioral data were univariately analyzed through an analysis of variance (ANOVA) and a Tukey *post hoc* test for multiple comparisons among agrochemical treatments using R software with the stats package (R Core Team, 2020).

## 2.3. Machine learning (ML) approaches

### 2.3.1. Feature selection

A recursive feature elimination (RFE) was applied to select a subset of the most relevant behavioral features. During this procedure, an ML algorithm starts with all dataset features to calculate the importance of each feature. The least important features were then pruned from the current dataset. This step is recursively repeated until the desired number of features to be selected is reached (Guyon et al., 2002). RFE was used along with ML algorithms, i.e., random forest (RF), support vector machine (SVM) with a linear kernel, and a linear discriminant analysis (LDA). The most relevant features were ranked and selected based on the average accuracy obtained from the three algorithms with a three-fold cross-validation.

### 2.3.2. Hyper-parameter optimization

Hyperparameters are not directly learned by the model and must be configured in some ML algorithms (Bergstra and Bengio, 2012). Therefore, to find a set of hyper-parameters that improve the performance of the algorithms, hyperparameter optimization was conducted through a grid search. This procedure consists of an exhaustive search over a specified hyperparameter space to evaluate the performance of the ML algorithms (Bergstra and Bengio, 2012). Thus, we set up the RF, quadratic discriminant analysis (QDA), LDA, k-nearest neighbors (KNN), Gaussian naive Bayes (NB), support vector machine (SVM), gradient boosting (GB), and multilayer perceptron (MLP) algorithms repeatedly three times and used a three-fold cross-validation with data randomization for each algorithm.

### 2.3.2. Algorithm performance

To train the ML algorithms defined after hyper-parameter optimization (RF, QDA, LDA, KNN, NB, SVM, GB, and MLP), we used 70% of the dataset with the most relevant features selected (Section 2.3.1). The predictive performance of the trained algorithms was then evaluated with the other 30% of the dataset for an independent validation. Thus, confusion matrices were constructed to calculate the predictive performance metrics, that is, the accuracy, kappa, weighted precision, weighted recall, and F1 score, according to the following formulas:

$$\text{accuracy} = \frac{\sum_{i=1}^k x_{ii}}{N}, \quad (1)$$

$$\text{kappa} = \frac{N * \sum_{i=1}^k x_{ii} - \sum_{i=1}^k x_{i\oplus} * x_{\oplus i}}{N^2 - \sum_{i=1}^k x_{i\oplus} * x_{\oplus i}}, \quad (2)$$

$$\text{precision} = \sum_{i=1}^k \left( \frac{1}{N_i} \right) \left( \frac{x_{ii}}{x_{i\oplus}} \right), \quad (3)$$

$$\text{recall} = \sum_{i=1}^k \left( \frac{1}{N_i} \right) \left( \frac{x_{ii}}{x_{\oplus i}} \right), \quad (4)$$

$$\text{F1} = \frac{2(\text{precision} * \text{recall})}{\text{precision} + \text{recall}}, \quad (5)$$

where  $k$  is the number of classes,  $x_{ii}$  indicates the observations classified within the correct population (diagonal of the confusion matrix),  $N$  is the sample size,  $N_i$  is the sample size of the given class  $i$ ,  $x_{i\oplus}$  is the marginal total of the confusion matrix line  $i$ , and  $x_{\oplus i}$  is the marginal total of the confusion matrix column  $i$ .

Based on the values of kappa ( $K$ ) and kappa variance ( $\sigma_k^2$ ), z-tests were carried out to indicate whether the prediction was different from random ( $Z_a$ ) and for a statistical comparison between the ML algorithms ( $Z_b$ ) at a significance level of 5%.

$$Z_a = \frac{K}{\sqrt{\sigma_k^2}}, \quad (6)$$

$$Z_b = \frac{\hat{K}_a - \hat{K}_b}{\sqrt{\sigma_{\hat{K}_a}^2 + \sigma_{\hat{K}_b}^2}}, \quad (7)$$

where  $a$  and  $b$  are the ML algorithms under analysis.

Principal component analysis (PCA) was carried out to reduce the data to two dimensions (PC1 and PC2) and examine the decision boundaries of the trained ML algorithms in terms of the PCA scores. Python language (version 3.6.8) was used in the analyses and development of the ML approaches, including Numpy (Harris et al., 2020), Pandas (McKinney,

2010), and SciKit-learn (Pedregosa et al., 2011). All analyses were carried out on a machine with the following features: Intel i7-9750H CPU @ 2.60 GHz  $\times$  12, 8 GB RAM, and an NVIDIA® GeForce® GTX 1660 (6 GB) Ti Max-Q GPU.

## 2.4. Physiological bioassay

The physiological responses to agrochemical exposures were assessed using immunofluorescence to detect proteins (*in situ*) related to proliferation, differentiation, and death in the midgut. After 24 h of exposure to agrochemicals, the bees were dissected in a saline solution (0.1 M NaCl, 20 mM KH<sub>2</sub>PO<sub>4</sub>, and 20 mM Na<sub>2</sub>HPO<sub>4</sub>). The guts were transferred to Zamboni's fixative (2% paraformaldehyde containing 15% picric acid in a 0.1 M sodium phosphate buffer) for 1 h at  $\pm$  25°C. Then, the guts were washed three times with sterile phosphate-buffered saline (PBS; 0.1M, pH 7.2) and incubated at 0.1 M PBS/1% Triton X-100 (PBST) for 2 h, followed by incubation for 24 h at 4°C in the following primary antibodies: rabbit anti-ERK1/2, rabbit anti-Notch (Cell Signaling Technology, Inc., Beverly, MA, USA), mouse anti-JNK, mouse anti-Prospero, and mouse anti-Wg and mouse anti-Armadillo (Developmental Studies Hybridoma Bank, Iowa City, IA, USA). After incubation, the samples were washed three times (10 min each) with PBS and incubated with FITC-conjugated secondary antibodies (anti-rabbit; green fluorescence) or TRITC-conjugated secondary antibody (anti-mouse; red fluorescence) (Sigma-Aldrich Corp., St Louis, MO, USA) (1:500). The cell nuclei were stained with diamidino-2-phenylindole (DAPI; Biotium, Inc., Hayward, CA, USA) for 30 min, washed in PBS, and mounted on slides with coverslips in a 30% sucrose solution. The slides were analyzed and photographed under a fluorescence microscope (Evos M5000; Thermo Fisher Scientific, Carlsbad, CA, USA). The number of labeled cells in five guts per treatment was quantified using a 20 $\times$  objective lens. Five guts from each treatment group were prepared without incubation with primary antibodies as negative controls. Because the midgut is a large organ, cell counts were conducted separately, considering the anterior, middle, and posterior regions of the organ. The total number of cells per organ was determined by summing the number of cells detected in each of the three regions. Cell quantification was conducted using Image-Pro 4.5 software (Media Cybernetics, Silver Spring, EUA).

Data from protein detection were subjected to PCA. Because the data were at the same scale, the eigenvalues and eigenvectors in the PCA were defined using the covariance matrix. The principal components were selected based on eigenvalues higher than the mean values of

all eigenvalues. The significance of the groups formed by the PCA was tested using a permutational multivariate analysis of variance (PERMANOVA) with 9999 permutations and the Euclidean distance. A homogeneity test of multivariate dispersion (PERMDISP) was used to check the assumption of the homogeneity of the PERMANOVA (Anderson, 2017). Pairwise contrasts among agrochemical treatments were applied with a Bonferroni adjustment. These analyses were conducted in R software (R Core Team, 2020) using the factextra (Kassambara and Mundt, 2020) and vegan (Oksanen et al., 2019) packages.

### 3. Results

#### 3.1. Mortality

Oral exposure of foragers to imidacloprid caused significant mortality in comparison to foragers exposed to glyphosate and a control ( $\chi^2 = 18.2$ ,  $df = 13$ ,  $p < 0.0001$ ). However, the mortality caused by the ingestion of glyphosate was not different from that of the control group ( $\chi^2 = 1.4$ ,  $df = 11$ ,  $p = 0.24$ ) (Figure 1).

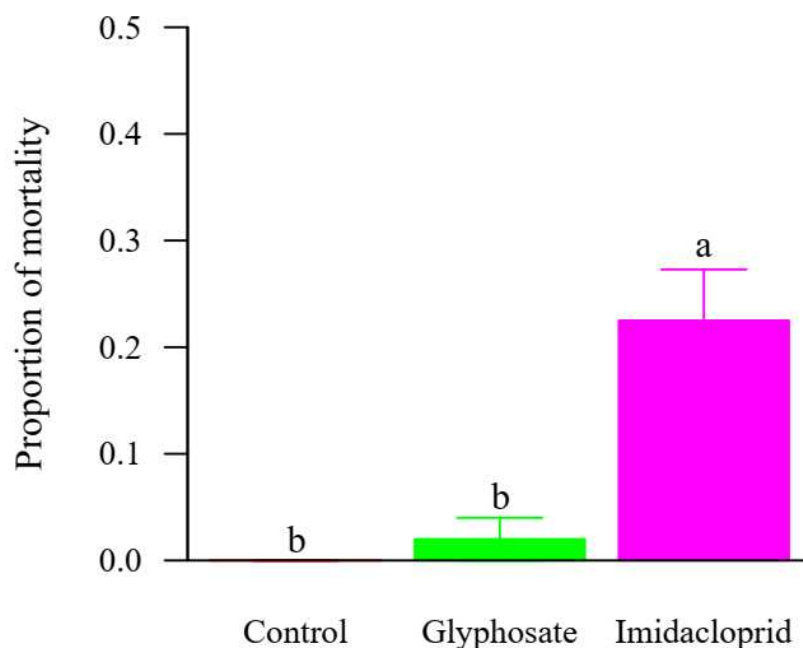


**Figure 1.** Mortality of the stingless bee *Melipona quadrifasciata* 24 h after exposure to glyphosate and imidacloprid agrochemicals. Different letters indicate statistically significant differences in GLM ( $p < 0.05$ ). The bars represent the means, and vertical bars are the standard errors.

#### 3.2. Collective behavior

There was a significant difference among agrochemicals in all behavioral features exhibited by the foragers ( $p < 0.05$ , Figure 2). Imidacloprid-exposed bees were more debilitated (shortest tracked distance and more significant resting), more disoriented (more significant swarm and transition), and fed more than the control (Supplementary video S1). Glyphosate-exposed bees and the control showed a similar pattern for most features, except that these bees interacted more with each other after glyphosate exposure (Supplementary videos S2 and S3).

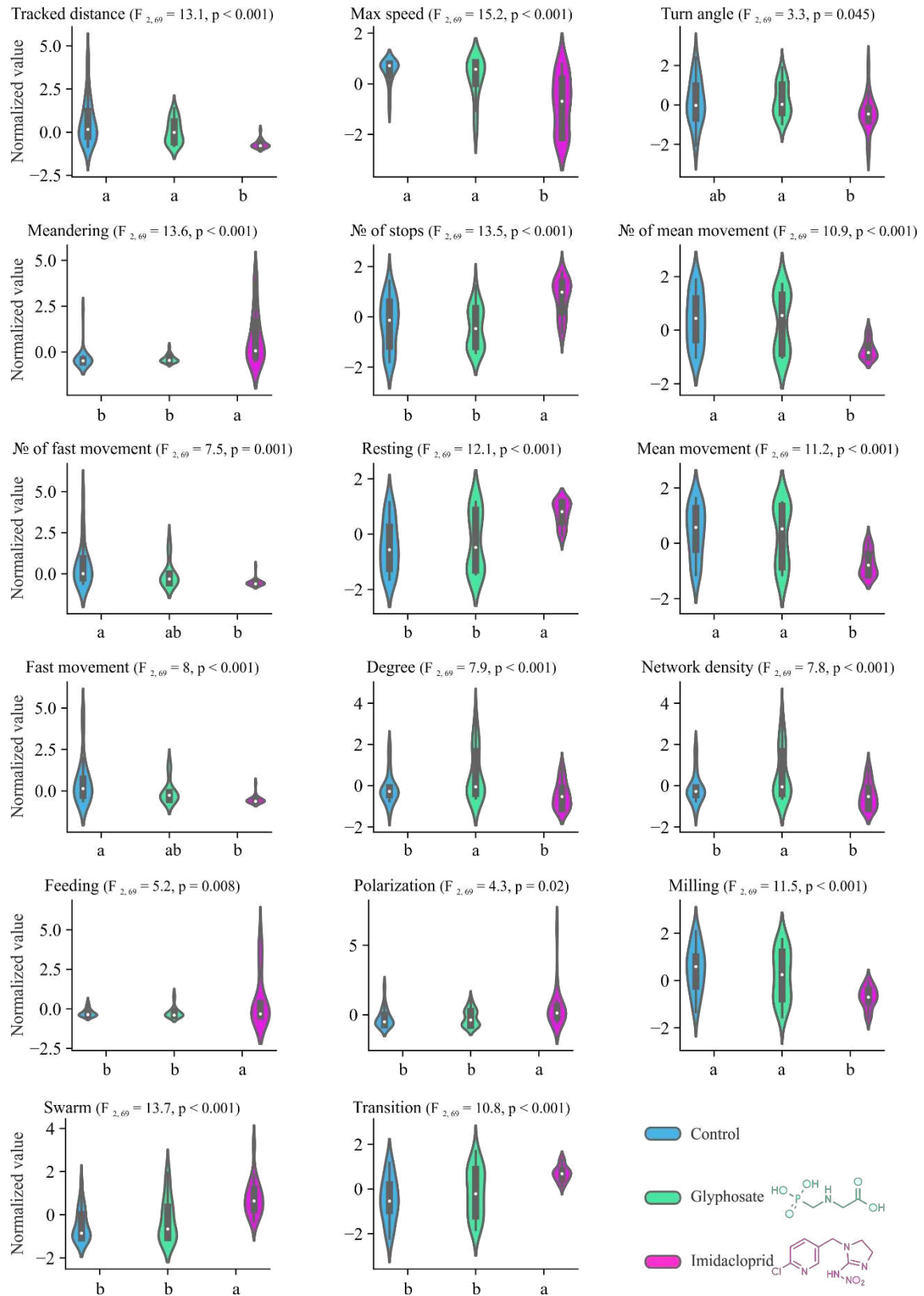


**Figure 2.** Boxplots with violin distribution of the multivariate behavioral data assessed in foragers of *Melipona quadrifasciata* exposed to glyphosate or imidacloprid. Each feature was scaled to the standard range (mean = 0 and standard deviation = 1), subtracting the mean and

dividing by the standard deviation. Different letters on the x-axis indicate a significant difference based on a Tukey test ( $p < 0.05$ ); in addition, the statistic output for each feature is given.

### **3.3. Machine learning approaches**

#### **3.3.1. Feature selection**

The most parsimonious ML algorithms used in feature selection were prioritized to choose the number of relevant features. Thus, the smallest number of variables in which a given algorithm reached the highest precision was selected. With the RF, 17 features were selected, followed by LDA with 10 features, and SVM with 5 features (Figure 3A). Therefore, following the ranking of importance, the five most relevant features were the tracked distance, number of stops, transition, meandering, and degree (Figure 3B).

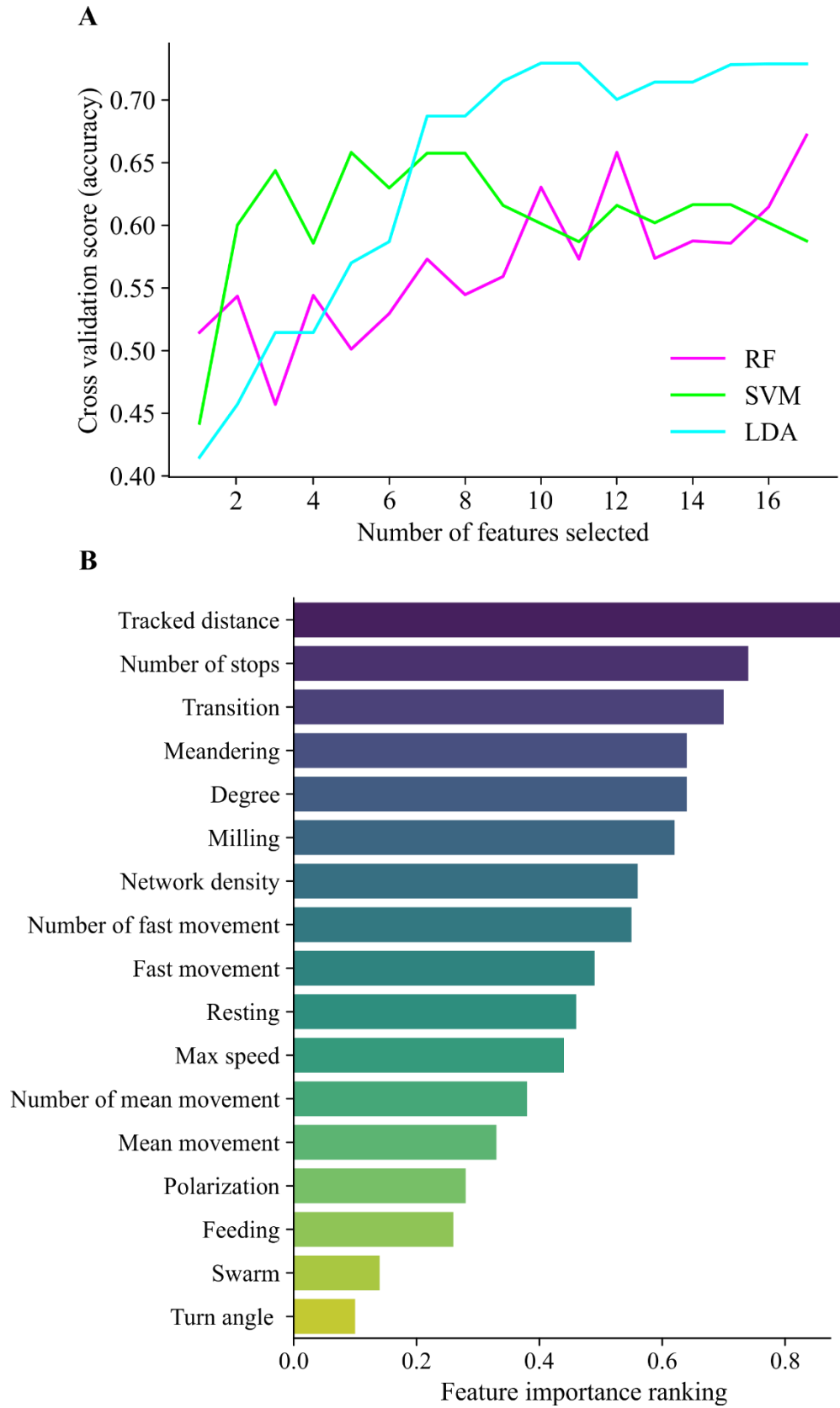


**Figure 3.** Selection of the most relevant behavioral features exhibited by foragers of *Melipona quadrifasciata* exposed to glyphosate or imidacloprid. **(A)** Establishment of the number of

features and **(B)** feature importance ranking with recursive feature elimination. The ML algorithms providing information about the feature importance are random forest (RF), support vector machine (SVM), and linear discriminant analysis (LDA). **(A)** Lines represent the average of a 3-fold cross-validation. **(B)** Bars represent the average ranking among the three ML algorithms.

### 3.3.2. Hyper-parameter optimization

After the hyper-parameter optimization, the models were trained using the parameters listed in Table 1. Because the algorithms QDA and NB have essentially only one hyper-parameter for tuning, the default in the SciKit-learn library was used (Pedregosa et al., 2011). All grid search interactions are shown in Supplementary Table 1.

Table 1. Hyper-parameters use in the machine learning algorithms after hyper-parameter optimization through a grid search. The definition of hyper-parameters and values was based on the SciKit-learn library (Pedregosa et al., 2011)

Algorithms	Hyper-parameters	Values
Random forest	trees	50
	max features	sqrt
Quadratic discriminant analysis	reg	0
Linear discriminant analysis	shrinkage	auto
	solver	lsqr (least squares)
K-nearest neighbors	metric	Euclidean
	neighbors	3
	weight function	distance
Gaussian naive bayes	variance smoothing	$1 \times 10^{-9}$
	regularization	10
Support vector machine	kernel	polynomial
	gamma	scale

Gradient boosting	learning rate	0.1
	max depth	9
	boosting stages	1000
	subsample	0.7
Multi-layer Perceptron	activation function	relu
	network layer sizes	100
	solver	adam

### 3.3.3. Algorithm performance

The algorithms were extremely efficient in discriminating the imidacloprid class with 100% true positives in all confusion matrices (Figure 4). Although the algorithms somewhat confused the glyphosate class with the control class, the MLP algorithm efficiently separated these two classes with 87.5% and 85.7% true positives for glyphosate and control, respectively (Figure 4). Interestingly, the QDA algorithm had high precision with 100% true positives for imidacloprid or control classes (Figure 4).

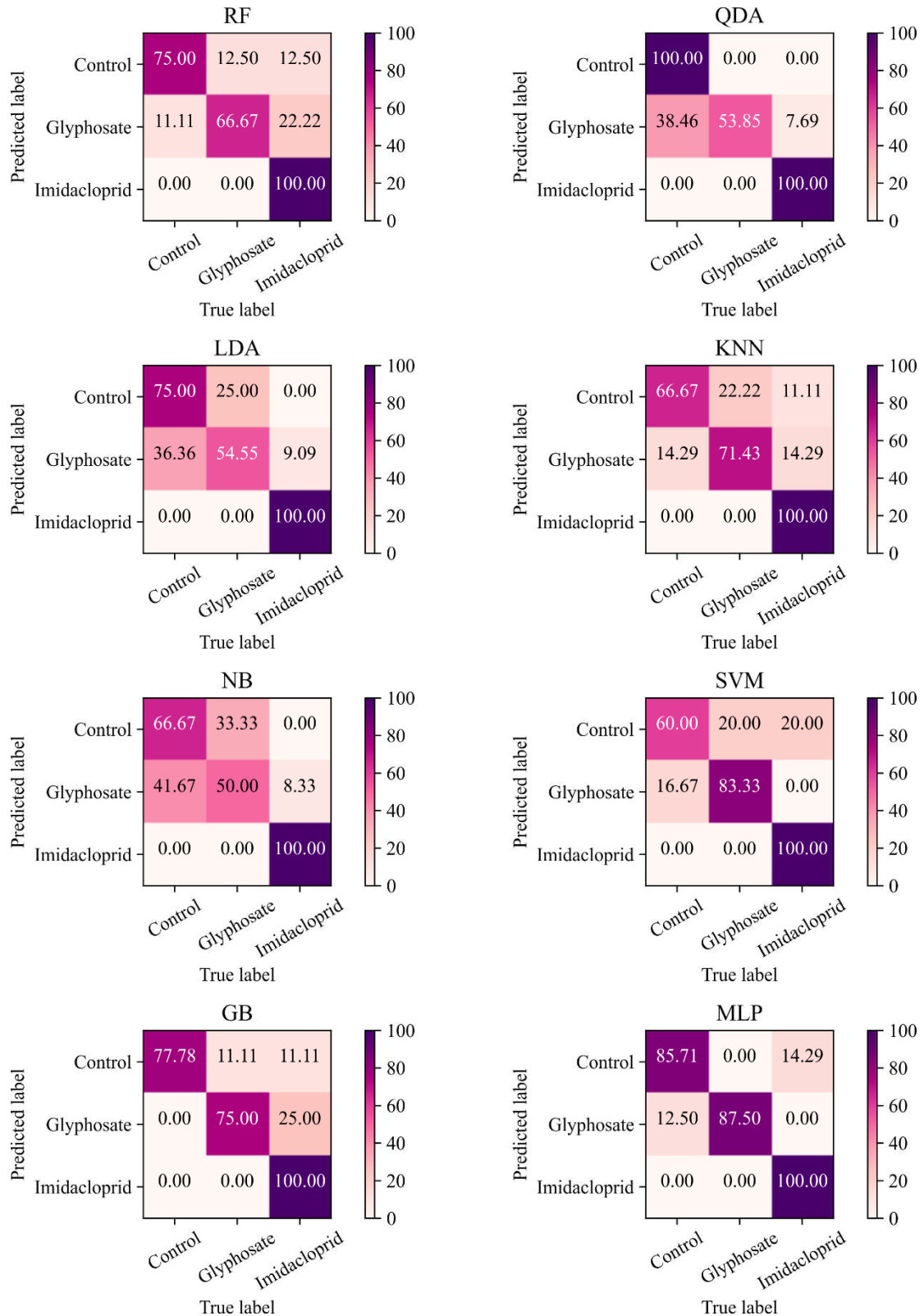


**Figure 4.** Confusion matrices of machine learning algorithms for predicting the agrochemical contamination (glyphosate or imidacloprid) in foragers of *Melipona quadrifasciata* based on behavioral features. The applied algorithms were a random forest (RF), quadratic discriminant

analysis (QDA), linear discriminant analysis (LDA), k-nearest neighbors (KNN), Gaussian naive Bayes (NB), support vector machine (SVM), gradient boosting (GB), and multi-layer perceptron (MLP). The confusion matrices reveal the number of correct and incorrect predictions for each class in percentage.

The ML algorithms were statistically significant in predicting the class of agrochemicals in which bees were contaminated ( $p < 0.001$ ; Figure 5). The algorithms exhibited accuracies between 67% and 91% (Figure 5). The MLP algorithm showed significant differences in QDA ( $Z = 1.972$ ,  $p = 0.048$ ), LDA ( $Z = 1.961$ ,  $p = 0.049$ ), and NB ( $Z = 2.064$ ,  $p = 0.039$ ). The MLP presented the best performance, reaching a kappa value of 0.86 and accuracy of 91% (Figure 5).

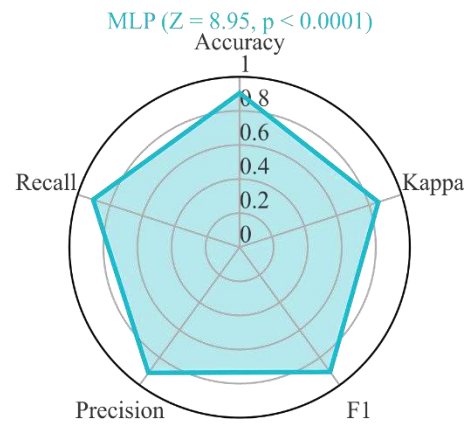
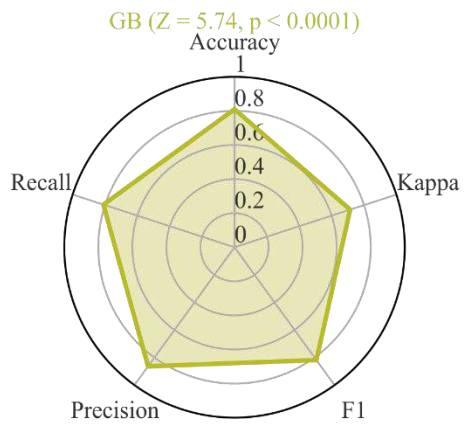
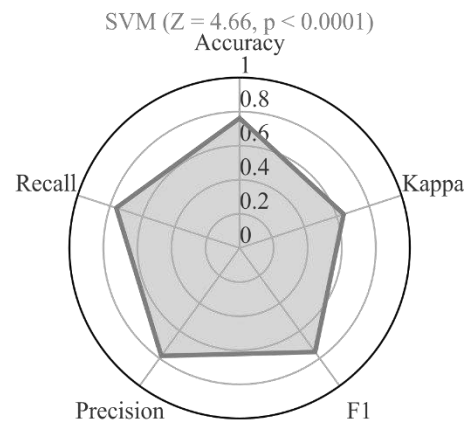
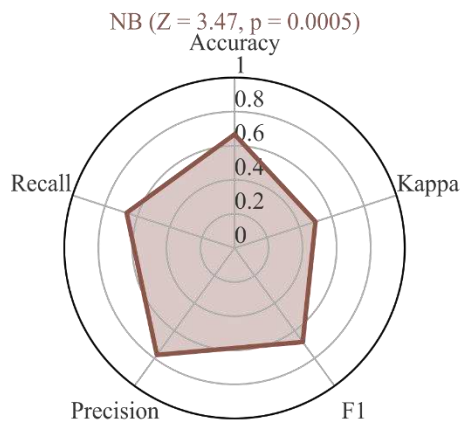
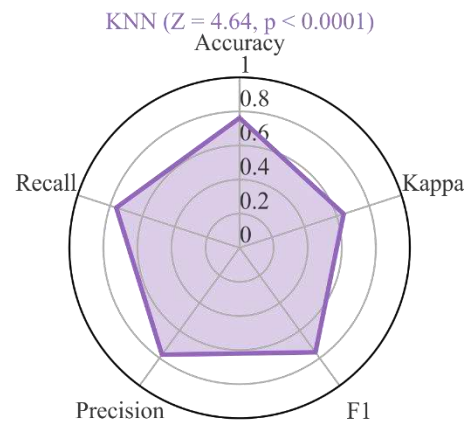
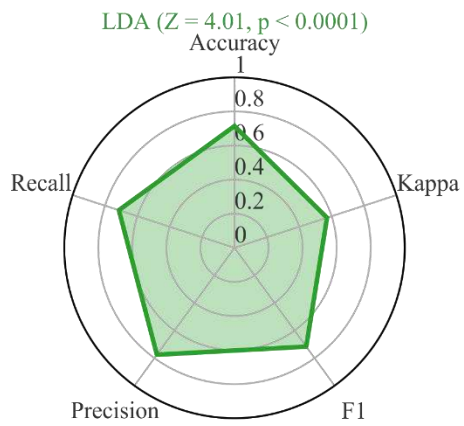
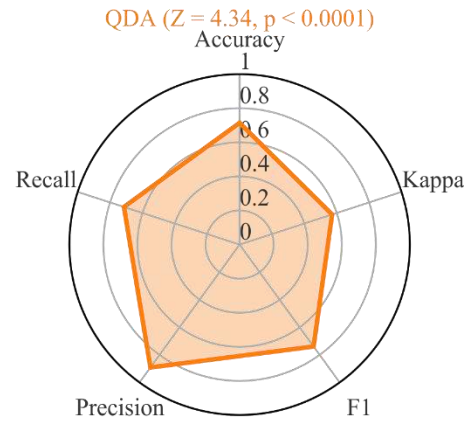
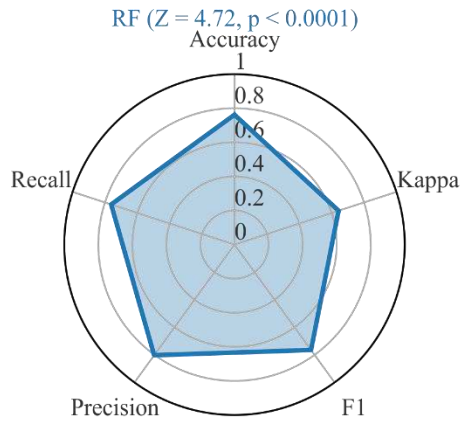


**Figure 5.** Validation of performance metrics (accuracy, kappa, precision, recall, and F1 score) of machine learning algorithms: random forest (RF), quadratic discriminant analysis (QDA), linear discriminant analysis (LDA), k-nearest neighbors (KNN), Gaussian naive Bayes (NB), support vector machine (SVM), gradient boosting (GB), and multi-layer perceptron (MLP). These algorithms were tested to predict the type of contamination (with glyphosate or imidacloprid) in foragers of *Melipona quadrifasciata* based on behavioral features. The z-test values are provided for each algorithm.

With the data containing the selected behavioral features, the PCA and the first two principal components explained 82% of the variation. The distinct separation between the glyphosate and control groups was not evident in the PCA scores (Figure 6). However, the algorithms that defined the decision boundaries among the classes well were mainly nonlinear algorithms (e.g., MLP, GB, and SVM).

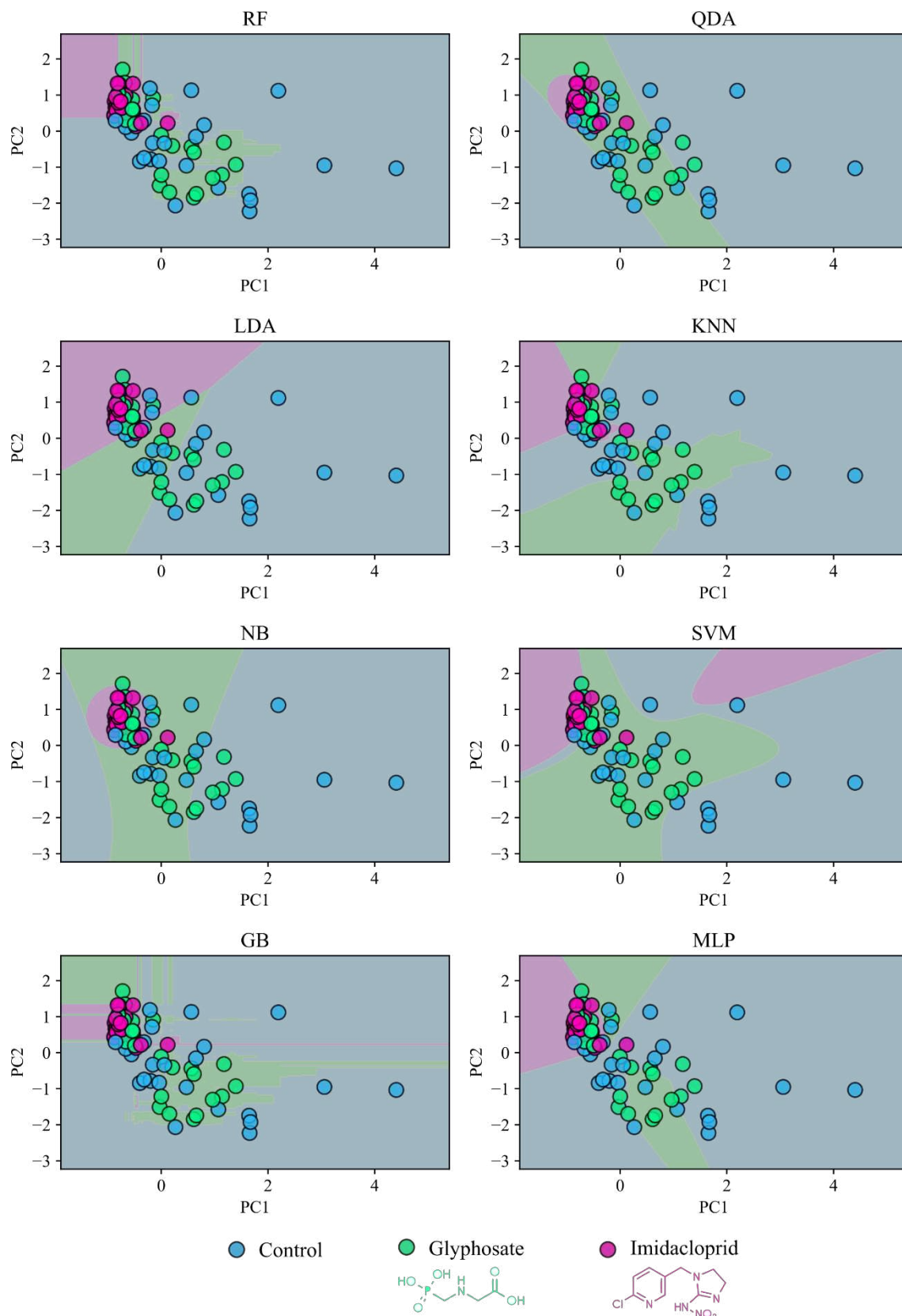


**Figure 6.** Decision boundaries of the machine learning algorithms in the principal component analysis (PCA) scores. The PCA was applied to the data with the selected behavioral features

of foragers of *Melipona quadrifasciata*, and the principal components (PC1 and PC2) explained 54% and 28% of the total data variation, respectively. The applied algorithms were random forest (RF), quadratic discriminant analysis (QDA), linear discriminant analysis (LDA), k-nearest neighbors (KNN), Gaussian naive Bayes (NB), support vector machine (SVM), gradient boosting (GB), and multi-layer perceptron (MLP).

### 3.4. Physiological response

The number of positive cells for different proteins in the midgut of forager *M. quadrifasciata* (mean  $\pm$  standard error) after 24 h of exposure to glyphosate were as follows:  $11.6 \pm 0.6$  (Armadillo),  $148 \pm 0.15$  (ERK1/2),  $31.8 \pm 1.30$  (JNK),  $224 \pm 1.7$  (Notch), and  $109 \pm 0.6$  (Prospero), and  $4 \pm 0.52$  (Wg). In addition, the numbers of positive cells for each protein after 24 h of exposure to imidacloprid were  $9.6 \pm 0.74$  (Armadillo),  $55.6 \pm 1.1$  (ERK1/2),  $37.4 \pm 1.18$  (JNK),  $38.8 \pm 0.61$  (Notch),  $164 \pm 1.06$  (Prospero), and  $9.8 \pm 0.4$  (Wg). Finally, the numbers of positive cells for each protein in the control were  $54.4 \pm 1.72$  (Armadillo),  $60.2 \pm 0.8$  (ERK1/2),  $3.2 \pm 0.12$  (JNK),  $32.8 \pm 0.91$  (Notch),  $94.2 \pm 1.02$  (Prospero), and  $17.4 \pm 0.31$  (Wg) (Figures 7 and 8).

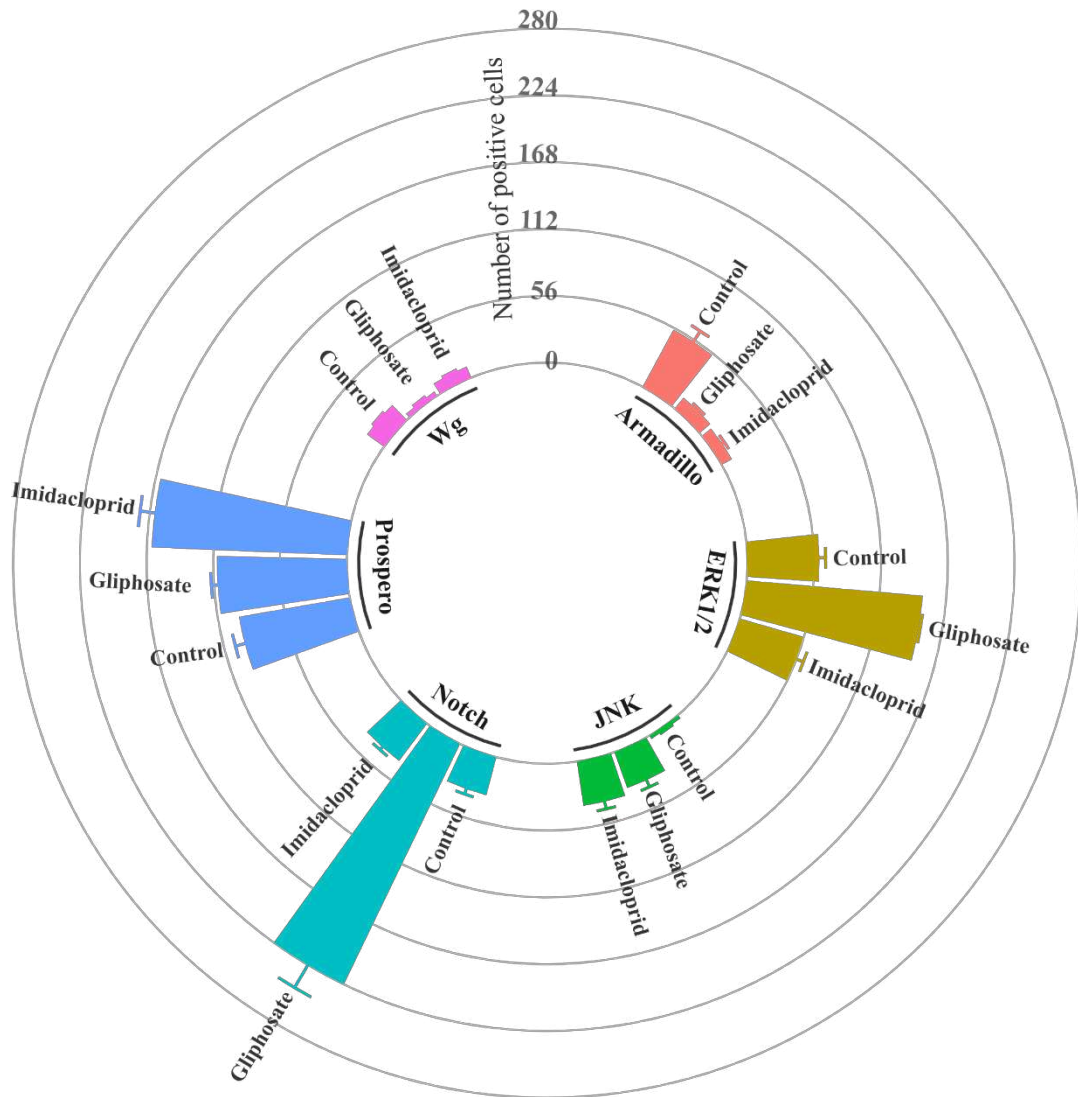
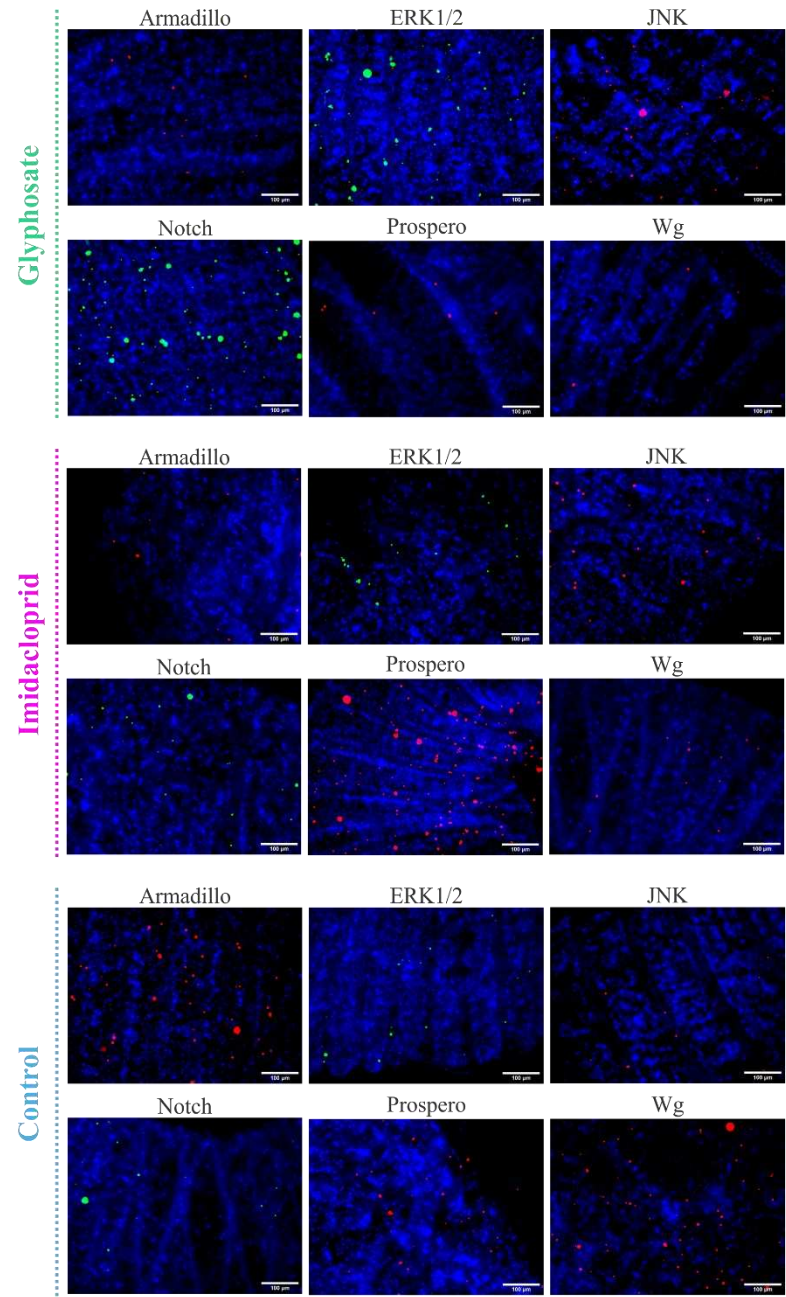


**Figure 7.** Number of positive cells for different proteins (Armado, ERK1/2, JNK, Notch, Prospero, and Wg) in the midgut of foragers of *Melipona quadrifasciata* 24 h after the treatment with glyphosate or imidacloprid, and the control. The axis numbers (from 0 to 280) indicate the number of positive cells. The bars are mean  $\pm$  standard error.

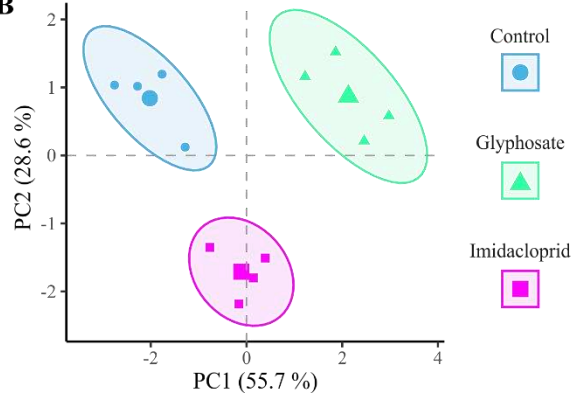
The assumption of homogeneity among samples within each treatment was accepted (homogeneous dispersion) (PERMIDISP:  $F_{2, 12} = 0.39$ ,  $p = 0.69$ ), indicating the suitability of PERMANOVA. There was a significant difference in protein detection patterns among treatments with agrochemicals ( $F_{2, 12} = 44.9$ ,  $p < 0.0001$ ,  $R^2 = 0.88$ , Figure 8B). Both glyphosate treatment ( $F = 55.26$ ,  $p = 0.015$ ,  $R^2 = 0.87$ ) and imidacloprid treatment ( $F = 12.13$ ,  $p = 0.039$ ,  $R^2 = 0.6$ ) were different from those of the control. Likewise, glyphosate treatment and imidacloprid treatment were different from each other ( $F = 56.04$ ,  $p = 0.021$ ,  $R^2 = 0.87$ ). An

ordination diagram of the PCA shows the relationship among treatments (Figure 8B) and the different proteins sampled through *in situ* detection (Figure 8C). Two proteins with eigenvalues of greater than the mean were selected. Thus, PC1 (first component of PCA) and PC2 (the second component of PCA) explained 55.7% and 28.6% of the total variance of the data, respectively.

A



B



C

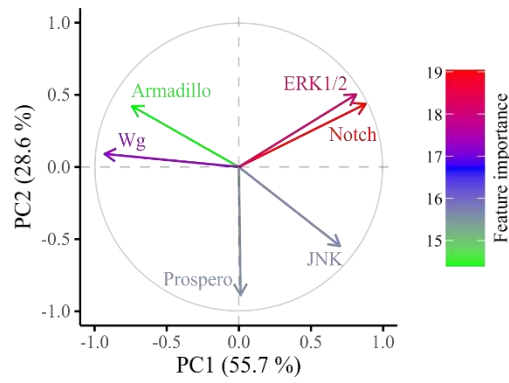


**Figure 8.** Detection (*in situ*) of positive cells for different proteins in the midgut of foragers of *Melipona quadrifasciata* 24 h after the treatment with glyphosate or imidacloprid, and the control. **(A)** Representative whole mounts of the midgut with positive cells (green or red) for Armadillo, ERK1/2, JNK, Notch, Prospero, and Wg. DNA (blue) was stained with DAPI. Scale bars: 100  $\mu$ m. **(B)** The principal component analysis (PCA) diagram shows the three treatments in two-dimensions based on Euclidean distance. Confidence ellipses are based on treatment centroids (95%). **(C)** PC loadings associated with the detection of positive cells for different proteins. Axis values (%) indicate how much the components explain the total data variance.

#### 4. Discussion

According to our results, acute oral exposure to glyphosate did not lead to lethal toxicity in *M. quadrifasciata* when tested at the recommended label concentrations for weed control (MAPA, 2021), which corresponds to a higher concentration compared to the residues found in the field from this agrochemical (Berg et al., 2018). Low mortality rates have also been reported for honeybees exposed to glyphosate either by contact or orally for both label-recommended concentrations and field-realistic concentrations (Abraham et al., 2018; Battisti et al., 2021; Faita et al., 2020; Helmer et al., 2015; Tomé et al., 2020). Moreover, contact exposure to glyphosate (only active ingredient) did not increase the mortality in adult bumblebees; however, glyphosate formulations containing surfactants can contribute to increase the mortality (Straw et al., 2021). The ingestion of glyphosate during post-embryonic development significantly increases the mortality of immature *M. quadrifasciata* (Seide et al., 2018). Thus, the lethal toxicity of glyphosate depends on the route, age, formulation composition, and time of exposure to the agrochemical (Battisti et al., 2021; Straw et al., 2021). In contrast to glyphosate, imidacloprid ingestion exhibited greater lethal toxicity to *M. quadrifasciata* even at a highly diluted concentration (300-times less concentrated than the field concentration). This insecticide has been reported to be highly toxic to bees (Blacqui re et al., 2012; EFSA, 2013; Pereira et al., 2020). Studies have confirmed the high mortality rate when stingless bees are exposed to this insecticide both in immature bees (Tom  et al., 2012) and adults (Costa et al., 2015; Tom  et al., 2015a; Valdovinos-N  n ez et al., 2009). In contrast to our results in adults, glyphosate ingestion is more lethal to larvae of *M. quadrifasciata* than imidacloprid (Seide et al., 2018).

Changes in locomotor behavior after exposure to agrochemicals are commonly used to indicate sublethal effects in bees (Desneux et al., 2007; Thompson and Maus, 2007). Imidacloprid led to the greatest changes in locomotor behavior features, unlike glyphosate exposure, which only increased the interaction among individuals of *M. quadrifasciata*. These findings may be related to the different modes of action of each agrochemical, whereby glyphosate acts on the shikimate pathway, found only in plants and microorganisms, and is absent in animals (Dill et al., 2010; Herrmann and Weaver, 1999). Despite the lack of evidence that glyphosate has a target site to act on insects, chronic exposure of honeybees to low-concentration glyphosate decreased the acetylcholinesterase enzyme (AChE) activity (Boily et al., 2013), which can modulate nerve impulses, and consequently, alter locomotor behavior. In addition, the sublethal effects of this herbicide in bees include impaired learning, disordered foraging behavior, and retrieval of memories (Farina et al., 2019; Luo et al., 2021; Vázquez et al., 2020).

Similar to our results, oral exposure to imidacloprid impaired the locomotor behavior of foragers of stingless bees and honeybees (Delkash-Roudsari et al., 2020; Jacob et al., 2019). Imidacloprid mimics acetylcholine (ACh) action binding on the postsynaptic neuron nAChR in insects. AChE cannot break down the imidacloprid, leading to an overstimulation and blocking of the nAChR, causing paralysis and death, and consequently affecting behavioral patterns (Buckingham et al., 1997; Tomizawa and Casida, 2005). In addition, imidacloprid maintains a sustained activation of the Kenyon cell nAChR in the mushroom bodies in bees, causing morphological changes in these structures and compromising the learning and sensory integration (Palmer et al., 2013; Tomé et al., 2012). Such changes in the behavior of foragers exposed to agrochemicals can compromise essential pollination activities in both natural and agricultural ecosystems (Ramírez et al., 2018; Schneider et al., 2012).

The ML algorithms used here to discriminate the sublethal effects of each agrochemical on the behavior of bees demonstrated high precision regardless of the different modes of action of glyphosate (herbicide) and imidacloprid (insecticide). The most divergent pattern among the behavioral features demonstrated by imidacloprid was 100% detected in all ML algorithms. Interestingly, the ML algorithms reached 87.5% of true positives for the glyphosate class despite the similarity of the behavioral features between the glyphosate and control. Our results also emphasize that combining AI-based approaches with multivariate assessment can detect patterns of sublethal alterations that are not found in univariate behavioral assessments.

In general, the effects of agrochemicals on the behavior of bees have been evaluated in a univariate manner (Barbosa et al., 2015; Botina et al., 2019; Tomé et al., 2015b). The availability of automated behavioral tools has facilitated multivariate behavioral measurements (Bernardes et al., 2021), whereas some irrelevant or less important features can negatively impact the performance of ML algorithms (Blum and Langley, 1997), and the assessment of highly correlated behavioral features produces multicollinearity (Yoo et al., 2014). When dealing with multivariate data, an important step is feature selection to optimize the ML performance (Blum and Langley, 1997). Among the 17 features studied here in *M. quadrifasciata*, the models achieved a better performance with the tracked distance, number of stops, transition, meandering, and degree. These five most relevant features are computed with a low computational demand from the Cartesian coordinates of the collective locomotory movement of insects (Bernardes et al., 2021). Therefore, these features can include important endpoints to predict the environmental factors influencing bee health, using features from radio-frequency identification tags, as an example (Nunes-Silva et al., 2020).

The ML algorithms had satisfactory kappa values, indicating appropriate ( $0.61 < \text{kappa} < 0.8$ ) and highly suitable ( $\text{kappa} > 0.81$ ) predictive performance (McHugh, 2012). As exhibited in the decision boundaries, the non-linear classifiers better fit the separation among treatments, highlighting the better performance of MLP and GB. However, GB has over-adjusted boundaries of the data, which may affect the ability to generalize to new datasets (Srivastava et al., 2014). MLP is an artificial neural network architecture that deals very well with nonlinear and complex data modeling (Rossi and Conan-Guez, 2005). The algorithm used here achieved a higher accuracy (91%) in the validation dataset, demonstrating a groundbreaking result in predicting agrochemical contamination in bees based on behavioral features.

Microscopy analyses revealed the sublethal effects of the two agrochemicals on the bee gut. The increase in Notch and ERK1/2, detected after glyphosate exposure, suggests that this compound causes injuries and cell death in the midgut of *M. quadrifasciata*, despite the absence of lethal effects. These proteins are related to cell proliferation, and their production might compensate for cell death in exposed foragers (Biteau and Jasper, 2011; Liu et al., 2010; Simon et al., 2009). The ingestion of glyphosate or imidacloprid also increased the number of positive midgut cells for JNK (9.5-times and 11.5-times, respectively), while decreasing the number of positive cells for Wg (−4-times for glyphosate and −1.8-times for imidacloprid) and Armadillo (−4.9-times to glyphosate and −5.6-times to imidacloprid) in comparison to the control. Based

on these results, it can be speculated that the ingestion of glyphosate or imidacloprid interferes with the integrity of the midgut epithelium because a decrease in Wg proteins activates the apoptotic pathway mediated by the JNK pathway in *Drosophila melanogaster* (Kockel et al., 2001; Tian et al., 2018). Ingestion of imidacloprid increased the number of positive cells for Prospero (1.5-times both the control and glyphosate exposure). Prospero, similar to Notch, is associated with cell renewal (Simon et al., 2009). Altogether, these changes in the detection of proteins in the midgut of *M. quadrifasciata* may be related to the stress caused by the ingestion of agrochemicals, and while some cells die, others proliferate to maintain the midgut homeostasis. The variation in the protein detection pattern in the midgut of adult bees after agrochemical contamination has already been reported elsewhere (Araújo et al., 2021; Farder-Gomes et al., 2021), and changes in the biochemical cascades caused by different agrochemicals deserve to be investigated in detail as sublethal effects in the future.

## 5. Conclusions

This study provides a holistic assessment of the sublethal effects of both glyphosate and imidacloprid on the foragers of *M. quadrifasciata*. Our pioneering study successfully integrated multivariate behavioral features with ML algorithms to predict agrochemical contamination in bees. ML built using a multivariate behavior dataset achieved a higher accuracy for classifying agrochemical contamination in foragers using the MLP algorithm. A multivariate assessment also revealed changes in protein detection in the midgut after exposure to glyphosate or imidacloprid. Ingestion of imidacloprid caused significant changes in behavior and protein detection in the midgut of bees, and the discrimination of bees exposed to this insecticide using ML was highly precise. Changes in protein detection in the midgut of glyphosate-exposed foragers have not implied changes in survival or in the majority of the behavior features studied, and despite this, it is worth mentioning that the ML model was able to classify bees contaminated with glyphosate. The method proposed herein can be widely applied to other insects, indicating further field applications of ML for predicting the environmental factors influencing their behavior and health.

## Acknowledgments

This research was supported by Conselho Nacional de Desenvolvimento Científico e Tecnológico (CNPq, 142206/2017-2), Coordenação de Aperfeiçoamento de Pessoal de Nível Superior, Brasil (CAPES, Finance Code 001), and Fundação de Amparo à Pesquisa do Estado de Minas Gerais (FAPEMIG, CBB-APQ-00247-14).

## 6. References

- Abraham, J., Benhotons, G.S., Krampah, I., Tagba, J., Amissah, C., Abraham, J.D., 2018. Commercially formulated glyphosate can kill non-target pollinator bees under laboratory conditions. *Entomol. Exp. Appl.* 166, 695–702. <https://doi.org/10.1111/eea.12694>
- Anderson, M.J., 2017. Permutational multivariate analysis of variance (PERMANOVA), in: Wiley StatsRef: Statistics Reference Online. American Cancer Society, pp. 1–15. <https://doi.org/https://doi.org/10.1002/9781118445112.stat07841>
- Araújo, R. dos S., Bernardes, R.C., Martins, G.F., 2021. A mixture containing the herbicides Mesotrione and Atrazine imposes toxicological risks on workers of *Partamona helleri*. *Sci. Total Environ.* 763, 142980. <https://doi.org/10.1016/j.scitotenv.2020.142980>
- Arena, M., Sgolastra, F., 2014. A meta-analysis comparing the sensitivity of bees to pesticides. *Ecotoxicology* 23, 324–334. <https://doi.org/10.1007/s10646-014-1190-1>
- Balbuena, M.S., Tison, L., Hahn, M.L.M.-L., Greggers, U., Menzel, R., Farina, W.M., 2015. Effects of sublethal doses of glyphosate on honey bee navigation. *J. Exp. Biol.* 218, 2799–2805. <https://doi.org/10.1242/jeb.117291>
- Barbosa, W.F., Tomé, H.V.V., Bernardes, R.C., Siqueira, M.A.L., Smagghe, G., Guedes, R.N.C., 2015. Biopesticide-induced behavioral and morphological alterations in the stingless bee *Melipona quadrifasciata*. *Environ. Toxicol. Chem.* 34, 2149–2158. <https://doi.org/10.1002/etc.3053>
- Battisti, L., Potrich, M., Sampaio, A.R., de Castilhos Ghisi, N., Costa-Maia, F.M., Abati, R., dos Reis Martinez, C.B., Sofia, S.H., 2021. Is glyphosate toxic to bees? A meta-analytical review. *Sci. Total Environ.* 767, 145397. <https://doi.org/10.1016/j.scitotenv.2021.145397>
- Berg, C.J., King, H.P., Delenstarr, G., Kumar, R., Rubio, F., Glaze, T., 2018. Glyphosate residue concentrations in honey attributed through geospatial analysis to proximity of large-scale agriculture and transfer off-site by bees. *PLoS One* 13, 1–18. <https://doi.org/10.1371/journal.pone.0198876>
- Bergstra, J., Bengio, Y., 2012. Random search for hyper-parameter optimization. *J. Mach.*

- Learn. Res. 13, 281–305.
- Bernardes, R.C., Lima, M.A.P., Guedes, R.N.C., da Silva, C.B., Martins, G.F., 2021. Ethoflow: computer vision and artificial intelligence-based software for automatic behavior analysis. *Sensors* 21. <https://doi.org/10.3390/s21093237>
- Biteau, B., Jasper, H., 2011. EGF signaling regulates the proliferation of intestinal stem cells in *Drosophila*. *Development* 138, 1045–1055. <https://doi.org/10.1242/dev.056671>
- Blacqui re, T., Smagghe, G., van Gestel, C.A.M., Mommaerts, V., 2012. Neonicotinoids in bees: a review on concentrations, side-effects and risk assessment. *Ecotoxicology* 21, 973–992. <https://doi.org/10.1007/s10646-012-0863-x>
- Blum, A.L., Langley, P., 1997. Selection of relevant features and examples in machine learning. *Artif. Intell.* 97, 245–271. [https://doi.org/10.1016/s0004-3702\(97\)00063-5](https://doi.org/10.1016/s0004-3702(97)00063-5)
- Boily, M., Sarrasin, B., DeBlois, C., Aras, P., Chagnon, M., 2013. Acetylcholinesterase in honey bees (*Apis mellifera*) exposed to neonicotinoids, atrazine and glyphosate: Laboratory and field experiments. *Environ. Sci. Pollut. Res.* 20, 5603–5614. <https://doi.org/10.1007/s11356-013-1568-2>
- Botina, L.L., Bernardes, R.C., Barbosa, W.F., Lima, M.A.P., Guedes, R.N.C., Martins, G.F., 2020. Toxicological assessments of agrochemical effects on stingless bees (Apidae, Meliponini). *MethodsX* 7, 100906. <https://doi.org/10.1016/j.mex.2020.100906>
- Botina, L.L., V lez, M., Barbosa, W.F., Mendon a, A.C., Pylro, V.S., T tola, M.R., Martins, G.F., 2019. Behavior and gut bacteria of *Partamona helleri* under sublethal exposure to a bioinsecticide and a leaf fertilizer. *Chemosphere* 234. <https://doi.org/10.1016/j.chemosphere.2019.06.048>
- Boyle, N.K., Pitts-Singer, T.L., Abbott, J., Alix, A., Cox-Foster, D.L., Hinarejos, S., Lehmann, D.M., Morandin, L., O'Neill, B., Raine, N.E., Singh, R., Thompson, H.M., Williams, N.M., Steeger, T., 2018. Workshop on pesticide exposure assessment paradigm for non-*Apis* bees: foundation and summaries. *Environ. Entomol.* 48, 4–11. <https://doi.org/10.1093/ee/nvy103>
- Brito, P., Elias, M., Silva-Neto, C., Sujii, E., Silva, D., Gon alves, B., Franceschinelli, E., 2020. The effects of field-realistic doses of imidacloprid on *Melipona quadrifasciata* (Apidae: Meliponini) workers. *Environ. Sci. Pollut. Res.* 27, 38654–38661. <https://doi.org/10.1007/s11356-020-08530-9>
- Brookes, G., Taheripour, F., Tyner, W.E., 2017. The contribution of glyphosate to agriculture

- and potential impact of restrictions on use at the global level. *GM Crops Food* 8, 216–228. <https://doi.org/10.1080/21645698.2017.1390637>
- Buckingham, S., Lapied, B., Corronc, H., Sattelle, F., 1997. Imidacloprid actions on insect neuronal acetylcholine receptors. *J. Exp. Biol.* 200, 2685–2692. <https://doi.org/10.1242/jeb.200.21.2685>
- Carrillo, M.P., Bovi, T. de S., Negrão, A.F., Orsi, R. de O., 2013. Influência dos agroquímicos fipronil e imidaclopride no aprendizado de abelhas *Apis mellifera* L. *Acta Sci. - Anim. Sci.* 35, 431–434. <https://doi.org/10.4025/actascianimsci.v35i4.18683>
- Cham, K.O., Nocelli, R.C.F., Borges, L.O., Viana-Silva, F.E.C., Tonelli, C.A.M., Malaspina, O., Menezes, C., Rosa-Fontana, A.S., Blochtein, B., Freitas, B.M., Pires, C.S.S., Oliveira, F.F., Contrera, F.A.L., Torezani, K.R.S., de Fátima Ribeiro, M., Siqueira, M.A.L., Rocha, M.C.L.S.A., 2018. Pesticide exposure assessment paradigm for stingless bees. *Environ. Entomol.* 48, 36–48. <https://doi.org/10.1093/ee/nvy137>
- Costa, L.M., Grella, T.C., Barbosa, R.A., Malaspina, O., Nocelli, R.C.F., 2015. Determination of acute lethal doses (LD50 and LC50) of imidacloprid for the native bee *Melipona scutellaris* Latreille, 1811 (Hymenoptera: Apidae). *Sociobiology*. <https://doi.org/10.13102/sociobiology.v62i4.792>
- Crawley, M.J., 2012. *The R book*, 2nd ed. Wiley, Chichester.
- Crisci, C., Ghattas, B., Perera, G., 2012. A review of supervised machine learning algorithms and their applications to ecological data. *Ecol. Modell.* <https://doi.org/10.1016/j.ecolmodel.2012.03.001>
- Delkash-Roudsari, S., Chicas-Mosier, A.M., Goldansaz, S.H., Talebi-Jahromi, K., Ashouri, A., Abramson, C.I., 2020. Assessment of lethal and sublethal effects of imidacloprid, ethion, and glyphosate on aversive conditioning, motility, and lifespan in honey bees (*Apis mellifera* L.). *Ecotoxicol. Environ. Saf.* 204, 111108. <https://doi.org/10.1016/j.ecoenv.2020.111108>
- Desneux, N., Decourtye, A., Delpuech, J.-M., 2007. The sublethal effects of pesticides on beneficial arthropods. *Annu. Rev. Entomol.* 52, 81–106. <https://doi.org/10.1146/annurev.ento.52.110405.091440>
- Dill, G.M., Sammons, R.D., Feng, P.C.C., Kohn, F., Kretzmer, K., Mehrsheikh, A., Bleeke, M., Honegger, J.L., Farmer, D., Wright, D., Haupfear, E.A., 2010. Glyphosate: discovery, development, applications, and properties, in: *Glyphosate Resistance in Crops and Weeds*.

- John Wiley & Sons, Inc., Hoboken, NJ, USA, pp. 1–33.  
<https://doi.org/10.1002/9780470634394.ch1>
- EFSA, 2013. Conclusion on the peer review of the pesticide risk assessment for bees for the active substance imidacloprid. EFSA J. 11, 3068. <https://doi.org/10.2903/j.efsa.2013.3068>
- Faita, M.R., Cardozo, M.M., Amandio, D.T.T., Orth, A.I., Nodari, R.O., 2020. Glyphosate-based herbicides and *Nosema* sp. microsporidia reduce honey bee (*Apis mellifera* L.) survivability under laboratory conditions. J. Apic. Res. 59, 332–342.  
<https://doi.org/10.1080/00218839.2020.1736782>
- Farder-Gomes, C.F., Fernandes, K.M., Bernardes, R.C., Bastos, D.S.S., Martins, G.F., Serrão, J.E., 2021. Acute exposure to fipronil induces oxidative stress, apoptosis and impairs epithelial homeostasis in the midgut of the stingless bee *Partamona helleri* Friese (Hymenoptera: Apidae). Sci. Total Environ. 774, 145679.  
<https://doi.org/10.1016/j.scitotenv.2021.145679>
- Farina, W.M., Balbuena, M.S., Herbert, L.T., Goñalons, C.M., Vázquez, D.E., 2019. Effects of the herbicide glyphosate on honey bee sensory and cognitive abilities: Individual impairments with implications for the hive. Insects.  
<https://doi.org/10.3390/insects10100354>
- Freitas, B.M., Imperatriz-Fonseca, V.L., Medina, L.M., de Matos Peixoto Kleinert, A., Galetto, L., Nates-Parra, G., Quezada-Euán, J.J.G., 2009. Diversity, threats and conservation of native bees in the Neotropics. Apidologie 40, 332–346.  
<https://doi.org/10.1051/apido/2009012>
- Ghahramani, Z., 2015. Probabilistic machine learning and artificial intelligence. Nature 521, 452–459. <https://doi.org/10.1038/nature14541>
- Giannini, K.M., 1997. Labor division in *Melipona compressipes fasciculata* Smith (Hymenoptera: Apidae: Meliponinae). An. da Soc. Entomológica do Bras. 26, 153–162.  
<https://doi.org/10.1590/s0301-80591997000100020>
- Gomes, P.A.B., Suhara, Y., Nunes-Silva, P., Costa, L., Arruda, H., Venturieri, G., Imperatriz-Fonseca, V.L., Pentland, A., Souza, P. de, Pessin, G., 2020. An Amazon stingless bee foraging activity predicted using recurrent artificial neural networks and attribute selection. Sci. Rep. 10, 1–12. <https://doi.org/10.1038/s41598-019-56352-8>
- Graving, J.M., Chae, D., Naik, H., Li, L., Koger, B., Costelloe, B.R., Couzin, I.D., 2019. DeepPoseKit, a software toolkit for fast and robust animal pose estimation using deep

- learning. *Elife* 8, e47994. <https://doi.org/10.7554/eLife.47994>
- Guruharsha, K.G., Kankel, M.W., Artavanis-Tsakonas, S., 2012. The Notch signalling system: recent insights into the complexity of a conserved pathway. *Nat. Rev. Genet.* <https://doi.org/10.1038/nrg3272>
- Guyon, I., Weston, J., Barnhill, S., Vapnik, V., 2002. Gene selection for cancer classification using support vector machines. *Mach. Learn.* 46, 389–422. <https://doi.org/10.1023/A:1012487302797>
- Harris, C.R., Millman, K.J., van der Walt, S.J., Gommers, R., Virtanen, P., Cournapeau, D., Wieser, E., Taylor, J., Berg, S., Smith, N.J., Kern, R., Picus, M., Hoyer, S., van Kerkwijk, M.H., Brett, M., Haldane, A., del R'io, J.F., Wiebe, M., Peterson, P., G'érard-Marchant, P., Sheppard, K., Reddy, T., Weckesser, W., Abbasi, H., Gohlke, C., Oliphant, T.E., 2020. Array programming with NumPy. *Nature* 585, 357–362. <https://doi.org/10.1038/s41586-020-2649-2>
- Helmer, S.H., Kerbaol, A., Aras, P., Jumarie, C., Boily, M., 2015. Effects of realistic doses of atrazine, metolachlor, and glyphosate on lipid peroxidation and diet-derived antioxidants in caged honey bees (*Apis mellifera*). *Environ. Sci. Pollut. Res.* 22, 8010–8021. <https://doi.org/10.1007/s11356-014-2879-7>
- Hendriksma, H.P., Härtel, S., Steffan-Dewenter, I., 2011. Honey bee risk assessment: new approaches for in vitro larvae rearing and data analyses. *Methods Ecol. Evol.* 2, 509–517. <https://doi.org/10.1111/j.2041-210X.2011.00099.x>
- Herbert, L.T., Vázquez, D.E., Arenas, A., Farina, W.M., 2014. Effects of field-realistic doses of glyphosate on honey bee appetitive behaviour. *J. Exp. Biol.* 217, 3457–3464. <https://doi.org/10.1242/jeb.109520>
- Herrmann, K.M., Weaver, L.M., 1999. The shikimate pathway. *Annu. Rev. Plant Physiol. Plant Mol. Biol.* 50, 473–503. <https://doi.org/10.1146/annurev.arplant.50.1.473>
- ICMBio, 2018. Instituto Chico Mendes de Conservação da Biodiversidade. Livro Vermelho da Fauna Brasileira Ameaçada de Extinção.
- Jacob, C.R. de O., Zanardi, O.Z., Malaquias, J.B., Souza Silva, C.A., Yamamoto, P.T., 2019. The impact of four widely used neonicotinoid insecticides on *Tetragonisca angustula* (Latreille) (Hymenoptera: Apidae). *Chemosphere* 224, 65–70. <https://doi.org/10.1016/j.chemosphere.2019.02.105>
- Johnson, R.M., 2015. Honey bee toxicology. *Annu. Rev. Entomol.* 60, 415–434.

- <https://doi.org/10.1146/annurev-ento-011613-162005>
- Kassambara, A., Mundt, F., 2020. Factoextra: extract and visualize the results of multivariate data analyses.
- Kerr, W.E., dos Santos Neto, G.R., 1956. Contribuição para o Conhecimento da Bionomia dos Meliponini 5. Divisão de Trabalho entre as operarias de *Melipona quadrifasciata quadrifasciata* Lep. Insectes Soc. 3, 423–430. <https://doi.org/10.1007/BF02225762>
- Kockel, L., Homsy, J.G., Bohmann, D., 2001. Drosophila AP-1: Lessons from an invertebrate. Oncogene. <https://doi.org/10.1038/sj.onc.1204300>
- Lima, M.A.P., Martins, G.F., Oliveira, E.E., Guedes, R.N.C., 2016. Agrochemical-induced stress in stingless bees: peculiarities, underlying basis, and challenges. J. Comp. Physiol. A 202, 733–747. <https://doi.org/10.1007/s00359-016-1110-3>
- Liu, J., Sato, C., Cerletti, M., Wagers, A., 2010. Notch signaling in the regulation of stem cell self-renewal and differentiation, Current Topics in Developmental Biology. Academic Press. [https://doi.org/10.1016/S0070-2153\(10\)92012-7](https://doi.org/10.1016/S0070-2153(10)92012-7)
- Liu, Z., Williamson, M.S., Lansdell, S.J., Han, Z., Denholm, I., Millar, N.S., 2006. A nicotinic acetylcholine receptor mutation (Y151S) causes reduced agonist potency to a range of neonicotinoid insecticides. J. Neurochem. 99, 1273–1281. <https://doi.org/10.1111/j.1471-4159.2006.04167.x>
- Luo, Q.H., Gao, J., Guo, Y., Liu, C., Ma, Y.Z., Zhou, Z.Y., Dai, P.L., Hou, C.S., Wu, Y.Y., Diao, Q.Y., 2021. Effects of a commercially formulated glyphosate solutions at recommended concentrations on honeybee (*Apis mellifera* L.) behaviours. Sci. Rep. 11, 2115. <https://doi.org/10.1038/s41598-020-80445-4>
- Maeda, H., Dudareva, N., 2012. The shikimate pathway and aromatic amino acid biosynthesis in plants. Annu. Rev. Plant Biol. 63, 73–105. <https://doi.org/10.1146/annurev-arplant-042811-105439>
- MAPA, 2021. Ministério da Agricultura, Pecuária e Abastecimento (MAPA) [WWW Document]. URL [http://agrofit.agricultura.gov.br/agrofit\\_cons/principal\\_agrofit\\_cons](http://agrofit.agricultura.gov.br/agrofit_cons/principal_agrofit_cons) (accessed 5.11.21).
- Matsuda, K., Buckingham, S.D., Kleier, D., Rauh, J.J., Grauso, M., Sattelle, D.B., 2001. Neonicotinoids: insecticides acting on insect nicotinic acetylcholine receptors. Trends Pharmacol. Sci. [https://doi.org/10.1016/S0165-6147\(00\)01820-4](https://doi.org/10.1016/S0165-6147(00)01820-4)
- McHugh, M.L., 2012. Interrater reliability: the kappa statistic. Biochem. Medica 22, 276–282.

- <https://doi.org/10.11613/bm.2012.031>
- McKinney, W., 2010. Data structures for statistical computing in Python, in: van der Walt, S., Millman, J. (Eds.), Proceedings of the 9th Python in Science Conference. pp. 56–61. <https://doi.org/10.25080/Majora-92bf1922-00a>
- Nunes-Silva, P., Costa, L., Campbell, A.J., Arruda, H., Contrera, F.A.L., Teixeira, J.S.G., Gomes, R.L.C., Pessin, G., Pereira, D.S., de Souza, P., Imperatriz-Fonseca, V.L., 2020. Radiofrequency identification (RFID) reveals long-distance flight and homing abilities of the stingless bee *Melipona fasciculata*. *Apidologie* 51, 240–253. <https://doi.org/10.1007/s13592-019-00706-8>
- Oksanen, J., Blanchet, F.G., Friendly, M., Kindt, R., Legendre, P., McGlinn, D., Minchin, P.R., O'Hara, R.B., Simpson, G.L., Solymos, P., Stevens, M.H.H., Szoecs, E., Wagner, H., 2019. Vegan: community ecology package.
- Palmer, M.J., Moffat, C., Saranzewa, N., Harvey, J., Wright, G.A., Connolly, C.N., 2013. Cholinergic pesticides cause mushroom body neuronal inactivation in honey bees. *Nat. Commun.* 4, 1634. <https://doi.org/10.1038/ncomms2648>
- Pedregosa, F., Varoquaux, G., Gramfort, A., Michel, V., Thirion, B., Grisel, O., Blondel, M., Prettenhofer, P., Weiss, R., Dubourg, V., Vanderplas, J., Passos, A., Cournapeau, D., Brucher, M., Perrot, M., Duchesnay, E., 2011. Scikit-learn: machine learning in Python. *J. Mach. Learn. Res.* 12, 2825–2830.
- Pereira, N.C., Diniz, T.O., Takasusuki, M.C.C.R., 2020. Sublethal effects of neonicotinoids in bees: a review. *Sci. Electron. Arch.* 13, 142. <https://doi.org/10.36560/13720201120>
- Pires, C.S.S., Torezani, K.R.S., Cham, K.O., Viana-Silva, F.E.C., Borges, L.O., Tonelli, C.A.M., Saretto, C.O.S.D., Nocelli, R.C.F., Malaspina, O., Cione, A.P., 2018. Seleção de espécies de abelhas nativas para avaliação de risco de agrotóxicos. Ibama.
- R Core Team, 2020. R: A language and environment for statistical computing.
- Ramírez, V.M., Ayala, R., González, H.D., 2018. Crop pollination by stingless bees. *Pot-Pollen Stingless Bee Melittology*. [https://doi.org/10.1007/978-3-319-61839-5\\_11](https://doi.org/10.1007/978-3-319-61839-5_11)
- Rossi, F., Conan-Guez, B., 2005. Functional multi-layer perceptron: a non-linear tool for functional data analysis. *Neural Networks* 18, 45–60. <https://doi.org/https://doi.org/10.1016/j.neunet.2004.07.001>
- Schneider, C.W., Tautz, J., Grünewald, B., Fuchs, S., 2012. RFID tracking of sublethal effects of two neonicotinoid insecticides on the foraging behavior of *Apis mellifera*. *PLoS One* 7,

30023. <https://doi.org/10.1371/journal.pone.0030023>
- Seide, V.E., Bernardes, R.C., Pereira, E.J.G., Lima, M.A.P., 2018. Glyphosate is lethal and Cry toxins alter the development of the stingless bee *Melipona quadrifasciata*. *Environ. Pollut.* 243, 1854–1860. <https://doi.org/10.1016/J.ENVPOL.2018.10.020>
- Sgolastra, F., Hinarejos, S., Pitts-Singer, T.L., Boyle, N.K., Joseph, T., Lückmann, J., Raine, N.E., Singh, R., Williams, N.M., Bosch, J., 2019. Pesticide exposure assessment paradigm for solitary bees. *Environ. Entomol.* 48, 22–35. <https://doi.org/10.1093/ee/nvy105>
- Siefert, P., Hota, R., Ramesh, V., Grünewald, B., 2020. Chronic within-hive video recordings detect altered nursing behaviour and retarded larval development of neonicotinoid treated honey bees. *Sci. Rep.* 10, 1–15. <https://doi.org/10.1038/s41598-020-65425-y>
- Simon, F., Fichelson, P., Ghosh, M., Audibert, A., 2009. Notch and Prospero repress proliferation following cyclin E overexpression in the *Drosophila* bristle lineage. *PLoS Genet.* 5, e1000594. <https://doi.org/10.1371/journal.pgen.1000594>
- Singh, D., Singh, B., 2020. Investigating the impact of data normalization on classification performance. *Appl. Soft Comput.* 97, 105524. <https://doi.org/10.1016/j.asoc.2019.105524>
- Slaa, E.J., Chaves, L.A.S., Malagodi-Braga, K.S., Hofstede, F.E., 2006. Stingless bees in applied pollination: practice and perspectives. *Apidologie* 37, 293–315. <https://doi.org/10.1051/apido:2006022>
- Srivastava, N., Hinton, G., Krizhevsky, A., Sutskever, I., Salakhutdinov, R., 2014. Dropout: a simple way to prevent neural networks from overfitting. *J. Mach. Learn. Res.* 15, 1929–1958.
- Straw, E.A., Carpentier, E.N., Brown, M.J.F., 2021. Roundup causes high levels of mortality following contact exposure in bumble bees. *J. Appl. Ecol.* <https://doi.org/10.1111/1365-2664.13867>
- Swarup, S., Verheyen, E.M., 2012. Wnt/wingless signaling in *Drosophila*. *Cold Spring Harb. Perspect. Biol.* 4, 1–15. <https://doi.org/10.1101/cshperspect.a007930>
- Thompson, H.M., Maus, C., 2007. The relevance of sublethal effects in honey bee testing for pesticide risk assessment, in: *Pest Management Science*. John Wiley & Sons, Ltd, pp. 1058–1061. <https://doi.org/10.1002/ps.1458>
- Tian, A., Benchabane, H., Ahmed, Y., 2018. Wingless/Wnt signaling in intestinal development, homeostasis, regeneration and tumorigenesis: a *Drosophila* perspective. *J. Dev. Biol.*

- <https://doi.org/10.3390/jdb6020008>
- Tomé, H.V.V., Barbosa, W.F., Corrêa, A.S., Gontijo, L.M., Martins, G.F., Guedes, R.N.C., 2015a. Reduced-risk insecticides in Neotropical stingless bee species: impact on survival and activity. *Ann. Appl. Biol.* 167, 186–196. <https://doi.org/10.1111/aab.12217>
- Tomé, H.V.V., Barbosa, W.F., Martins, G.F., Guedes, R.N.C., 2015b. Spinosad in the native stingless bee *Melipona quadrifasciata*: regrettable non-target toxicity of a bioinsecticide. *Chemosphere* 124, 103–109. <https://doi.org/10.1016/j.chemosphere.2014.11.038>
- Tomé, H.V.V., Martins, G.F., Lima, M.A.P., Campos, L.A.O., Guedes, R.N.C., 2012. Imidacloprid-induced impairment of mushroom bodies and behavior of the native stingless bee *Melipona quadrifasciata anthidioides*. *PLoS One* 7, e38406.
- Tomé, H.V.V., Ramos, G.S., Araújo, M.F., Santana, W.C., Santos, G.R., Guedes, R.N.C., Maciel, C.D., Newland, P.L., Oliveira, E.E., 2017. Agrochemical synergism imposes higher risk to Neotropical bees than to honey bees. *R. Soc. Open Sci.* 4, 160866. <https://doi.org/10.1098/rsos.160866>
- Tomé, H.V. V, Schmehl, D.R., Wedde, A.E., Godoy, R.S.M., Ravaiano, S. V, Guedes, R.N.C., Martins, G.F., Ellis, J.D., 2020. Frequently encountered pesticides can cause multiple disorders in developing worker honey bees. *Environ. Pollut.* 256, 113420. <https://doi.org/10.1016/j.envpol.2019.113420>
- Tomizawa, M., Casida, J.E., 2005. Neonicotinoid insecticide toxicology: mechanisms of selective action. *Annu. Rev. Pharmacol. Toxicol.* <https://doi.org/10.1146/annurev.pharmtox.45.120403.095930>
- Valdovinos-Núñez, G.R., Quezada-Euán, J.J.G., Ancona-Xiu, P., Moo-Valle, H., Carmona, A., Sánchez, E.R., 2009. Comparative toxicity of pesticides to stingless bees (Hymenoptera: Apidae: Meliponini). *J. Econ. Entomol.* 102, 1737–1742. <https://doi.org/10.1603/029.102.0502>
- Vázquez, D.E., Balbuena, M.S., Chaves, F., Gora, J., Menzel, R., Farina, W.M., 2020. Sleep in honey bees is affected by the herbicide glyphosate. *Sci. Rep.* 10, 1–8. <https://doi.org/10.1038/s41598-020-67477-6>
- Yoo, W., Mayberry, R., Bae, S., Singh, K., Peter He, Q., Lillard Jr, J.W., 2014. A study of effects of multicollinearity in the multivariable analysis. *Int. J. Appl. Sci. Technol.* 4, 9–19.

## Appendix A

The tracked distance is measured as the distance that an animal walks during a video recording. The max speed is the maximum speed achieved by the animal. The turn angle is the average angle that the individual rotates in each video frame. Meandering is the average angle that the individual rotates during the video. The number of stops is the count associated with no activity of the animal (the tracked distance of  $\leq 0.046$  cm frame<sup>-1</sup> was counted as a stop). The mean number of movements is the number associated with the intermediated activity (the tracked distance of  $> 0.046$  and  $\leq 0.53$  cm frame<sup>-1</sup> was counted as the mean movement). The number of fast movements is the number associated with high activity (the tracked distance of  $> 0.53$  cm frame<sup>-1</sup> was counted as fast movement). Resting, mean movement, and fast movement were calculated as the proportion of time the animals stayed in each state of activity. Degree is the sum of all interactions of an individual with other animals of the group (an interaction was considered when the individuals approached a distance of  $\leq 1.41$  cm). The network density is the proportion of interactions in an animal group. Feeding is the proportion of time that individuals spent feeding during the video. Polarization is the proportion of individuals that are highly aligned in a group. Milling is the proportion of the group with a high degree of rotation about its center of mass. Swarm is the proportion of individuals in a group that are in a disordered movement. Transition is the proportion of the group that was in a transition among the polarization, milling, and swarm states. The mathematical definition of these features can be found in Bernardes et al. (2021).

## Supplementary Material

<https://drive.google.com/file/d/1id78fiSnCU3JHvmXKUwgAJ7yKXo7sZkx/view?usp=sharing>

## Supplementary videos

Video S1. Representative video showing the collective behavior of *Melipona quadrifasciata* foragers exposed to neonicotinoid imidacloprid. The target letters in the bees are individual identities assigned automatically by the software used in the video analyses. <https://drive.google.com/file/d/1xvLwjElc2NJRfPcfNXEUqpEHppuUtIBkf/view?usp=sharing>

Video S2. Representative video showing the collective behavior of *Melipona quadrifasciata* foragers exposed to the herbicide glyphosate. The target letters in the bees are individual identities assigned automatically by the software used in the video analyses.

<https://drive.google.com/file/d/1arszjtBK5FulDjUgPbbY-tiq1Rt9sV-/view?usp=sharing>

Video S3. Representative video showing the collective behavior of a non-exposed *Melipona quadrifasciata* forager (control). The target letters in the bees are individual identities assigned automatically by the software used in the video analyses.

<https://drive.google.com/file/d/17zAWMiQXpQaBbi7Uxnwe-CfWl-YAjD7V/view?usp=sharing>

### **CHAPTER 3. Impact of copper sulfate on survival, behavior, midgut morphology, and antioxidant activity of *Partamona helleri* (Apidae: Meliponini)**

*Accepted for publication in Environmental Science and Pollution Research*

Ref.:

Ms. No. ESPR-D-21-03773R2

Impact of copper sulfate on survival, behavior, midgut morphology, and antioxidant activity of *Partamona helleri*  
(Apidae: Meliponini)

Environmental Science and Pollution Research

Dear Dr. Araújo,

I am pleased to tell you that your work has now been accepted for publication in Environmental Science and Pollution Research. This letter serves as an acceptance certificate. Your article has been sent to the production service and you will receive the proofs soon.

If you have any question, please contact Dennis Villahermosa + [dennis.villahermosa@springer.com](mailto:dennis.villahermosa@springer.com)

Thank you for submitting your work to this journal.

With kind regards,

Dr. Giovanni Benelli

Editor

Environmental Science and Pollution Research

## Impact of copper sulfate on survival, behavior, midgut morphology, and antioxidant activity of *Partamona helleri* (Apidae: Meliponini)

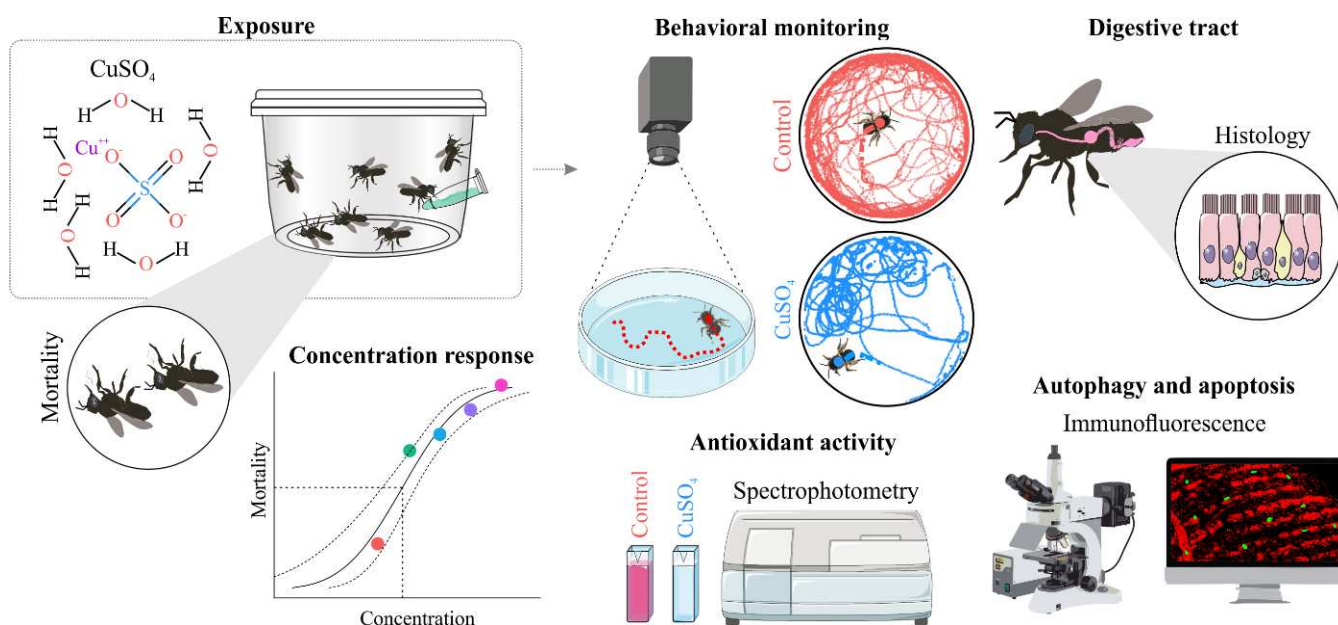
Rodrigo Cupertino Bernardes<sup>a</sup>, Kenner Moraes Fernandes<sup>b</sup>, Daniel Silva Sena Bastos<sup>b</sup>, André Filipe Penha Aires Freire<sup>c</sup>, Marcos Pereira Lopes<sup>b</sup>, Leandro Licursi de Oliveira<sup>b</sup>, Mara Garcia Tavares<sup>b</sup>, Renan dos Santos Araújo<sup>a\*</sup> and Gustavo Ferreira Martins<sup>b</sup>

<sup>a</sup>Departamento de Entomologia, Universidade Federal de Viçosa, Viçosa, MG 36570-900, Brazil

<sup>b</sup>Departamento de Biologia Geral, Universidade Federal de Viçosa, Viçosa, MG 36570-900, Brazil

<sup>c</sup>Departamento de Ciências Biológicas, Universidade Federal do Maranhão, São Luís, Maranhão, 65080-805, Brazil

### Graphical abstract



## Abstract

Copper sulfate ( $\text{CuSO}_4$ ) is widely used in agriculture as a pesticide and foliar fertilizer. However, the possible environmental risks associated with  $\text{CuSO}_4$  use, particularly related to pollinating insects, have been poorly studied. In this study, we evaluated the both lethal and sublethal effects of  $\text{CuSO}_4$  on the stingless bee *Partamona helleri*. Foragers were orally exposed to five concentrations of  $\text{CuSO}_4$  and the concentration killing 50% ( $\text{LC}_{50}$ ) was estimated. This concentration was subsequently used in behavioral, midgut morphology, and antioxidant activity analyses. We detected increases in bee mortality with the ingestion of increasing concentrations of  $\text{CuSO}_4$ . Ingestion at the estimated  $\text{LC}_{50}$  ( $142.95 \mu\text{g mL}^{-1}$ ) resulted in altered walking behavior and damage to the midgut epithelium and peritrophic matrix of bees. Furthermore, the  $\text{LC}_{50}$  caused an increase in the activities of catalase and superoxide dismutase, and in levels of the lipid peroxidation biomarker malondialdehyde. Furthermore, the *in situ* detection of caspase-3 and LC3, proteins related to apoptosis and autophagy, respectively, revealed that these processes are intensified in the midgut of treated bees. These data highlight that the ingestion of  $\text{CuSO}_4$  can have considerable sublethal effects on the walking behavior and midgut of stingless bees, and therefore could pose potential risks to pollinators including native bees.

**Keywords:** Bioassays,  $\text{CuSO}_4$ , heavy metal,  $\text{LC}_{50}$ , stingless bee, toxicological effects

## 1. Introduction

Heavy metals such as copper (Cu), zinc (Zn), and manganese (Mn) are found in numerous agrochemical formulations that are used to enhance agricultural production (Deng et al. 2007; Worku and Hailu 2018). Depending on the concentration, heavy metals can be toxic and have potentially adverse effects on intracellular components, including organelles, cell membranes, and enzymes (Peña et al., 1999; Wang and Shi 2001; reviewed by Tchounwou et al. 2012). Following their application to crops, agrochemical products based on heavy metals can accumulate in the leaves and flowers, and can accordingly be transferred to pollinating insects that forage on the treated plants (Hladun et al. 2015, 2016; Cai et al. 2019) or accumulate directly in the bodies of insects (Hongxia et al. 2010; Baghban et al. 2014; Botina et al. 2019; Goretti et al. 2020).

The salt copper sulfate ( $\text{CuSO}_4$ ) is widely used as a fungicide, insecticide, and foliar fertilizer (Michaud and Grant 2003; Rodrigues et al. 2016), and it has been demonstrated that chronic intoxication with  $\text{CuSO}_4$  can reduce the locomotor activity (Bonilla-Ramirez et al. 2011) and central nervous system neuronal function (Hwang et al. 2014) of the fly *Drosophila melanogaster*. In coccinellid beetles, chronic intoxication with  $\text{CuSO}_4$  has been found to increase the time of development, reduce fertility, and extend the pre-reproductive period of females (Michaud and Grant 2003). The ingestion of  $\text{CuSO}_4$  has been shown to alter the color and thickness of the midgut in the flesh fly *Sarcophaga peregrina* (Wu et al. 2009), and the integrity of the peritrophic matrix (PM) in *Aedes aegypti* larvae (Rayms-Keller et al. 1998). In the stingless bees, the ingestion of  $\text{CuSO}_4$  affects the survival and the walking behavior of the workers of *Friesella schrottkyi* and the respiration rate of *Partamona helleri* (Rodrigues et al. 2016; Botina et al. 2019).

Debates provoked by recent widespread reductions in pollinator populations, particularly bees, have addressed several factors, including both biotic risks (mites, viruses, fungi, and bacteria) and abiotic ones (habitat degradation, climate change, and agrochemicals) (vanEngelsdorp and Meixner 2010; Lima et al. 2016; Steinhauer et al. 2018; Cham et al. 2019; Tomé et al. 2020). Among these, stress attributable to the use of agrochemicals, and its consequences, in stingless bees have received prominent attention in recent years, mainly due to the associated sublethal effects (Tomé et al. 2015, 2017; Bernardes et al. 2018; Araújo et al. 2021).

Among the sublethal effects associated with the exposure of stingless bees to agrochemicals, those that stand out are the impairment of locomotor activity (Tomé et al. 2012; Barbosa et al. 2015; Bernardes et al. 2017; Marques et al. 2020), changes in the expression of genes related to immune response and detoxification (Viana et al. 2021), and damage to cells in the nervous ganglion (Jacob et al. 2015; Tomé et al. 2012) and midgut (Araújo et al. 2019). In addition, oxidative damage and cell death in the digestive tract have recently been investigated (Araujo et al. 2021; Farder-Gomes et al. 2021).

Stingless bees play essential roles in pollinating a substantial proportion of the flora in tropical regions and, depending on the ecosystem, are known to pollinate between 40% and 90% of native trees (Kerr et al. 2001; Braga et al. 2012; Pedro 2014). *P. helleri*, for instance, is an important pollinator of trees in the Atlantic Forest (Camargo and Pedro 2003; Ramalho 2004); this species has been widely used as a model for toxicological studies related to stingless bees due to its large number and their relative facility of being found in the environment (Bernardes et al. 2018; Araújo et al. 2019; Pereira et al. 2020; Fader-Gomes et al. 2021). During foraging, workers can be directly exposed to  $\text{CuSO}_4$  through contact or ingestion. In addition, they may collect copper contaminated resources (e.g., pollen, nectar, and resins), since heavy

metals can accumulate in different parts of plants (Fageria et al. 2002). The larvae can be intoxicated with these collected resources and potentially suffer lethal and sublethal effects (Lima et al. 2012)

Given the knowledge gap about CuSO<sub>4</sub> effects in non-target organisms, such as stingless bees, and the ecological significance of these bees, we sought to evaluate the lethal and sublethal effects of ingested CuSO<sub>4</sub> in foragers of the *P. helleri*. In the present study, we estimated the LC<sub>50</sub> and assessed walking behavior in this stingless bee. In addition, we assessed, for the first time, the CuSO<sub>4</sub> sublethal effects on processes of apoptosis, autophagy, and antioxidant activity of the *P. helleri* midgut.

## **2. Material and methods**

### **2.1. Bees and chemicals**

Five different colonies of *P. helleri* were collected in Viçosa (MG, Brazil; 20°, 45' S, and 42° 52' W) with permission from the Chico Mendes Institute for Biodiversity Conservation (SISBIO, ID 75536) and established in the experimental apiary at the Universidade Federal de Viçosa (UFV) for at least two years before the beginning of the experiment. These number of colonies assure the genetic variability, as workers from different colonies are descendants of different queens. Foragers were collected at the entrance of the colonies using glass jars when they exit the hive to forage, avoiding harm to the original colonies. These bees were between 20 to 30 days old; age that workers perform most foraging activity (Giannini 1997; Kerr and Santos-Neto 1956; Simões and Bego 1979). The collected specimens were taken to the laboratory where they acclimatized without food, in an incubator at  $28 \pm 1^{\circ}\text{C}$  and  $70\% \pm 5\%$  humidity in the dark for a period of 1 h before experimental exposure. This acclimatization was

necessary to standardise the feeding condition of the tested workers and based on an exposure protocol for stingless bees (Botina et al. 2020) and previous works (Tomé et al. 2015, 2017).

Copper sulfate [CuSO<sub>4</sub>: Penta 24 (240 g kg<sup>-1</sup> Cu and 110 g kg<sup>-1</sup> S); Multitécnica Industrial, Sete Lagoas, MG, Brazil] was diluted in 50% aqueous sucrose solution to obtain the concentration of 5000 µg mL<sup>-1</sup>, which was gradually diluted to obtain the other concentrations used in the mortality bioassay (see below). This is the concentration that is routinely used to spray the leaves of Brazilian tomato crops (MAPA 2020), and this stock solution was used to prepare solutions of different concentrations for use in a mortality bioassay. To prepare the solutions for all bioassays, we used 30 mg of copper sulfate and the residue was properly discarded following local waste management protocols. After bioassays, contaminated bees were also discarded properly.

## **2.2. Bee mortality**

The collected foragers were transferred to plastic containers (250 mL) separated according to colony (10 bees per colony), each of which was considered an experimental unit (Botina et al. 2020). In total, we set up 30 containers with 300 sampled bees (10 bees in each container for each of the five colonies, which were exposed to each of the six concentrations of the CuSO<sub>4</sub>, including the control). The control group received a non-contaminated sucrose solution (sucrose:distilled water, 1:1). We used the average natural mortality of control bees to correct for the mortality recorded in the other treatments (Abbott 1925). Diets were offered in 1.5 mL feeders constructed from perforated microcentrifuge tubes, which were inserted into a hole in the wall of the plastic containers. Maintenance of bees in plastic containers, as well as the feeding method used here, followed exposure protocol for stingless bees (Botina et al. 2020) and previous works (Araújo et al. 2021; Farder-Gomes et al. 2021). The bees were subjected to a 3-h exposure (acute exposure) to the following six concentrations of CuSO<sub>4</sub> diluted in 50%

sucrose solution: 5000, 1666.7, 554.2, 183.4, 58.4, and 0.0  $\mu\text{g mL}^{-1}$  (control). To obtain this range in concentrations ( $c$ ), in a preliminary experiment, we identified the concentration that caused low mortality ( $l$ ) (close to 10%) and the one that caused high mortality ( $h$ ) (close to 90%). Then we calculate the dilution rate ( $k$ ) in relation to the concentrations ( $n$ ) as  $k = (\log_{10}(h) - \log_{10}(l)) / (n-1)$ , and determinate each concentration ( $cn$ ) as the previous concentration plus the dilution rate ( $c_n = c_{n-1} + 10^k$ ).

Following exposure, the bees were allowed to feed on 50% uncontaminated sucrose solution *ad libitum*. We evaluated mortality at 24 h after commencing exposure and used these data to estimate the mortality curve and determine the 50% lethal concentration ( $\text{LC}_{50}$ ). The absence of movement was taken to be indicative of bee mortality (Botina et al. 2020). Throughout the experimental period, the foragers were maintained in the aforementioned incubator under dark conditions.

### 2.3. Bee behavior

The behavior of bees was monitored 24 h after exposure to the  $\text{LC}_{50}$  ( $142.95 \mu\text{g mL}^{-1}$ ) of  $\text{CuSO}_4$  or the control diet. The bees were exposure in groups during 3 hours (item 2.1). The bees were individually transferred to a Petri dish arena (9 cm diameter and 0.8 cm high) containing a filter paper base and covered with transparent plastic film to prevent bee escape (Botina et al. 2020). The movements of the bees were recorded for 10 min using a digital camera operating at 30 frames per second and analyzed using Ethoflow® software (Bernardes et al., 2021), based on which, we calculated walking distance (cm), mean velocity ( $\text{cm s}^{-1}$ ), resting time (s), and the number of stops. The bioassays were carried out between 10:00 and 14:00 under artificial fluorescent lighting at  $25 \pm 2^\circ\text{C}$ . In total, we monitored the behavior of 32 bees (four bees for each colony exposed to each of the two treatments - in this case, it was used four colonies and not five).

## 2.4. Midgut morphology

From bees exposed (item 2.1) to the  $LC_{50}$  ( $142.95 \mu\text{g mL}^{-1}$ ) of  $\text{CuSO}_4$  and control, we choose randomly 10 bees to dissect (5 for  $LC_{50}$  and 5 for control) in saline solution for insects ( $0.1 \text{ M NaCl}$ ,  $0.1 \text{ M KH}_2\text{PO}_4$ , and  $0.1 \text{ M Na}_2\text{HPO}_4$ ). The midgut of bees was transferred to Zamboni's fixative solution (2% paraformaldehyde, containing 15% picric acid in  $0.1 \text{ M}$  sodium phosphate buffer), and maintained therein for 2 h at  $25 \pm 2^\circ\text{C}$ . Thereafter, the samples were washed three times in  $0.1 \text{ M}$  phosphate-buffered saline (PBS), dehydrated in a graded ethanol series (70% to 95%), and embedded in Historesin (Leica Biosystems, Nussloch, Germany). Sections of the embedded material ( $5 \mu\text{m}$  thick) were obtained using a Leica RM 2255 microtome, and were stained with hematoxylin and eosin (HE). Samples were observed under an Olympus BX-53 light microscope, coupled with an Olympus DP 73 digital camera (Olympus Optical Corp., Tokyo, Japan).

To detect the PM (glycoconjugates and polysaccharides containing  $\beta$ -1-4 *N*-acetylglucosamine residues) in the midgut lumen, other unstained sections were washed twice in PBS and incubated for 1 h with  $10 \text{ g mL}^{-1}$  fluorescein isothiocyanate (FITC)-conjugated lectin [wheat germ agglutinin (WGA)-FITC: L4895; Sigma-Aldrich, Israel] diluted (1:500) in  $0.1 \text{ M}$  PBS. After a triple wash in PBS, the sections were stained with diamidino-2-phenylindole (DAPI: 1:500; Biotium, Inc., Hayward, CA, USA) for 30 min to label the cell nuclei. Sections were subsequently washed a further three times and mounted with a 50% sucrose solution. As a negative control, sections were stained only with DAPI and mounted with a 50% sucrose solution. The slides were observed and photographed using an Olympus BX53 fluorescence microscope, coupled with an Olympus XM 10 digital camera (Olympus Optical Corp., Tokyo, Japan).

## 2.5. Abdomen antioxidant activity

The abdomen of bees that had been exposed to  $LC_{50}$  ( $142.95 \mu\text{g mL}^{-1}$ ) of  $\text{CuSO}_4$  and control were homogenized separately in 1 mL of PBS, using a Tissue Master 125 homogenizer (OMNI) and centrifuged at  $10000 \times g$  for 10 min at  $4^\circ\text{C}$  (Heraeus Fresco 16 centrifuge; Thermo Scientific). For each of the 10 samples, we prepared a homogenate, collected the supernatant, and spectrophotometrically assayed antioxidant activity based on the activity of the enzymes catalase (CAT), glutathione *S*-transferase (GST), and superoxide dismutase (SOD), and contents of the lipid peroxidation biomarker malondialdehyde (MDA).

The activity of CAT was measured at 374 nm, based on quantification of the kinetics of the decomposition of  $\text{H}_2\text{O}_2$  to  $\text{O}_2$  and  $\text{H}_2\text{O}$  (Hadwan and Abed 2016); GST activity was determined at 340 nm by monitoring thioester formation, using 1-chloro-2,4-dinitrobenzene (CDNB) as a substrate (Habig et al. 1974); SOD activity was assessed at 320 nm using the pyrogallol autoxidation method (Marklund and Marklund 1974); and the content of MDA was assessed at 535 nm using the thiobarbituric acid reactive substances (TBARS) method (Buege and Aust 1978). For each of the 10 samples (five abdomens per two treatments), we performed multiple measurements to enhance the variance structure of the data, totaling 60 measurements (six measurements for each of the 10 samples). Thereby, in statistical analyses, we carried out bootstrap sampling to randomly generate confidence intervals from the observed data (item 2.7) (Efron 1992). The results were expressed as kilo units of protein per milliliter ( $\text{kU protein mL}^{-1}$ ) for CAT activity, units of protein per milliliter ( $\text{U protein mL}^{-1}$ ) for GST and SOD, and micromoles of protein per milliliter ( $\mu\text{mol protein mL}^{-1}$ ) for MDA.

## 2.6. Midgut immunofluorescence

Fixed midguts (see section 2.4) were washed three times and incubated in 0.1 M PBS/1% Triton X-100 (PBST) for 2 h. The organs were incubated separately, for 24 h at  $4^\circ\text{C}$ ,

with the PBS-diluted primary antibodies anti-LC3 (1:500: Cell Signaling Technology, Beverly, MA, EUA) and anti-caspase-3 cleaved (1:500: Sigma-Aldrich, St. Louis Mo., EUA), indicative of autophagy and apoptosis, respectively. Immunostaining was performed using midguts obtained from five bees exposed to the LC<sub>50</sub> of CuSO<sub>4</sub> and the control, totaling 20 individuals (five bees for each of the two treatments, analyzed using each of the two primary antibodies).

After initial incubation with the primary antibodies, the samples were washed three times and then re-incubated with secondary antibody conjugated to FITC (Sigma-Aldrich Corp., St Louis, MO, USA) in PBS (1: 500) for 24 h at 4°C. After subsequent washing, the nuclei of midgut cells were stained with TO-PRO-3 (Life Technologies, Eugene, EUA) for 30 min and mounted in a Mowiol solution (Fluka, St. Louis, MO, EUA). As a negative control, the midguts of five exposed bees and five control bees were treated as described above, excluding the step corresponding to incubation with the primary antibody. The samples were examined under a Zeiss 510 Meta confocal microscope (Carl Zeiss AG, Oberkochen, Germany) at the Núcleo de Microscopia e Microanálise (NMM-UFV). The quantification of cells staining positive for LC3 or caspase-3 was performed using Image-Pro 4.5 software (Media Cybernetics, Silver Spring, EUA), for which, six images obtained under a ×20 objective lens were randomly selected for each sample.

## 2.7. Statistical analysis

All statistical analyses were performed using R software (R Core Team, version 4.0.0, 2020). For the data obtained in the mortality bioassay, we fitted a concentration-response (Probit) model and estimated the LC<sub>50</sub> of CuSO<sub>4</sub> in *P. helleri*.

Principal component analysis (PCA) was performed for variables associated with walking behavior (distance, velocity, resting time, and number of stops). Given that these variables do not have the same scales, the components were defined based on a correlation

matrix. Bartlett's test was used to assess the suitability of the proposed model. We selected principal components (PCs) with eigenvalues that were higher than the mean value of all eigenvalues. We fitted generalized linear mixed models (GLMMs) with PC1 and PC2 scores as response variables and using Gamma error distribution structure (a suitable distribution for continuous data where the variance increases with the square of the mean) (Crawley 2012). The colonies were included as random effects in GLMMs to compensate for the identical background of bees (Hendriksma et al. 2011).

Considering the different measurements used for the detection of antioxidant activity on the same sample, we carried out bootstrap with 1000 interactions, taking 10 samples per treatment in each interaction. Bootstrap sampling enabled us to randomly generate confidence intervals from the data observed empirically (Efron 1992). In each bootstrap sample, permutation tests were executed with 1,000 interactions to assess differences between treatments. A permutation test was necessary to determine statistical inference in the distribution of the data generated in each bootstrap interaction (Lunneborg 2014). Consequently, the test hypothesis for each variable (CAT, GTS, SOD, and MDA) was based on  $10^6$  random interactions.

We fitted generalized linear models (GLMs) with Poisson distribution (a suitable distribution for count data) (Crawley 2012) to the immunofluorescence dependent variables (i.e., the mean number of cells staining positive for LC3 or caspase-3). In addition, given that the measured variables have the same scale, we performed hierarchical cluster analysis using a complete linkage method and Euclidean distance.

### 3. Results and Discussion

#### 3.1. Toxicity of CuSO<sub>4</sub>

The hypothesis assuming the suitability of the model was accepted ( $F_{4,27} = 1.02$ ,  $p = 0.42$ ), indicating that the Probit concentration-response model is suitable for analysis of the mortality bioassay results. The LC<sub>50</sub> (confidence interval) estimated using this concentration-response model was 142.95  $\mu\text{g mL}^{-1}$  (69.5–231.76, Fig. 1).

The exposure to CuSO<sub>4</sub> in label rate (5000  $\mu\text{g mL}^{-1}$ ) caused 100% mortality on *P. helleri* foragers, as previously reported for *P. helleri* (Botina et al. 2019) and *F. schrottkyi* (Rodrigues et al. 2016) exposed to this compound. This mortality reflects the oral intoxication caused by CuSO<sub>4</sub>, as heavy metal intoxication reduces the viability of bees (Di et al. 2016). The LC<sub>50</sub> found in the present study is thirty-five times lower than that recommended for use in the field (5000  $\mu\text{g/mL}$ ); therefore, CuSO<sub>4</sub> may present a risk for these bees when they go out to forage. The foragers can also collect pollen, nectar, and resins containing heavy metals, which can favor the accumulation of heavy metals in the colonies. These heavy metals can also be ingested by the larvae (Desoky et al. 2019; Lima et al. 2016; Yarsan et al. 2007).

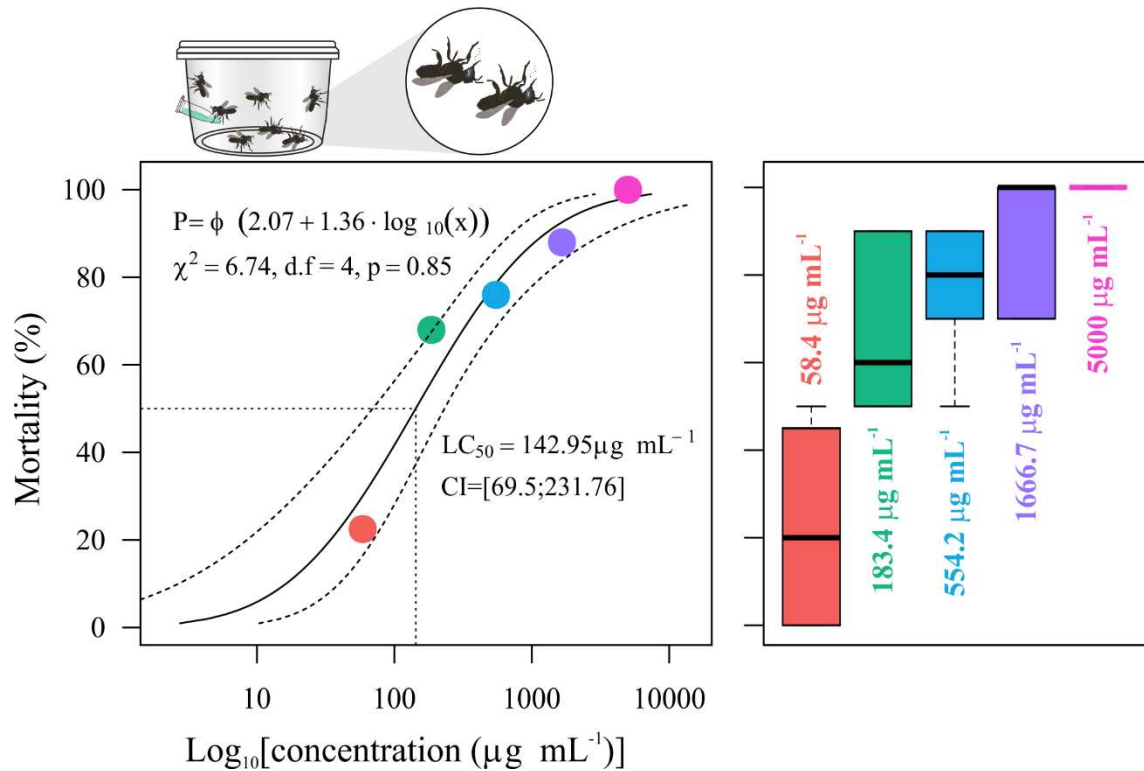


**Figure. 1.** Concentration–mortality curve for *Partamona helleri* foragers exposed to copper sulfate ( $\text{CuSO}_4$ ). The dots represent the means of five observations at each exposure concentration, obtained for a total of 30 bees (including the controls). The dashed lines above and below the fitted regression curve indicate the 95% confidence interval. The box plot (right panel) shows the variation in mortality data (median, lower, and upper quartiles).

### 3.2. Walking activity

Bartlett's test indicated the suitability of the selected PCA model ( $\chi^2 = 259.47$ ,  $\text{df} = 6$ ,  $p < 0.001$ ). Principal components 1 (PC1) and 2 (PC2) explained 88.9% and 6.4% of the total variance in the data, respectively (Fig. 2A). PC1 compared the variables velocity and distance with resting time and number of stops. These variables had opposite loadings signals (Fig. 2B), thereby enabling us to separate fast from slow individuals. Negative loadings indicate higher velocities and distances walked, whereas positive loadings indicate longer resting times and a larger number of stops. Significant differences among treatments were detected in PC1, with

values obtained for exposed individuals being more positive, which is taken to be indicative of slow movements ( $\chi^2 = 4.6$ ,  $df = 6$ ,  $p = 0.032$ , Fig. 2C, and 2D). PC2 compared the number of stops with the other variables (Fig. 2B). However, we found that oral exposure to  $\text{CuSO}_4$  did not result in any significant differences in PC2 ( $\chi^2 = 0.01$ ,  $df = 6$ ,  $p = 0.99$ , Fig. 2C).

Our findings indicate that the oral intoxication with the  $\text{LC}_{50}$  of  $\text{CuSO}_4$  reduced the walking activity of *P. helleri*, since the treated individuals presented more positive loadings in PC1. This behavioral change could be attributed to physiological changes in the nervous system. The exposure to copper and other heavy metal altered the feeding behavior of honeybees (Burden et al. 2019). Moreover, copper poisoning was associated with neurological changes in *D. melanogaster*, indicating that the intoxication with copper-based compounds leads to disruptions of vital behaviors, such as dispersion and reproduction (Arcaya et al. 2013).

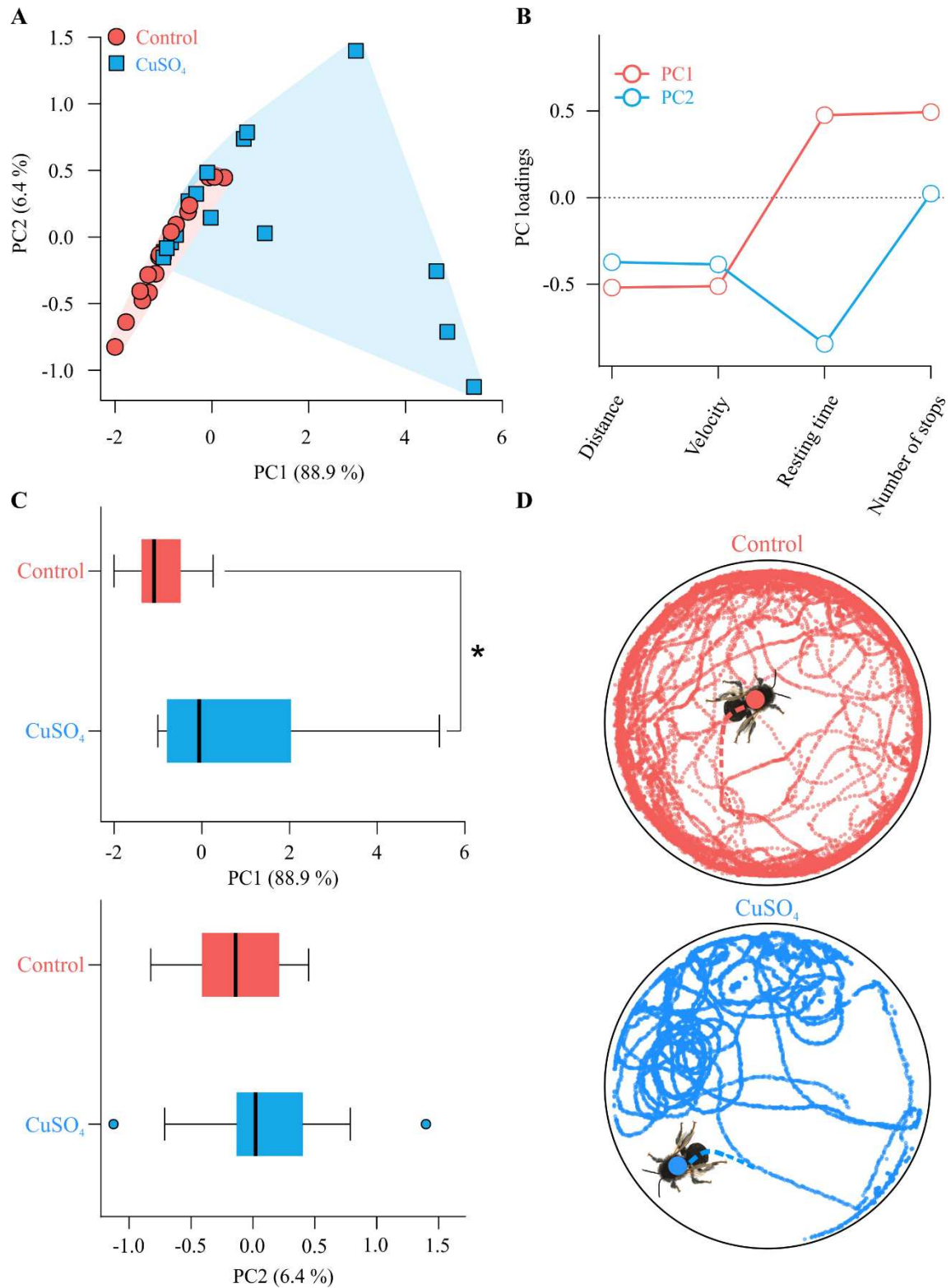


**Figure 2.** Walking behavior of *Partamona helleri* foragers 24 h after exposure to CuSO<sub>4</sub> (LC<sub>50</sub>; 142.95  $\mu\text{g mL}^{-1}$ ) for 3 h. (A) An ordination diagram of the principal component analysis

categorized according to CuSO<sub>4</sub> exposure and control, N = 32 (n = 16 per treatment). The percentage values shown in the axis labels indicate the proportion of the total variance explained by each component. (B) Loadings of the two principal components associated with each behavioral variable. (C) A box plot of the median and range of dispersion (lower and upper quartiles and outliers) of the PC1 (top panel) and PC2 (bottom panel) scores. \*  $p < 0.05$  in GLMM. (D) Individual representative tracks showing the walking behavior of control and CuSO<sub>4</sub>-exposed *P. helleri* foragers.

### 3.3. Morphology of the midgut

The midgut of *P. helleri* foragers comprises an epithelium containing digestive and regenerative cells (Fig. 3A, C). In foragers that ingested the uncontaminated diet (control), the digestive cells have an evident striated border at their apex, and a well-developed PM was observed in the gut lumen, as confirmed by WGA-FITC staining (Fig. 3E). In contrast, the midgut epithelium of bees that ingested the LC<sub>50</sub> of CuSO<sub>4</sub> was characterized by collapsed cells that lacked a striated border (Fig. 3B, D). Moreover, compared with that of the control foragers, the PM was thin (Fig. 3F).

Cellular disintegration in the midgut epithelium, as observed in the present study, has also been reported in adult workers of the honey bee *Apis mellifera* in response to chronic exposure to sublethal doses of calcium oxide nanoparticles and lead oxide (Dabour et al. 2019). Similarly, exposure to the heavy metals cadmium and copper has been observed to affect the size and thickness of the midgut of the fly *Boettcherisca peregrina* (Diptera) and even causes destruction or condensation of the mitochondria of gut cells (Wu et al. 2009). Collectively, these findings indicate that damage caused by nanoparticles (Dabour et al. 2019) or compounds containing heavy metals such as cadmium and copper (Wu et al. 2009) (e.g., CuSO<sub>4</sub> in the present study), have the potential to impair organ function and compromise individual survival.

The weak signal we detected for WGA-FITC fluorescence in the gut lumen of treated bees indicates that oral intoxication with the  $LC_{50}$  of  $CuSO_4$  adversely affects PM synthesis. Similar observations of a perturbed PM have been made in larvae of *A. aegypti* that had ingested heavy metals (Hg, Cd, and Cu) (Rayms-Keller et al. 1998). Moreover, oral intoxication with heavy metals (Cd, Cu, or Zn) has been reported to impair the digestion of ingested food in the third-instar larvae of *Helicoverpa armigera* (Lepidoptera) (Baghban et al. 2014). Based on these observations, we can thus infer that the epithelial degradation induced by  $CuSO_4$  reduces PM synthesis, thereby confirming that heavy metal intoxication negatively influences the structure and homeostasis of the midgut in *P. helleri*.

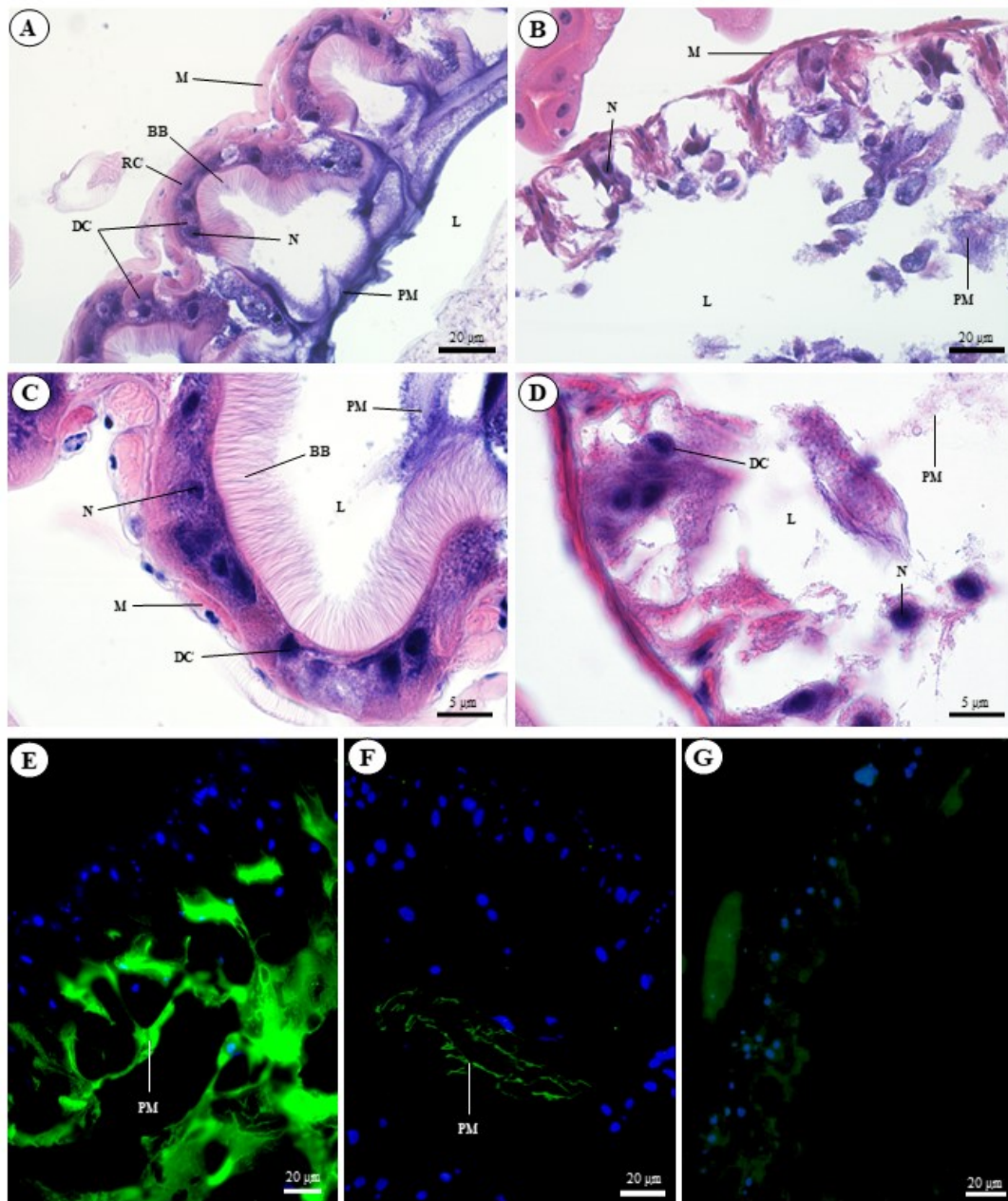


**Figure 3.** Histological sections of the midgut epithelium of *Partamona helleri* foragers orally exposed to a control diet (A, C, E, and G) or to the  $LC_{50}$  of  $CuSO_4$  ( $142.95 \mu g mL^{-1}$ ) (B, D, and F). A-D: Sections stained with hematoxylin and eosin (HE). E-F: Sections stained with wheat germ agglutinin-fluorescein isothiocyanate (WGA-FITC) (green). Cell nuclei are stained with DAPI (blue). (G) Negative control for WGA staining. DC: Digestive cells; RC: regenerative cells; BB: brush border; L: midgut lumen; M: muscle; N: nuclei; PM: peritrophic matrix.

### 3.4. Enzyme activity

Bees orally exposed to CuSO<sub>4</sub> showed a significant increase in CAT (bootstrap = 0.606,  $p = 0.005$ , Fig. 4A) and SOD (bootstrap = 2.21,  $p = 0.01$ , Fig. 4C) activities, as well in levels of MDA (bootstrap = 0.598,  $p = 0.003$ , Fig. 4 D), whereas in contrast, the activity of GST was not significantly altered in response to exposure (bootstrap = 0.686,  $p = 0.11$ , Fig. 4B).

Consistently, it has previously been observed that the activities of both CAT and SOD increased in the foragers of *P. helleri* that were exposed to the insecticide fipronil (Farder-Gomes et al. 2021), indicating that different agrochemicals can induce oxidative stress on these bees. Under these circumstances, elevated SOD and CAT activities would perhaps be expected, given that these enzymes are among the main endogenous defense-related enzymes of the antioxidant system deployed to counter the generation of reactive oxygen species (ROS) (Birben et al. 2012; Hsieh and Hsu 2013), which is known to increase in response to exposure to CuSO<sub>4</sub> (Alaraby et al. 2016; Yang et al. 2019). Moreover, the observed increase in MDA levels indicative of the cell membrane damage promoted by CuSO<sub>4</sub>, as membrane lipids are susceptible to peroxidative attack in response to exposure to CuSO<sub>4</sub> (Buege and Aust 1978; Kalita et al. 2018).

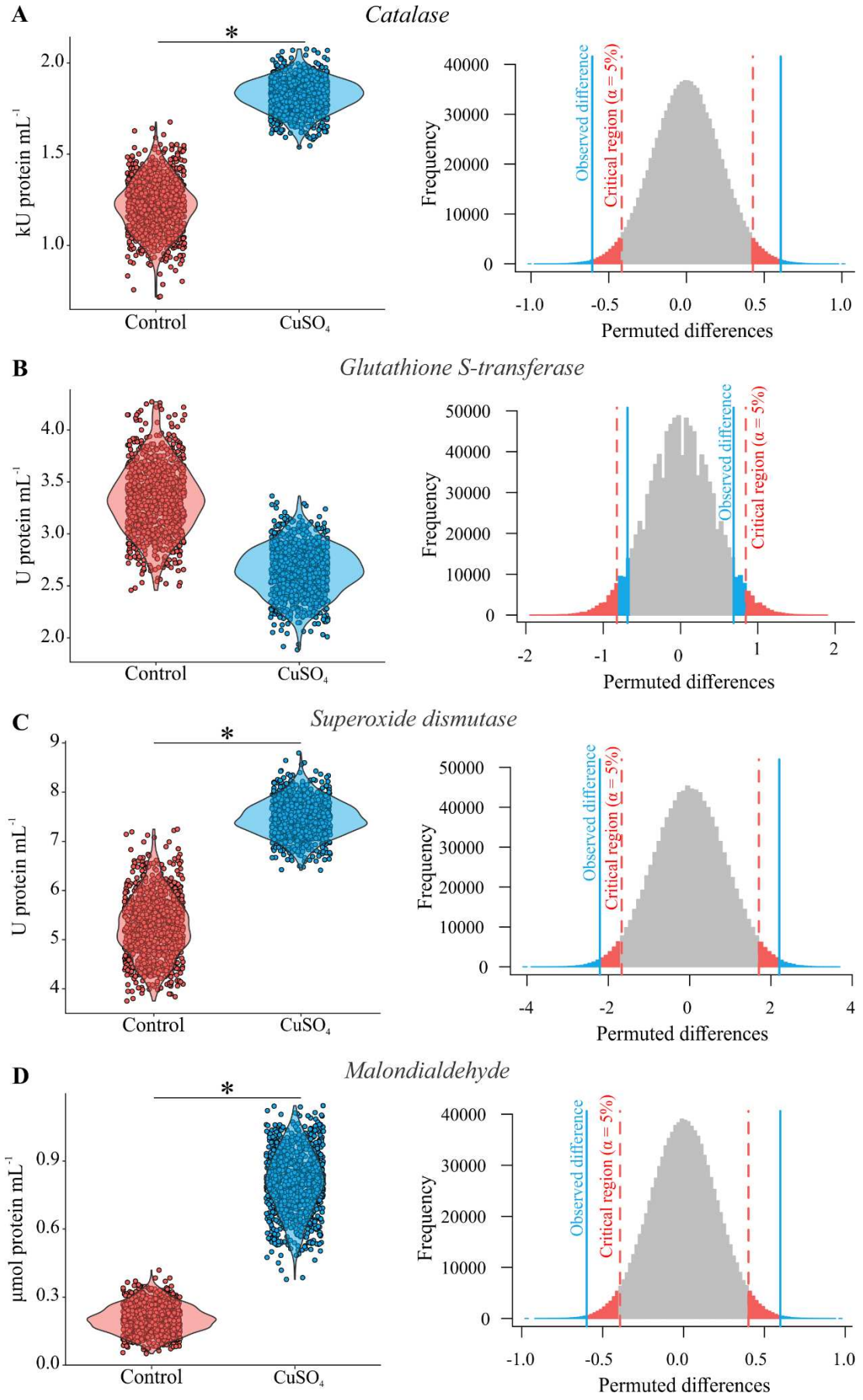


**Figure. 4.** Quantification of the activity of the enzymes catalase (A), glutathione *S*-transferase (B), and superoxide dismutase (C), and of the levels of malondialdehyde (D) in *Partamona helleri* orally exposed to the LC<sub>50</sub> of CuSO<sub>4</sub> (142.95 µg mL<sup>-1</sup>). The violin plots (left panel) show the distribution of the observed data com bootstrap and dots correspond to amostrated values in each 1000 bootstrap interactions in raw dataset (i.e., 6 resamples in each of the 5 replicates in each of the 2 treatments). Histogram (right panel) of the probability distribution of the random difference (permutational difference) in each of the 1000 permutational tests within each of the 1000 bootstrap interaction, totaling 10<sup>6</sup> interactions. The blue lines represent the mean observed difference after all bootstrap interactions. The dashed red lines are the quantiles at 2.5 and 97.5% of the distribution of the permutational difference, that is, it shows the region of rejection of the null hypothesis (i.e., the treatment and control do not differ) at 5% bilateral probability. \*  $p < 0.05$  in permutation tests.

### 3.5. LC3- and caspase-3-positive cells in the midgut

Immunofluorescence analysis revealed that the number of LC3-positive cells in the midgut of control bees was significantly lower ( $1.2 \pm 0.37$ ; mean  $\pm$  standard error) than that in the midgut of CuSO<sub>4</sub>-exposed bees ( $16.8 \pm 1.88$ ) ( $\chi^2 = 7.95$ , d.f. = 8,  $p < 0.001$ , Fig. 5). These data are consistent with the findings of previous studies that have indicated that oral intoxication with the insecticide spinosad or an herbicide mixture (Atrazine + Mesotrione) increased the number of cells positive for LC3 in the midgut of *P. helleri* (Araújo et al. 2019, 2021). In this regard, the higher proportion of autophagic cells in the midgut of exposed bees compared with the controls can be explained in terms of the response to stress induced by the ingestion of CuSO<sub>4</sub>.

Caspase-3-positive cells were only detected in the midgut of exposed bees (mean  $20.4 \pm 1.33$ ; Fig. 5), thereby indicating the occurrence of apoptotic cell death in the midgut

epithelium can be attributed to the oral intoxication with CuSO<sub>4</sub>. This type of cell death is known to occur in response to multiple stimuli, including the accumulation of ROS and oxidative stress (Kannan and Jain 2000; Rost-Roszkowska et al. 2010; Gregorc and Ellis 2011).

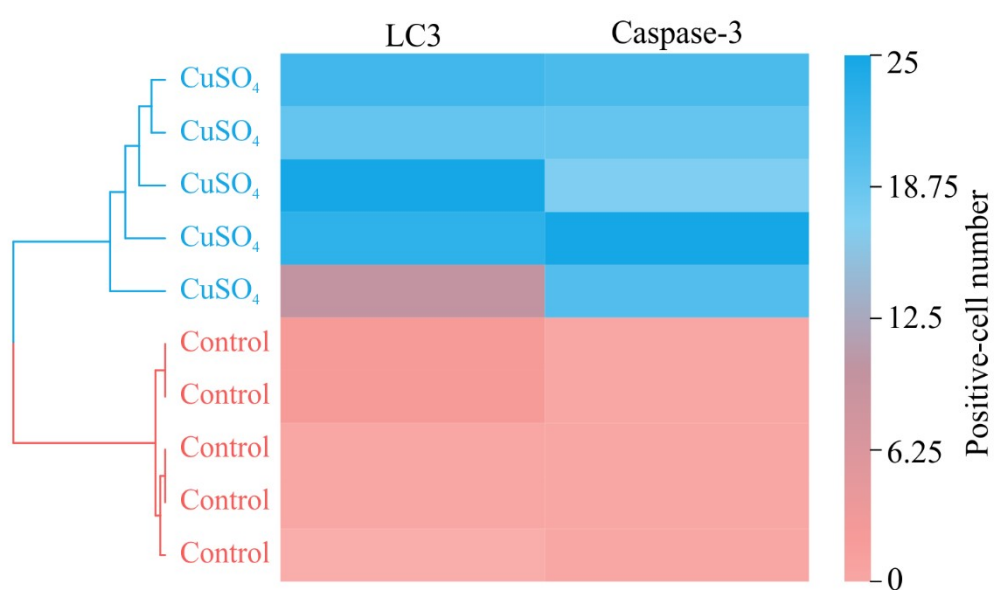


**Figure. 5.** Representative whole mounts (top panel) of the midgut of *Partamona helleri* foragers orally exposed to the LC<sub>50</sub> of CuSO<sub>4</sub> (142.95 µg mL<sup>-1</sup>), showing LC3- and caspase-3-positive cells (green). The nuclei are stained with TO-PRO-3 (red). Hierarchical cluster analysis and heat map representation (bottom panel) were based on the complete linkage method and Euclidean distance of the number of positive cells. N = 10 (five bees for each of the two treatments) for each of the two primary antibodies.

#### 4. Conclusion

In this study, we demonstrate that the CuSO<sub>4</sub> acute ingestion, in a concentration (estimated LC<sub>50</sub> - 142.95 µg mL<sup>-1</sup>) lower than that recommended for use in the field, impaired walking activity, and disrupted midgut morphology and homeostasis in foragers of the stingless bee *P. helleri*. Furthermore, CuSO<sub>4</sub> was found to promote increases in midgut antioxidant activity, autophagy, and apoptosis. Collectively, our findings indicate that when applied as a pesticide/fertilizer, CuSO<sub>4</sub> can have considerable sublethal effects on the midguts of stingless bees, and therefore could pose a potential threat to pollinating insects of native trees as stingless bees.

#### Acknowledgements

We thank the Apiário Central and the Núcleo de Microscopia e Microanálises (NMM-UFV) for technical support.

#### Funding

The project has been supported by the Conselho Nacional de Desenvolvimento Científico e Tecnológico (CNPq, 142206/2017-2 and 301725/2019-5) and Fundação de Amparo à Pesquisa do Estado de Minas Gerais (FAPEMIG, CBB-APQ-00247-384 14). The research was financed by the Universidade Federal de Viçosa and Coordenação de Aperfeiçoamento de Pessoal de Nível Superior (CAPES, Finance code 001),

## References

- Abbott WS (1925) A method of computing the effectiveness of an insecticide. *J Econ Entomol* 18:265–267. <https://doi.org/10.1093/jee/18.2.265a>
- Alaraby M, Hernández A, Marcos R (2016) New insights in the acute toxic/genotoxic effects of CuO nanoparticles in the *in vivo Drosophila* model. *Nanotoxicology* 10:749-760. <http://dx.doi.org/10.3109/17435390.2015.1121413>
- Araújo RS, Bernardes RC, Martins GF (2021) A mixture containing the herbicides Mesotrione and Atrazine imposes toxicological effects on workers of *Partamona helleri* (Friese, 1900). *Sci Total Environ* 763:142980. <https://doi.org/10.1016/j.scitotenv.2020.142980>
- Araújo RS, Lopes MP, Barbosa WF, Gonçalves WG, Fernandes KM, Martins GF, Tavares M.G (2019) Spinosad-mediated effects on survival, overall group activity and the midgut of workers of *Partamona helleri* (Hymenoptera: Apidae). *Ecotoxicol Environ Saf* 175:148-154. <https://doi.org/10.1016/j.ecoenv.2019.03.050>
- Arcaya JL, Tejeda CM, Salazar U, Silva EJ, Urdaneta K, Varela K (2013) Copper intoxication decreases lifespan and induces neurologic alterations in *Drosophila melanogaster*. *Invest Clin* 54:47-57. <https://europepmc.org/article/med/23781712>
- Baghban A, Sendi J, Khosravi R, Zibaee A (2014) Effect of heavy metals (Cd, Cu, and Zn) on feeding indices and energy reserves of the cotton boll worm *Helicoverpa armigera* Hübner (Lepidoptera: Noctuidae). *J Plan Protec Res* 54:367-373. <https://doi.org/10.2478/jppr-2014-0055>
- Barbosa WF, Tomé HVV, Bernardes RC, Siqueira MAL, Smagghe G, Guedes RNC (2015) Biopesticide-induced behavioral and morphological alterations in the stingless bee *Melipona quadrifasciata*. *Environ Toxicol Chem* 34:2149-2158. <https://doi.org/10.1002/etc.3053>

Bernardes RC, Barbosa WF, Martins GF, Lima MAP (2018) The reduced-risk insecticide azadirachtin poses a toxicological hazard to stingless bee *Partamona helleri* (Friese, 1900) queens. *Chemosphere* 201:550-556. <https://doi.org/10.1016/j.chemosphere.2018.03.030>

Bernardes RC, Lima MAP, Guedes RNC, Silva CB, Martins GF (2021) Ethoflow: computer vision and artificial intelligence-based software for automatic behavior analysis. *Sensors* 21. <https://doi.org/10.3390/s21093237>

Bernardes RC, Tomé HVV, Barbosa WF, Guedes RNC, Lima MAP (2017) Azadirachtin-induced antifeeding in Neotropical stingless bees. *Apidologie* 48:275-285. <https://doi.org/10.1007/s13592-016-0473-3>

Birben E, Sahiner UM, Sackesen C, Erzurum S, Kalayci O (2012) Oxidative stress and antioxidant defense. *W All Organ J* 5:9-19. <https://doi.org/10.1097/WOX.0b013e3182439613>

Bonilla-Ramirez L, Jimenez-Del-Rio M, Velez-Pardo C (2011) Acute and chronic metal exposure impairs locomotion activity in *Drosophila melanogaster*: a model to study Parkinsonism. *Biometals* 24:1045-1057. <https://doi.org/10.1007/s10534-011-9463-0>

Botina LL, Bernardes RC, Barbosa WF, Lima MP, Guedes RN, Martin G (2020) Toxicological assessments of agrochemical effects on stingless bees (Apidae, Meliponini). *MethodsX* 7:100906. <https://doi.org/10.1016/j.mex.2020.100906>

Botina LL, Velez M, Barbosa WF, Mendonça AC, Pylro VS, Totola MR, Martins GF (2019) Behavior and gut bacteria of *Partamona helleri* under sublethal exposure to a bioinsecticide and a leaf fertilizer. *Chemosphere* 234:187-195. <https://doi.org/10.1016/j.chemosphere.2019.06.048>

Braga J, Sales É, Neto J, Conde M, Barth OM, Lorenzon MC (2012) Floral sources to *Tetragonisca angustula* (Hymenoptera: Apidae) and their pollen morphology in a Southeastern

Brazilian Atlantic Forest. Rev Biol Trop 60:1491-1501.

[https://www.scielo.sa.cr/scielo.php?script=sci\\_arttext&pid=S0034-77442012000400007](https://www.scielo.sa.cr/scielo.php?script=sci_arttext&pid=S0034-77442012000400007)

Buege JA, Aust SD (1978) Microsomal lipid peroxidation. Meth Enz 52:302-310.  
[https://doi.org/10.1016/S0076-6879\(78\)52032-6](https://doi.org/10.1016/S0076-6879(78)52032-6)

Burden CM, Morgan MO, Hladun KR, Amdam G, Trumble JJ, Smit BH (2019) Acute sublethal exposure to toxic heavy metals alters honey bee (*Apis mellifera*) feeding behavior. Sci Rep 9:1–10. <https://doi.org/10.1038/s41598-019-40396-x>

Cai LM, Wang QS, Wen HH, Luo J, Wang S (2019) Heavy metals in agricultural soils from a typical township in Guangdong Province, China: occurrences and spatial distribution. Ecotoxicol Environ Saf 168:184-191. <https://doi.org/10.1016/j.ecoenv.2018.10.092>

Camargo JM, Pedro SR (2003) Neotropical Meliponini: the genus *Partamona* Schwarz, 1939 (Hymenoptera, Apidae, Apinae) - bionomy and biogeography. Rev Bras Entom 47:311-372. <https://doi.org/10.1590/S0085-56262003000300001>

Cham KO, Nocell RC, Borges LO, Viana-Silva FEC, Tonelli CAM, Malaspina O, Menezes C, Rosa-Fontana AS, Blochtein B, Freitas BM, Pires CSS (2019) Pesticide exposure assessment paradigm for stingless bees. Environ Entom 48:36-48.  
<http://hdl.handle.net/11449/190115>

Crawley MJ (2012) The R book, 2nd edn. Wiley, Chichester.

Dabour K, Al Nagggar Y, Masry S, Naiem E, Giesy JP (2019) Cellular alterations in midgut cells of honey bee workers (*Apis mellifera* L.) exposed to sublethal concentrations of CdO or PbO nanoparticles or their binary mixture. Sci Total Environ 651:1356-1367.  
<https://doi.org/10.1016/j.scitotenv.2018.09.311>

Deng DM, Shu WS, Zhang J, Zou HL, Lin Z, Ye ZH, Wong M (2007) Zinc and cadmium accumulation and tolerance in populations of *Sedum alfredii*. Environ Pollut 147:381-386. <https://doi.org/10.1016/j.envpol.2006.05.024>

Desoky AEAS, Omran NS, Omar MOM, Hussein MH, Abd-Allah MM (2019) Heavy metals concentrations in bee products collected from contaminated and non-contaminated areas from Upper Egypt Governorates. J Adv Agric 10:1657–1666. <https://doi.org/10.24297/jaa.v10i0.8149>

Di N, Hladu KR, Zhang K, Liu TX, Trumble JT (2016) Laboratory bioassays on the impact of cadmium, copper and lead on the development and survival of honeybee (*Apis mellifera* L.) larvae and foragers. Chemosphere 152:530-538. <http://dx.doi.org/10.1016/j.chemosphere.2016.03.033>

Efron B (1992) Bootstrap methods: another look at the jackknife. In: Kotz S., Johnson N.L. (eds) Breakthroughs in Statistics. Springer Series in Statistics (Perspectives in Statistics). Springer, New York, NY.

Fageria NK, Baligar C, Clark RB (2002) Micronutrients in crop production. Adv Agron 77: 185-268. [https://doi.org/10.1016/s0065-2113\(02\)77015-6](https://doi.org/10.1016/s0065-2113(02)77015-6)

Farder-Gomes CF, Fernandes KM, Bernardes RC, Bastos DSS, Martins GF, Serrão JE (2021) Acute exposure to fipronil induces oxidative stress, apoptosis and impairs epithelial homeostasis in the midgut of the stingless bee *Partamona helleri* Friese (Hymenoptera: Apidae). Sci. Total Environ. 774:145679. <https://doi.org/10.1016/j.scitotenv.2021.145679>

Giannini KM (1997) Labor division in *Melipona compressipes fasciculata* Smith (Hymenoptera: Apidae: Meliponinae). An Soc Entomol Bras 26:153–162. <https://doi.org/10.1590/S0301-80591997000100020>

Goretti E, Pallottini M, Rossi R, La Porta G, Gardi T, Goga BC, Elia AC, Galletti M, Moroni B, Petroselli C, Selvaggi R, Cappelletti D (2020) Heavy metal bioaccumulation in honey bee matrix, an indicator to assess the contamination level in terrestrial environments. *Environ Pollut* 256:113388. <https://doi.org/10.1016/j.envpol.2019.113388>

Gregorc A, Ellis JD (2011) Cell death localization in situ in laboratory reared honey bee (*Apis mellifera* L.) larvae treated with pesticides. *Pest Biochem Phys* 99:200-207. <https://doi.org/10.1016/j.pestbp.2010.12.005>

Habig WH, Pabst MJ, Jakoby WB (1974) Glutathione S-transferases the first enzymatic step in mercapturic acid formation. *J Biol Chem* 249:7130-7139. [https://doi.org/10.1016/S0021-9258\(19\)42083-8](https://doi.org/10.1016/S0021-9258(19)42083-8)

Hadwan MH, Abed HN (2016) Data supporting the spectrophotometric method for the estimation of catalase activity. *Data Brief* 6:194-199. <http://dx.doi.org/10.1016/j.dib.2015.12.012>

Hendriksma HP, Härtel S, Steffan-Dewenter I (2011) Honey bee risk assessment: new approaches for in vitro larvae rearing and data analyses. *Meth Ecol Evo* 2:509-517. <https://doi.org/10.1111/j.2041-210X.2011.00099.x>

Hladun KR, Di N, Liu TX, Trumble JT (2016) Metal contaminant accumulation in the hive: consequences for whole-colony health and brood production in the honey bee (*Apis mellifera* L.). *Environ Toxicol Chem* 35:322-329. <https://doi.org/10.1002/etc.3273>

Hladun KR, Parker DR, Trumble JT (2015) Cadmium, Copper, and Lead accumulation and bioconcentration in the vegetative and reproductive organs of *Raphanus sativus*: implications for plant performance and pollination. *J Chem Ecol* 41:386-395. <https://doi.org/10.1007/s10886-015-0569-7>

Hongxia S, Ying LIU, Guren Z (2010) Effects of heavy metal pollution on insects. Europe PMC 178-185. <https://europepmc.org/article/cba/634314>

Hsieh YS, Hsu CY (2013) Oxidative stress and anti-oxidant enzyme activities in the trophocytes and fat cells of queen honeybees (*Apis mellifera*). Rejuvenation Res 16:295-303. <https://doi.org/10.1089/rej.2013.1420>

Hwang JE, Bruyne M, Warr CG, Burke R (2014) Copper overload and deficiency both adversely affect the central nervous system of *Drosophila*. Metallomics 6:2223-2229. <https://doi.org/10.1039/c4mt00140k>

Jacob CRO, Soares HM, Nocelli RC, Malaspina O (2015) Impact of fipronil on the mushroom bodies of the stingless bee *Scaptotrigona postica*. Pest Manag Sci 71:114-122. <https://doi.org/10.1002/ps.3776>

Kalita J, Kumar V, Misra UK, Bora HK (2018) Memory and learning dysfunction following copper toxicity: biochemical and immunohistochemical basis. Mol Neurobiol 55: 3800-3811. <https://doi.org/10.1007/s12035-017-0619-y>

Kannan K, Jain SK (2000) Oxidative stress and apoptosis. Pathophysiology 7:153-163. 10.1016/s0928-4680(00)00053-5

Kerr WE, Carvalho GA, Silva ACD, Assis MDGPD (2010) Aspectos pouco mencionados da biodiversidade amazônica. Parc Estrat 6:20-41. [http://200.130.27.16/index.php/parcerias\\_estrategicas/article/viewFile/183/177](http://200.130.27.16/index.php/parcerias_estrategicas/article/viewFile/183/177)

Kerr WE, Santos-Neto GR (1956) Contribuição para o Conhecimento da Bionomia dos Meliponini 5. Divisão de Trabalho entre as operárias de *Melipona quadrifasciata quadrifasciata* Lep. Insectes Soc 3:423–430. <https://doi.org/10.1007/BF02225762>

Lima MAP, Martins GF, Oliveira EE, Guedes RNC (2016) Agrochemical induced stress in stingless bees: peculiarities, underlying basis, and challenges. *J Comp Physiol A Neuroethol Sens Neural Behav Physiol* 202:733-747. 10.1007/s00359-016-1110-3

Lima MAP, Pires CSS, Guedes RNC, Campos, LAO (2013) Lack of lethal and sublethal effects of Cry1Ac Bt-toxin on larvae of the stingless bee *Trigona spinipes*. *Apidologie* 44:21–28. <https://doi.org/10.1007/s13592-012-0151-z>

Lunneborg CE (2014) Permutation based inference. In *Wiley StatsRef: Statistics Reference Online* (eds N. Balakrishnan, T. Colton, B. Everitt, W. Piegorisch, F. Ruggeri and J.L. Teugels). 18445112.stat06178.

MAPA, 2020. AGROFIT - Sistema de Agrotóxicos Fitosanitários [Ministério da Agricultura Pecuária e Abastecimento]. Available at: [http://extranet.agricultura.gov.br/agrofit\\_cons/principal\\_agrofit\\_cons](http://extranet.agricultura.gov.br/agrofit_cons/principal_agrofit_cons).

Marklund S, Marklund G (1974) Involvement of the superoxide anion radical in the autoxidation of pyrogallol and a convenient assay for superoxide dismutase. *Eur J Biochem* 47:469-474. <https://doi.org/10.1111/j.1432-1033.1974.tb03714.x>

Marques RD, Lima MAP, Marques RD, Bernardes RC (2020) A spinosad-based formulation reduces the survival and alters the behavior of the stingless bee *Plebeia lucii*. *Neotropical Entomology* 49:578-585. <https://doi.org/10.1007/s13744-020-00766-x>

Michaud JP, Grant AK (2003) Sub-lethal effects of a copper sulfate fungicide on development and reproduction in three coccinellid species. *J Insect Sci* 3:1-6. <https://doi.org/insectscience.org/3.16>

Pedro SRM (2014) The stingless bee fauna in Brazil (Hymenoptera: Apidae). *Sociobiology* 61:348-354. <https://doi.org/10.13102/sociobiology.v61i4.348-354>

Peña MM, Lee J, Thiele DJ (1999) A delicate balance: homeostatic control of copper uptake and distribution. *J Nutr* 129:1251-1260. <https://doi.org/10.1093/jn/129.7.1251>

Pereira, R.C., Barbosa, W.F., Lima, M.A.P., Vieira, J.O.L., Guedes, R.N.C., da Silva, B.K.R., Fernandes, F.L., 2020. Toxicity of botanical extracts and their main constituents on the bees *Partamona helleri* and *Apis mellifera*. *Ecotoxicology* 29:246-257. <https://doi.org/10.1007/s10646-020-02167-7>

Ramalho M (2004) Stingless bees and mass flowering trees in the canopy of Atlantic Forest: a tight relationship. *Acta Bot Bras* 181:37-47. <http://dx.doi.org/10.1590/S0102-33062004000100005>

Rayms-Keller A, Olson KE, McGaw M, Oray C, Carlson JO, Beaty BJ (1998) Effect of heavy metals on *Aedes aegypti* (Diptera: Culicidae) larvae. *Ecotoxicol Environ Saf* 39:41-47. <http://dx.doi.org/10.1006/eesa.1997.1605>

R Core Team (2020) R: A language and environment for statistical computing. R foundation for statistical computing, Vienna, Austria. <https://www.R-project.org/>.

Rodrigues CG, Krüger AP, Barbosa WF, Guedes RNC (2016) Leaf fertilizers affect survival and behavior of the neotropical stingless see *Friesella schrottkyi* (Meliponini: Apidae: Hymenoptera). *J Econ Entomol* 109:1001-1008. <http://dx.doi.org/10.1093/jee/tow044>

Rost-Roszkowska MM, Poprawa I, Chachulska-Zymelka A (2010) Apoptosis and autophagy in the midgut epithelium of *Acheta domesticus* (Insecta, Orthoptera, Gryllidae). *Zool Sci* 27:740-745. <https://doi.org/10.2108/zsj.27.740>

Simões D, Bego LR (1979) Estudo da regulação social em *Nannotrigona* (*Scaptotrigona*) *postica* Latreille, em duas colônias (normal e com rainhas virgens, com especial referência ao polietismo etário (Hym., apidae, Meliponinae). *Bol Zool* 4:89-98. <https://doi.org/10.11606/issn.2526-3358.bolzoo.1979.121832>

Steinhauer N, Kulhanek K, Antúnez K, Human H, Chantawannakul P, Chauzat MP (2018) Drivers of colony losses. *Curr Opin Insect Sci* 26:142-148. <https://doi.org/10.1016/j.cois.2018.02.004>

Tchounwou PB, Yedjou CG, Patlolla AK, Sutton DJ (2012) Heavy metal toxicity and the environment. *Molecular, Clinical and Environmental Toxicology* 101, 133-164. [https://doi.org/10.1007/978-3-7643-8340-4\\_6](https://doi.org/10.1007/978-3-7643-8340-4_6)

Tomé HVV, Barbosa WF, Martins GF, Guedes RNC (2015) Spinosad in the native stingless bee *Melipona quadrifasciata*: regrettable non-target toxicity of a bioinsecticide. *Chemosphere* 124:103-109. <http://dx.doi.org/10.1016/j.chemosphere.2014.11.038>

Tomé HVV, Martins GF, Lima MAP, Campos LAO, Guedes RNC (2012) Imidacloprid-induced impairment of mushroom bodies and behavior of the native stingless bee *Melipona quadrifasciata* anthidioides. *PLoS One* 7:e38406. <http://dx.doi.org/10.1371/journal.pone.0038406>

Tomé HV, Ramos GS, Araújo MF, Santana WC, Santos GR, Guedes RNC, Maciel CD, Newland PL, Oliveira EE (2017). Agrochemical synergism imposes higher risk to Neotropical bees than to honeybees. *R Soc Open Sci* 4:160866. <http://dx.doi.org/10.1098/rsos.160866>

Tomé HV, Schmeh DR, Wedde AE, Godoy RS, Ravaiano SV, Guedes RN, Martins GF, Ellis JD (2020) Frequently encountered pesticides can cause multiple disorders in developing worker honey bees. *Environ Pollut* 256:113420. <http://dx.doi.org/10.1016/j.envpol.2019.113420>

vanEngelsdorp D, Meixner MD (2010) A historical review of managed honey bee populations in Europe and the United States and the factors that may affect them. *J Invertebr Pathol* 103:80-95. <http://dx.doi.org/10.1016/j.jip.2009.06.011>

Viana, T.A., Barbosa, W.F., Lourenço, A.P., Santana, W.C., Campos, L.A.O, Martins, G.F., 2021. Changes in innate immune response and detoxification in *Melipona quadrifasciata* (Apinae: Meliponini) on oral exposure to azadirachtin and spinosad. *Apidologie* 52:252-261. <http://dx.doi.org/10.1007/s13592-020-00814-w>

Wang S, Shi X (2001) Molecular mechanisms of metal toxicity and carcinogenesis. *Mol Cell Biochem* 222:3-9.

Worku Y, Hailu B (2018) The effects of compost and effective microorganism on taking up tending of heaving metals by vegetables. *Int J Adv Res Biol Sci* 5:51-59. <http://dx.doi.org/10.22192/ijarbs.2018.05.03.007>

Wu GX, Gao X, Ye GY, Li K, Hu C, Cheng JA (2009) Ultrastructural alterations in midgut and Malpighian tubules of *Boettcherisca peregrina* exposure to cadmium and copper. *Ecotoxicol Environ Saf* 72:1137-1147. <http://dx.doi.org/10.1016/j.ecoenv.2008.02.017>

Yang F, Pei R, Zhang Z, Liao J, Yu W, Qiao N, Pan J (2019) Copper induces oxidative stress and apoptosis through mitochondria-mediated pathway in chicken hepatocytes. *Toxicol Vitro* 54:310-316. <https://doi.org/10.1016/j.tiv.2018.10.017>

Yarsan E, Karacal F, Ibrahim IG, Dikmen B, Koksall A, Das YK (2007) Contents of some metals in honeys from different regions in Turkey. *Bull Environ Contam Toxicol* 79:255–258. <https://doi.org/10.1007/s00128-007-9034-9>

**CHAPTER 4. A mixture containing the herbicides Mesotrione and Atrazine imposes toxicological risks on workers of *Partamona helleri***



Contents lists available at ScienceDirect

Science of the Total Environment

journal homepage: [www.elsevier.com/locate/scitotenv](http://www.elsevier.com/locate/scitotenv)

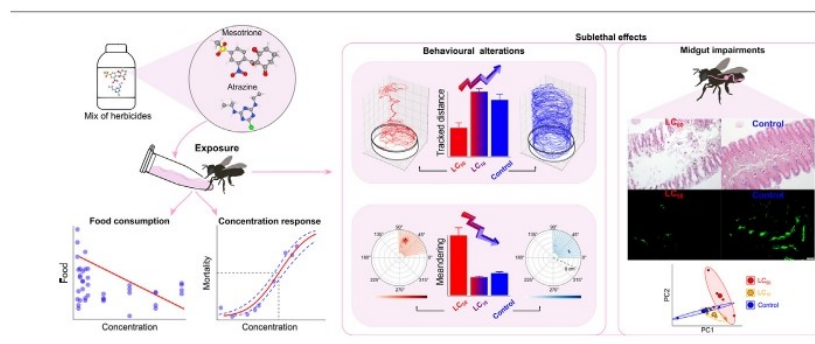
# A mixture containing the herbicides Mesotrione and Atrazine imposes toxicological risks on workers of *Partamona helleri*

Renan dos Santos Araújo<sup>a,\*</sup>, Rodrigo Cupertino Bernardes<sup>a</sup>, Gustavo Ferreira Martins<sup>b</sup><sup>a</sup> Departamento de Entomologia, Universidade Federal de Viçosa, Viçosa, MG 36570-900, Brazil<sup>b</sup> Departamento de Biologia Geral, Universidade Federal de Viçosa, Viçosa, MG 36570-900, Brazil

## HIGHLIGHTS

- The oral exposure to the mix of herbicides interfered with behaviour and food consumption of *Partamona helleri*.
- The exposure led to damages of the midgut epithelium and peritrophic matrix.
- The exposure changed the number of cells positive for signalling-pathway proteins.

## GRAPHICAL ABSTRACT



## ARTICLE INFO

## Article history:

Received 24 July 2020

Received in revised form 30 September 2020

Accepted 4 October 2020

Available online 14 October 2020

Editor: Henner Hollert

## Keywords:

Stingless bee

Herbicide

Midgut

Peritrophic matrix

Cell signalling

## ABSTRACT

A mixture of Mesotrione and Atrazine (Calaris®) has been reported as an improvement of the atrazine herbicides, which are agrochemicals used for weed control. However, its possible harmful effects on non-target organisms, including pollinators, needs to be better understood. In this work, the effects of the mix of herbicides on food consumption, behaviour (walking distance, and meandering), and the morphology of the midgut of the stingless bee *Partamona helleri* were studied. Foragers were orally exposed to different concentrations of the mix. The concentrations leading to 10% and 50% mortality ( $LC_{10}$  and  $LC_{50}$ , respectively) were estimated and used in the analysis of behaviour and morphology. The ingestion of contaminated diets (50% aqueous sucrose solution + mix) led to a reduction in food consumption by the bees when compared to the control, bees fed a non-contaminated diet (sucrose solution). Ingestion of the  $LC_{50}$  diet reduced locomotor activity, increased meandering, induced the degradation of the epithelium and peritrophic matrix, and also changed the number of cells positive for signalling-pathway proteins in the midgut. These results show the potential toxicological effects and environmental impacts of the mix of herbicides in beneficial insects, including a native bee.

© 2020 Elsevier B.V. All rights reserved.

## 1. Introduction

Stingless bees (Apidae: Meliponini) are considered efficient pollinators of many species of wild flora and various crops of economic value in tropical and subtropical regions (Hrncir et al., 2016; Azmi et al., 2019;

Machado et al., 2020). These generalist bees are visitors of flowers of countless species (Heard, 1999). During the visits, they may be exposed to agrochemicals, such as herbicides, sprayed on many crops, which may represent a threat to the survival and maintenance of the bee colonies (Revised in Lima et al., 2016; Seide et al., 2018; Belsky and Joshi, 2020; Vázquez et al., 2020).

Herbicides are used to control weeds that absorb these compounds through the leaves, stems, or roots (Kraehmer et al., 2014a, 2014b;

\* Corresponding author.

E-mail addresses: [renan.s.araujo@ufv.br](mailto:renan.s.araujo@ufv.br) (R.S. Araújo), [gmartins@ufv.br](mailto:gmartins@ufv.br) (G.F. Martins).

Wang et al., 2018; Albuquerque et al., 2020). Herbicides interfere with specific metabolic pathways and kill the target weed by acting on growth regulators, inhibitors (seedling growth, photosynthesis, and biosynthesis of amino acids, lipids, and pigments) or act as cell membrane disruptors (Peterson et al., 2015; Revised in Lushchak et al., 2018).

Mesotrione [2-(4-mesyl-2-nitrobenzoyl)cyclohexane-1,3-dione] and Atrazine (2-chloro-4-ethylamino-6-isopropylamino-1,3,5-triazine) are among the most used herbicides worldwide (Barchanska et al., 2012). Mesotrione, a tricyclic, is an inhibitor of the enzyme 4-hydroxyphenylpyruvate dioxygenase and is one of the best-selling herbicides in the world (Dumas et al., 2017; Carles et al., 2017). Atrazine inhibits the photosystem II by binding on the plastoquinone (Farland et al., 2008). Although banned in the European Union since 2007, Atrazine is widely used in countries, including Brazil and the United States (Fernandes et al., 2020; MAPA, 2020). A formulation (Calaris®) containing a mixture of Mesotrione and Atrazine was developed by Syngenta and has been considered an upgrading of atrazine herbicides (Matte et al., 2018; Syngenta, 2020).

Poisoning by Mesotrione or Atrazine can cause damage to arthropods. For example, Mesotrione increases the mortality of the mite *Tetranychus urticae* (Schmidt-Jeffris and Cutulle, 2019), and Atrazine delays the maturation and induces molting errors in the spider *Pardosa milvina* (Godfrey and Rypstra, 2018). Atrazine poisoning in insects can result in changes in survival, reproduction, longevity, development time, body size, and locomotion, depending on the species (Vogel et al., 2015; Marcus and Fiumera, 2016; Ejomah et al., 2020). In addition, Atrazine poisoning can cause changes in the physiology of insects, such as dysfunction in the endocrine system (McCallum et al., 2013), neurotransmission (Papaefthimiou et al., 2003), and in the expression of genes associated with detoxification (Le Goff et al., 2006), and proteins related to oxidative stress and energy production (Thornton et al., 2010). In *Apis mellifera* bees, Atrazine poisoning decreased acetylcholine activity (Boily et al., 2013) and increased lipid peroxidation (Helmer et al., 2015). However, the toxicological effects of these herbicides on stingless bees are still unknown.

The toxicological risk of agrochemicals in bees includes, among other stressors, the lethal and sublethal effects (Rortais et al., 2017; Delkash-Roudsari et al., 2020). Sublethal effects are relevant because they can interfere with the development, behaviour, reproduction, and physiology of organs such as the midgut. The midgut epithelium of bees comprises the enterocytes (or digestive cells), which synthesise digestive enzymes and absorb nutrients; regenerative or stem cells, responsible for the cell renewal; and enteroendocrine cells that synthesise neuropeptides (Martins et al., 2006; Cruz Landim, 2009; Christie, 2020). The midgut epithelium or peritrophic matrix (PM; an extracellular matrix that protects the midgut epithelium) may also be compromised after oral exposure of bees to agrochemicals with different spectra of action (Desneux et al., 2007; Oliveira et al., 2013; Lopes et al., 2018; Araujo et al., 2019a, 2019b; Carneiro et al., 2020). However, the effects of herbicides on endocrine cells and proteins of signalling pathways related to the process of proliferation and differentiation of cells in the midgut have not yet been studied.

Given that herbicides potentially cause damage to bees, this work aims to evaluate the effects of oral exposure to the mix of herbicides (Mesotrione + Atrazine) on the stingless bee workers, *Partamona helleri*. The food consumption, behaviour (walking distance and meandering), and morphology of the midgut epithelium were assessed after oral intoxication and compared to the controls (non-intoxicated individuals). In addition to identifying the effects of intoxication with the mix of herbicides, the integrity of the PM was checked, and the midgut cells were tested for different cell markers, including the FMRFamide neuropeptide (H-Phe-Met-Arg-Phe-NH<sub>2</sub>) and proteins related to cell proliferation and differentiation.

## 2. Material and methods

### 2.1. Bees and herbicide mix

Adult workers of *P. helleri* were collected from four colonies kept in the experimental apiary at the Universidade Federal de Viçosa (UFV), Viçosa, MG, Brazil (20° 75'S 42° 86'W) under the license ID 75536 (ICMBio – SISBIO, Ministério do Meio Ambiente, Brazil). Foragers were used in all experiments; these bees go out to collect food resources in the field and can be exposed to agrochemicals during their outside activities (Tomé et al., 2017; Botina et al., 2020). The bees (20–30 days old) were collected at the entrance of each colony with a glass Erlenmeyer flask which was placed at the exit of the hive. The collected foragers were taken to the laboratory and were kept in an incubator at 28 °C and 80% humidity in the dark for 1 h for acclimation (Botina et al., 2020).

The bees were exposed to a mix of Mesotrione and Atrazine in their commercial formulation [Calaris® - active ingredients: Mesotrione (50 g/L) and Atrazine (500 g/L); formulation adjuvants (597 g/L); concentrated suspension; Syngenta, São Paulo, SP, (Brazil)] registered for agricultural use in Brazil. A stock solution was prepared by diluting the commercial formulation of the mix at the maximum recommended rate for the field (i.e., 240 mL of the mix in 20 L of water) in 50% aqueous sucrose solution, according to the manufacturer's recommendations for the control of morning glory weeds (*Ipomoea hederifolia*, *Ipomoea nil*, *Ipomoea quamoclit*, and *Merremia cissoides*) and crabgrass (*Digitaria ciliaris*, and *Digitaria nuda*) in sugarcane (*Saccharum officinarum*) cultivation. The dilution of the stock solution of the mix was prepared by diluting 300 µL in 25 mL of 50% aqueous sucrose solution. This herbicide solution was considered as the 100% concentration and was used as a basis to acquire eight more successive dilutions that resulted in the concentrations used in the concentration-mortality bioassay (Section 2.2).

### 2.2. Concentration-mortality and food consumption bioassays

After the acclimation period, ten foragers from each colony were transferred to plastic pots with a volume of 250 mL, with each pot equivalent to an experimental unit. The bees were exposed orally to the solution of the mix of herbicides through a hole made in microtubes (1.5 mL) of a centrifuge which was inserted into the wall of each plastic pot. The mix of herbicides was used in the following concentrations: 100%, 75%, 50%, 25%, 10%, 7.5%, 5%, 2.5%, and 1% (OECD, 2017; Botina et al., 2020). These concentrations (except 100%) are below than recommended for the use in the field according to the manufacturer's instructions and, similar to the ingestion of food contaminated by herbicides in natural conditions. The contaminated diet was offered to the bees for 3 h (Tomé et al., 2015; Bernardes et al., 2018; Araujo et al., 2019a). After this period, the microtubes were replaced, and the bees were fed *ad libitum* with a 50% sucrose solution (without herbicide) for 24 h. This 50% sucrose solution was offered to the control group only once, which had ten foragers from each colony, and was sufficient to feed the bees during the experiment (27 h). All bees were kept under controlled conditions as described above. Bees devoid of the movement were described as dead. In this bioassay, 50% and 10% lethal concentrations (LC<sub>50</sub> and LC<sub>10</sub>, respectively) were estimated and used in subsequent bioassays.

The effects on bees' food consumption after oral exposure to the mix of herbicides were analysed by weighing the microtubes containing the diets. The microtubes with different concentrations (Section 2.2) were weighed separately, before and after 3 h of the exposure, on an analytical balance (XS3DU, Mettler Toledo, Columbus, OH). Therefore, food consumption was recorded in grams (g), corresponding to the average consumption of the ten bees in each experimental unit (Botina et al., 2020).

### 2.3. Behavioural bioassay

The behaviour was monitored for 24 h after the workers' exposure for three hours to the LC<sub>50</sub> and LC<sub>10</sub> concentrations determined in the concentration-mortality bioassay and control. The behaviour of groups of five workers from each of the four colonies for each of the three treatments (total  $N = 60$ ) was recorded for 10 min with a digital video camera (HDR-XR520V, Sony) at 30 frames per second and in high definition (1920 × 1080 pixels). These records were made in a bright room with artificial led light at  $25 \pm 3$  °C. The videos were analysed using the EthoFlow® software (Instituto Nacional de Propriedade Industrial - INPI, Brazil, BR 512020 000737-6; Bernardes et al., 2020) to calculate the distance travelled (cm) by the workers in the arenas (Petri dishes of 9 cm diameter x 2 cm high). This software was also used to evaluate the behaviour of meandering ( $^{\circ} \text{cm}^{-1}$ ), which is based on the polar coordinates of the movement (defined as the sum of the azimuth angles divided by the sum of the rays of the movement).

### 2.4. Histology of the midgut and WGA-FITC staining

Foragers exposed to the LC<sub>50</sub> ( $n = 5$ ) and LC<sub>10</sub> ( $n = 5$ ) concentrations and the controls ( $n = 5$ ) were anaesthetised at  $-20$  °C for 1.5 min and dissected in insect physiological solution (0.1 M NaCl, 20 mM KH<sub>2</sub>PO<sub>4</sub> and 20 mM Na<sub>2</sub>HP<sub>4</sub>). The midguts were fixed in Zamboni solution (4% paraformaldehyde, Sorensen's phosphate buffer, and saturated picric acid solution) for 2 h at  $25 \pm 2$  °C. The organs were washed and stored overnight in sodium phosphate buffer (0.1 PBS, pH 7.2). Samples were dehydrated in an ascending series of ethanol (70%, 80%, 90%, 95%, and 99%) embedded in Leica® historesin (Leica Biosystems Nussloch GmbH, Heidelberg, Germany) and sectioned at 5  $\mu\text{m}$  thick with a glass knife on an automatic microtome. The sections were stained with hematoxylin and eosin for 15 min and 1 min, respectively, analysed, and photographed with an Olympus BX53 light microscope connected to a DP 73 digital camera (Olympus Optical Co., Tokyo, Japan).

Histological sections were also used to detect the PM. Sections were incubated for 1 h at room temperature with FITC-conjugated lectin (WGA-FITC, Sigma-Aldrich, # L4895, Israel) diluted (1:400) in PBS to detect glycoconjugates and polysaccharides containing  $\beta$ -1-4 N-acetylglucosamine residues. The sections were washed three times and incubated for 30 min with DAPI (diamidino-2-fenilindole; Biotium, Inc.,

Hayward, CA, EUA; 1:500) for DNA (cell nuclei) staining. After a triple wash, the sections were mounted in a 50% sucrose solution, analysed, and photographed under fluorescence microscopy coupled to an Olympus XM10 digital camera (Olympus Optical Co., Tokyo, Japan). The intensity of the WGA-FITC fluorescence signal in the images was measured with Image-ProPlus 4.5 software (Media Cybernetics, Silver Spring, USA). In this measurement, five images were selected at random from each treatment acquired with a final magnification of 1600 $\times$ .

### 2.5. Immunofluorescence

Fixed midguts (session 2.4) were washed three times and incubated for 2 h in 0.1 M PBS with 1% Triton X-100 (PBST). The organs were incubated for 72 h at 4 °C with primary antibodies diluted in PBS. The primary antibodies used were: anti-FMRP-amide XP Rabbit mAb (1:500 dilution) (Gene Tex, San Antonio, TX, USA), anti-LC3 B (D11) XP Rabbit mAb (1:500), anti-phospho-p44/42 MAPK (Erk1/2) XP Rabbit mAb (1:200) and anti-NOTCH 1 (D6F11) XP Rabbit mAb (1:400) (Cell Signaling Technology, Inc., Beverly, MA, USA); anti-WNT Mouse (Wingless protein, monoclonal, *Drosophila* – Brook and Cohen, 1996) (1:600) and anti-PROSPERO Mouse (MR1A – Campbell et al., 1994) (1:400) (Developmental Studies Hybridoma Bank, Iowa City, Iowa, USA). For each antibody, five midguts of bees treated with LC<sub>50</sub>, LC<sub>10</sub>, and control were used, totalling fifteen individuals.

After the primary incubation, the organs were washed three times and incubated for 24 h with conjugated secondary antibody anti-Rabbit TRITC (1:500) (Thermo Fisher-Scientific, Waltham, Mass., EUA) or anti-Mouse IgG Goat pAb (1:500) (Gene Tex, San Antonio, TX, USA) in PBS at 4 °C. The samples were stained with DAPI for 1 h, washed again, and mounted on glass slides with 50% sucrose solution. Samples were analysed and photographed under fluorescence microscopy. Differences between treatments were quantified by counting positive cells detected throughout the organ, which was carefully analysed using the 20 $\times$  objective.

Five midguts from each treatment (LC<sub>50</sub>, LC<sub>10</sub>, and control) were used as a negative control. The organs were treated as previously described, except for the step referring to the incubation with the primary antibody.

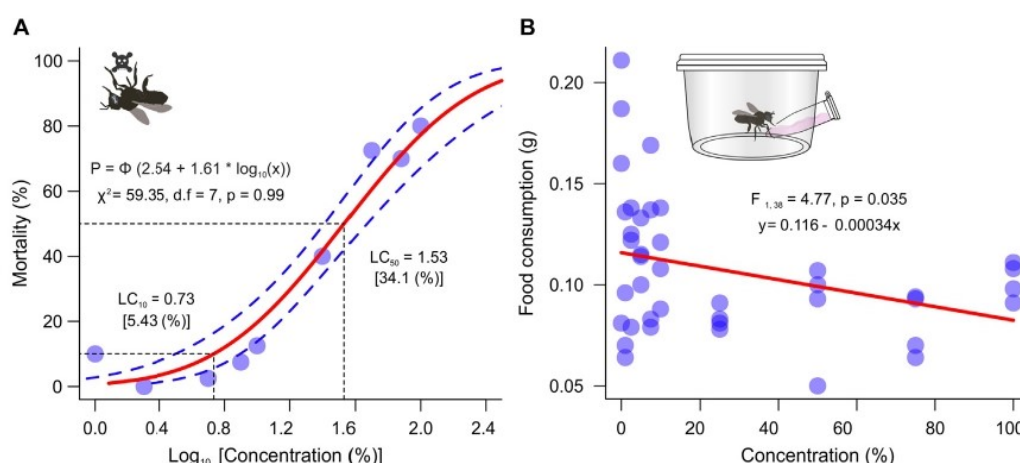


**Fig. 1.** Mortality and food consumption of the stingless bee *Partamona helleri* exposed to different concentrations of the mix of herbicides (Mesotrione + Atrazine). (A) Concentration – mortality curve. The dots represent the observed values. The red line is the estimate based on the probit model. The dotted blue lines represent the 95% confidence intervals. LC<sub>50</sub> and LC<sub>10</sub> are indicated (black dotted lines). (B) Food consumption (g) per experimental unit. The red line indicates linear regression. The points represent the observed values of a total  $N = 36$  ( $n = 4$  pots with ten workers for each of the nine concentrations in the mix).

## 2.6. Data analyses

For mortality bioassay data, a concentration-response model (probit) was created and used to estimate the lethal concentrations at 50% and 10% ( $LC_{50}$ , and  $LC_{10}$ ). The results of food consumption were subjected to linear regression analysis. Mixed linear models (LMMs) were adjusted for behavioural data (walking distance and meandering). These data were adequate for Gaussian distribution, and the colony was considered as a random effect since groups of individuals from the same colony were evaluated together in the same arena. Wheat Germ Agglutinin (WGA - peritrophic matrix staining) data were analysed using generalised linear models (GLM) with gamma distribution, a suitable distribution for continuous data where the variance increases with the square of the mean (Crawley, 2012).

To evaluate changes in the detection of intracellular proteins (immunostaining) caused by acute toxicity to the mix of herbicides, an analysis of permutational multivariate variance (PERMANOVA) with 999 permutations and Euclidean distance was performed. The variables were standardised to a mean = 0 and standard deviation = 1 to eliminate the scale effect. Paired combinations (contrasts) were performed with Bonferroni adjustment. The multivariate dispersion homogeneity test (PERMDISP) was used to check the assumption of homogeneity of PERMANOVA (Anderson, 2014). Principal component analysis (PCA) was used to obtain an ordering of the samples in the treatments and the relationship of the variables with the treatments. The main components were defined by the covariance matrix, as the variables were standardised. Through GLM, univariate analyses were also performed to complement the cell signalling results. These models were adjusted with a negative binomial distribution because the variables are of the count type. In addition, this distribution avoids the occurrence of overdispersion (high residual deviance).

In LMMs and GLMs, when necessary, contrasts by gradual simplification of the models were performed to assess the difference between the levels of the explanatory variable (treatment with the mix of herbicides). The residues were checked on all models to verify the adequacy of the distributions. All analyses were performed using R software (R Core Team version 4.0.0, 2020).

## 3. Results

### 3.1. Mortality and food consumption

The effects of different concentrations of the mix of herbicides on mortality were verified for workers of *P. helleri*. The concentration-response model was adequate for the results of mortality after oral exposure ( $\chi^2 = 59.347$ , d.f. = 7,  $p = 0.99$ , Fig. 1A). The estimated concentrations (95% confidence interval) were  $LC_{50} = 34.1\%$  (25.86; 46.98) and  $LC_{10} = 5.43\%$  (3.16; 7.88). Workers decreased food consumption with increasing concentrations of the mix of herbicides ( $F_{1,38} = 4.77$ ,  $p = 0.035$ , Fig. 1B).

### 3.2. Behaviour

The walking distance was significantly different between treatments with the mix of herbicides ( $\chi^2 = 27.4$ , d.f. = 2,  $p < 0.0001$ ). Bees from the  $LC_{50}$  treatment walked less than bees from the  $LC_{10}$  and control treatments (Fig. 2A–D, and Movies S1–S3). Meandering behaviour was also different between treatments ( $\chi^2 = 39.2$ , d.f. = 2,  $p < 0.0001$ ). The  $LC_{50}$  treatment showed greater meandering behaviour (Fig. 3A–B) with greater azimuth angles occurring more frequently (Fig. 3C).

### 3.3. Midgut and peritrophic matrix (PM)

Digestive cells with high vacuolization and disintegrating protrusions in their apical region were observed in the epithelium treated with the  $LC_{50}$  of the mix (Fig. 4A–B). On the other hand, these signals

of degradation were less evident in the  $LC_{10}$  and control. Control bees did not have protrusions in the apical region and signals of the disintegration of digestive cells (Fig. 4C–F).

The analysis of the fluorescence signal intensity in the PM stained with WGA-FITC showed a significant difference ( $\chi^2 = 2.83$ , d.f. = 12,  $p = 0.027$ , Fig. 5A–B). The greater intensity of labelling for PM was detected in the control group.

### 3.4. Immunostaining

The assumption of homogeneous dispersion was not rejected (PERMDISP:  $F_{2,12} = 1.62$ ,  $p = 0.24$ ), demonstrating the suitability of the PERMANOVA analysis. The mix of herbicides caused significant changes in the pattern of *in situ* detection of proteins related to cell signalling (PERMANOVA:  $F_{2,12} = 1.85$ ,  $p = 0.013$ ,  $R^2 = 0.24$ ). The paired combinations demonstrated that the  $LC_{50}$  treatment differed from the control (Fig. 6A). In the first component (PC1), which explains most of the variance (29.84%), the variables PROSPERO and WNT presented the highest loads and, therefore, contributed more to the divergence between treatments (Figs. 6B, 7, and Fig. S1). The variables LC3 and NOTCH showed high positive loads for the second axis (PC2), which are more associated with the  $LC_{50}$  treatment, which presented the most positive PC2 scores (Fig. 8 and Fig. S2). These results were consistent with the univariate analysis performed for each cell signalling variable (Table S1).

## 4. Discussion

To our knowledge, this work was the first to study the toxicological effects of the formulation of the mix of herbicides (Mesotrione + Atrazine - Calaris®) on pollinators. Our data shows that the estimated concentrations ( $LC_{50}$ , and  $LC_{10}$  - Fig. 1), which are below the recommended concentration used in the field, imposed a risk on adult workers of *P. helleri* in laboratory conditions, that represent an extreme scenario of exposure of the mix of herbicides. Concentrations lower than that recommended for the field of an Atrazine-based herbicide were also toxic to workers of the termite *Macrotermes bellicosus* (Ejomah et al., 2020). These data are concerning because the main constituent of the mix of herbicides is Atrazine (Matte et al., 2018), an agrochemical that is considered to have a high relative environmental risk and is banned in the European Union (Barchanska et al., 2012). Thus, the ingestion of herbicide formulations based on Atrazine or a mix, in which Atrazine is the main component, can be harmful to the survival of beneficial insects, such as *P. helleri* (this work) and *M. bellicosus* (Ejomah et al., 2020). As a consequence, Atrazine can have broader adverse effects and affect the colony of these individuals. These effects need to be studied to understand their full impact.

The presence of the herbicides in the diet inhibited the consumption of food by *P. helleri*, and the amount ingested by the individuals was sufficient to increase their mortality in comparison to the control. This lower diet consumption can be caused by nutritional stress due to intoxication by the ingested xenobiotic and by the inhibitory phage effect of the contaminated food (Bernardes et al., 2017; Tong et al., 2019). The type of stress caused by oral exposure to agrochemicals (insecticides, and fungicides) increased mortality of bees, including *Apis mellifera* and stingless bees (e.g., *P. helleri*, and *Scaptotrigona xanthotricha*) (Tomé et al., 2015, 2017; Tosi et al., 2017).

The results of the behavioural response (Fig. 2, and Movies S1–S3) corroborate investigations that agrochemicals affect walking ability in stingless bees (Tomé et al., 2012, 2015; Barbosa et al., 2015; Marques et al., 2020), which can lead to changes in dispersion and reproduction. Even worse, oral intoxication by the mix of herbicides ( $LC_{50}$ ) increased the meandering behaviour of *P. helleri*, suggesting that this agrochemical may also be neurotoxic (Cheng et al., 2020). However, further studies are needed to understand the effect of the mix of herbicides on the nervous system of bees.

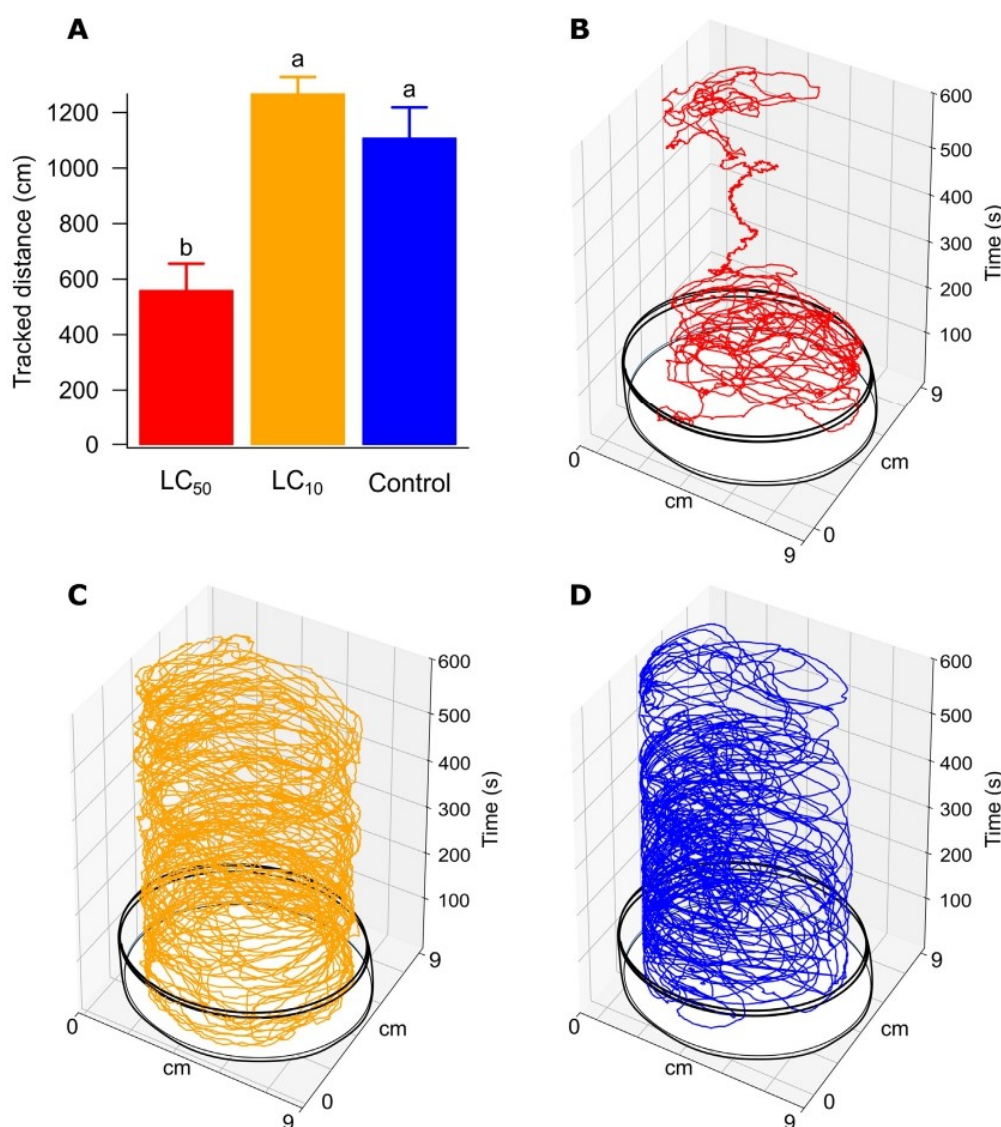


**Fig. 2.** Walking distance (cm) by workers of *Partamona helleri* exposed to different concentrations of the mix of herbicides (Mesotrione + Atrazine). (A) The bars are means  $\pm$  standard error of a total of  $N = 60$  ( $n = 5$  workers from each of the 4 colonies in each of the 3 treatments). Bars represented by different letters are significantly different according to the contrasts due to the gradual simplification of the model. (B), (C), and (D) represent movement tracks in the arenas (9 cm  $\times$  9 cm) over the monitoring time (600 s) for the LC<sub>50</sub>, LC<sub>10</sub>, and control treatments, respectively.

Exposure to the LC<sub>50</sub> of the mix of herbicides also harmed the midgut epithelium of *P. helleri*, leading the high cell vacuolisation, which is indicative of cell death (Araujo et al., 2019a). A greater number of LC3 B-positive cells was also detected in the midgut of bees that ingested the LC<sub>50</sub> of the mix of herbicides (Table S1). Therefore, these two results reinforce that the mix has the potential to stimulate autophagy and consequently, the degradation of the intestinal epithelium.

The decrease in the intensity of staining by WGA-FITC in orally exposed bees indicated that the degradation of the epithelium was so high that it compromised the maintenance of PM. Similar data have been reported in adult *A. mellifera* bees (Lopes et al., 2018) and during the development of *P. helleri* (Araujo et al., 2019b) after oral exposure to Spinosad. Together, these data show that ingestion of agrochemicals, including the mix of herbicides and insecticides, can negatively affect the PM, a structure responsible for protecting the midgut epithelium against abrasion of food particles, digestive enzymes, and pathogens

(Hegedus et al., 2009), and, because of that, drastically reduce the bee's life span.

Oral exposure to the mix of herbicides also reduced the number of cells positive for PROSPERO or FMRF in the midgut of intoxicated bees compared to the control. PROSPERO is a transcription factor that possibly regulates the differentiation of stem cells into enteroendocrine cells in insects (Micchelli and Perrimon, 2006; Zeng and Hou, 2015; Di Cara et al., 2018). It is hypothesized that a reduction in the number of cells positive for PROSPERO correlates to fewer enteroendocrine cells. Furthermore, the reduction in the amount of FMRF positive cells in the midgut of treated works of *P. helleri* suggests that the mix of herbicides leads to the death of differentiated enteroendocrine cells, which can affect midgut homeostasis (Amcheslavsky et al., 2014).

Unlike the results observed for PROSPERO and FMRF, the exposure of *P. helleri* to the LC<sub>50</sub> of the mix of herbicide caused an increase in the number of cells positive for WNT or NOTCH. It has been reported that

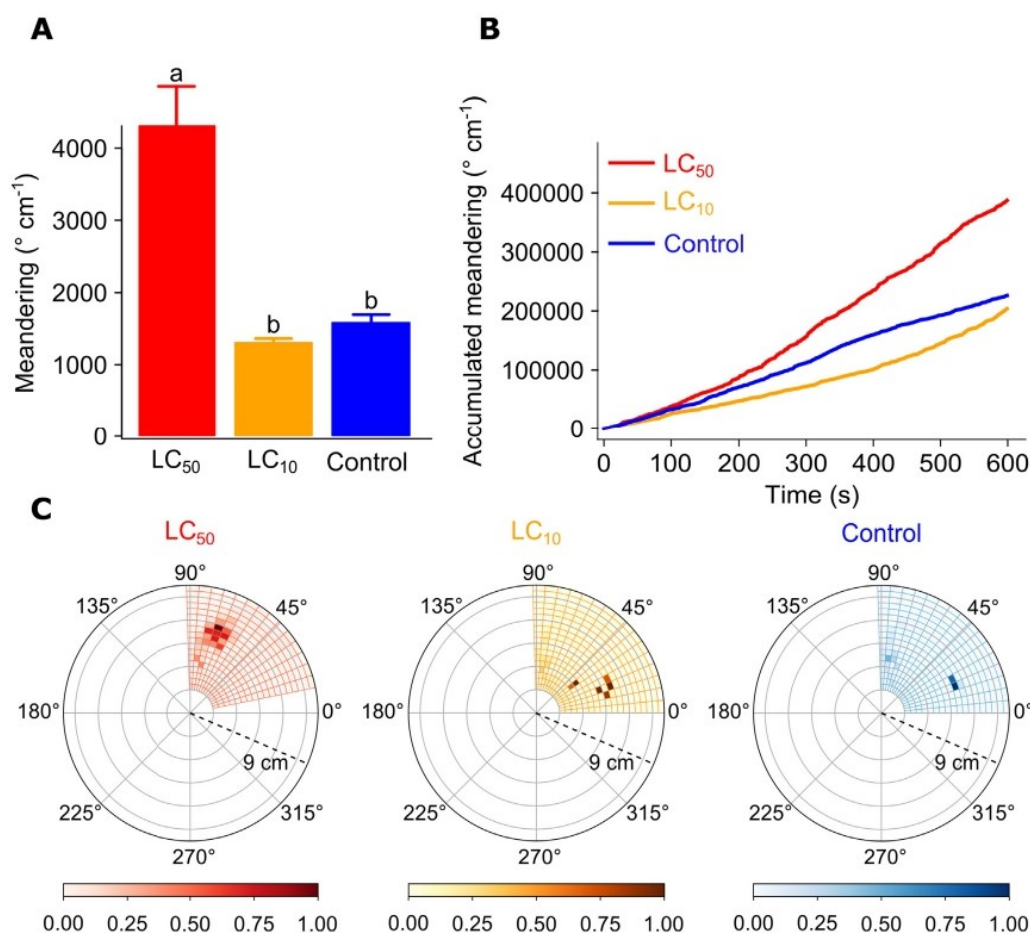


**Fig. 3.** Meandering behaviour presented by workers of *Partamona helleri* exposed to different concentrations of the mix of herbicides (Mesotrione + Atrazine). (A) The bars are means  $\pm$  standard error of a total of  $N = 60$  ( $n = 5$  workers from each of the 4 colonies in each of the 3 treatments). Bars represented by different letters are significantly different according to the contrasts by gradual simplification of the model. (B) Representation of meandering accumulated every second of monitoring (600 s) categorised by treatments. (C) Histograms of the polar coordinates showing the proportion of occurrence of the rays and azimuth angles of the walk in the different treatments.

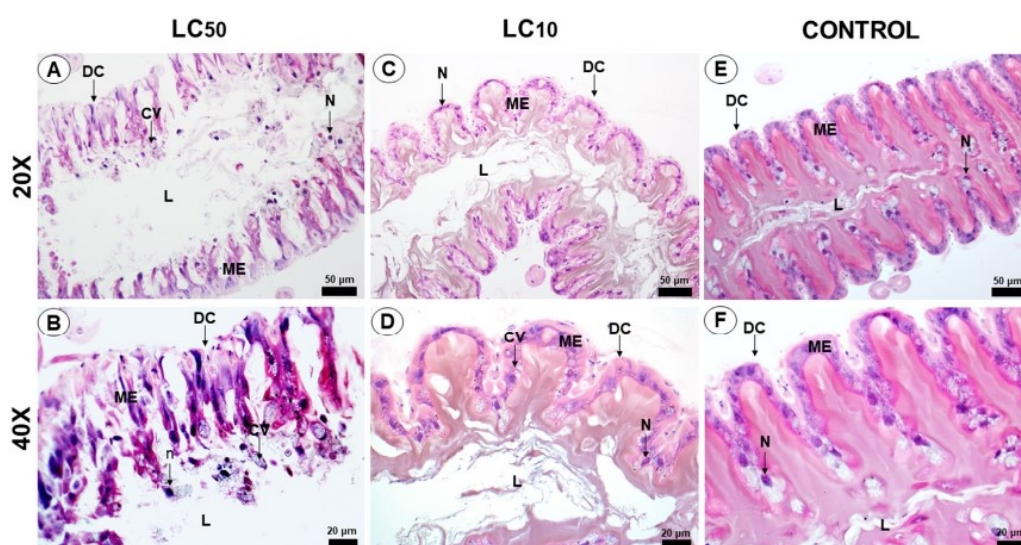


**Fig. 4.** Histological sections of the *Partamona helleri* midgut exposed orally to (A-B) LC<sub>50</sub> and (C-D) LC<sub>10</sub> of the mix of herbicides (Mesotrione + Atrazine) or to (E-F) 50% sucrose solution (control). DC: digestive cells, CV: cytoplasmic vacuolisation, L: lumen, ME: midgut epithelium, N: nuclei. Staining: hematoxylin and eosin.

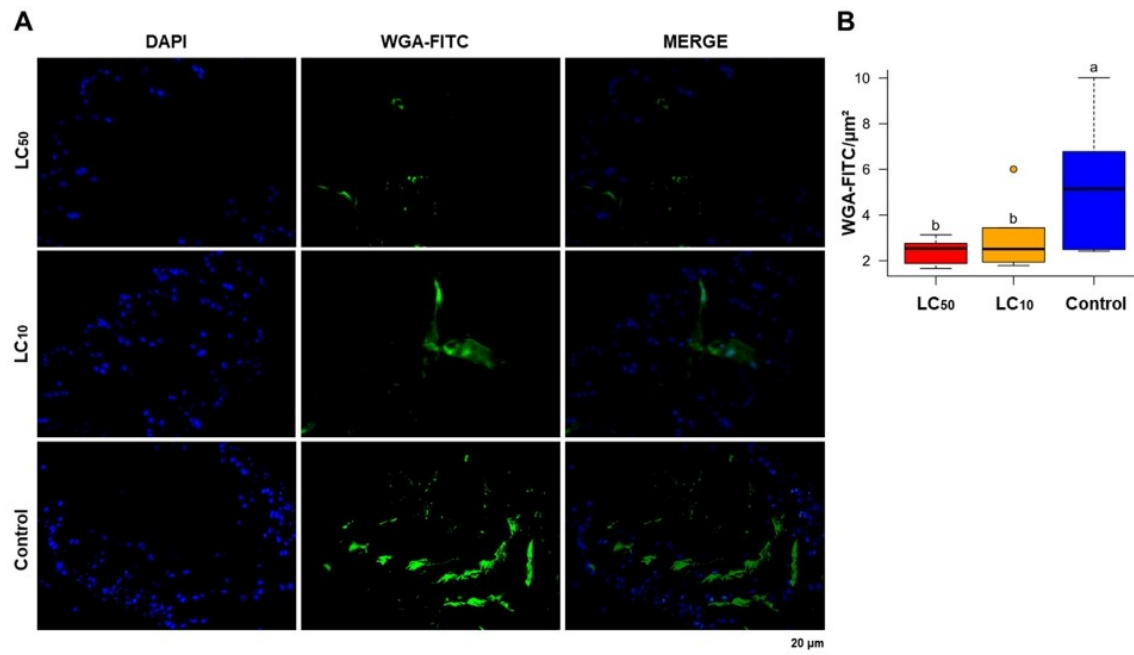


**Fig. 5.** Peritrophic matrix (PM) of the midgut of *Partamona helleri* exposed orally to the LC<sub>50</sub> and LC<sub>10</sub> of the mix of herbicides (Mesotrione + Atrazine) or the 50% sucrose solution (control). (A) Micrographs of the midgut stained with WGA-FITC (green = PM) and DAPI (blue = nucleus). (B) WGA-FITC fluorescence intensity. The boxes indicate the medians and the dispersion (lower and upper quartiles and outliers) of a total  $N = 15$  samples ( $n = 5$  midguts for each of the 3 treatments). The dot above the yellow bar indicates an outlier. Different letters indicate a significant difference according to the contrasts in the GLM ( $p < 0.05$ ).

WNT and NOTCH signalling pathways are related to the proliferation and differentiation of midgut stem cells in *Drosophila melanogaster* (Kuwamura et al., 2010, 2012). There was also an increase in the

detection of MAPK-positive cells in bees exposed to the mix. The MAPK protein regulates the proliferation and differentiation of insect midgut cells (Kondoh et al., 2005; Tong and Feng, 2018). Therefore,

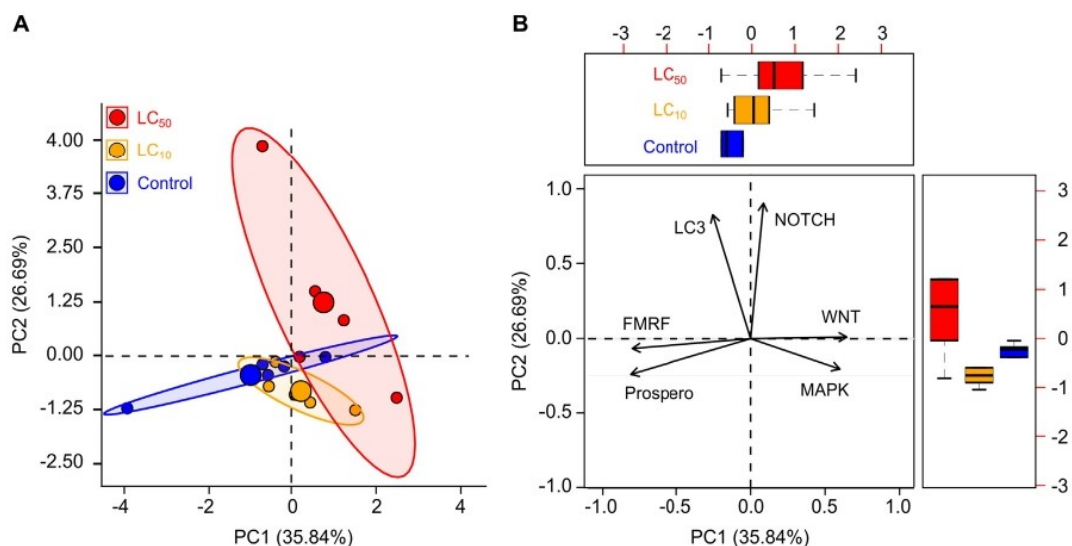


**Fig. 6.** Principal component analysis (PCA) considering the number of positive cells for proteins related to cell signalling in the midgut of *Partamona helleri* exposed orally to the LC<sub>50</sub> and LC<sub>10</sub> of the mix of herbicides (Mesotrione + Atrazine) or the 50% sucrose solution (control). (A) PCA ordering diagram with ellipses representing the confidence interval (95%) around the centroid of each treatment (major points) of a total  $N = 15$  samples ( $n = 5$  midguts for each of the 3 treatments). (B) Representation of loads of the variables associated with the first and second components. The directions and lengths of the arrows indicate the relative loads of the variables to the components. The boxplots indicate the median and dispersion range (lower and upper quartiles) of the scores for component 1 (upper panel) and component 2 (right panel), categorised by treatments with the mix of herbicides. The percentage values on the axes indicate how much each component explains the total variance of the data.

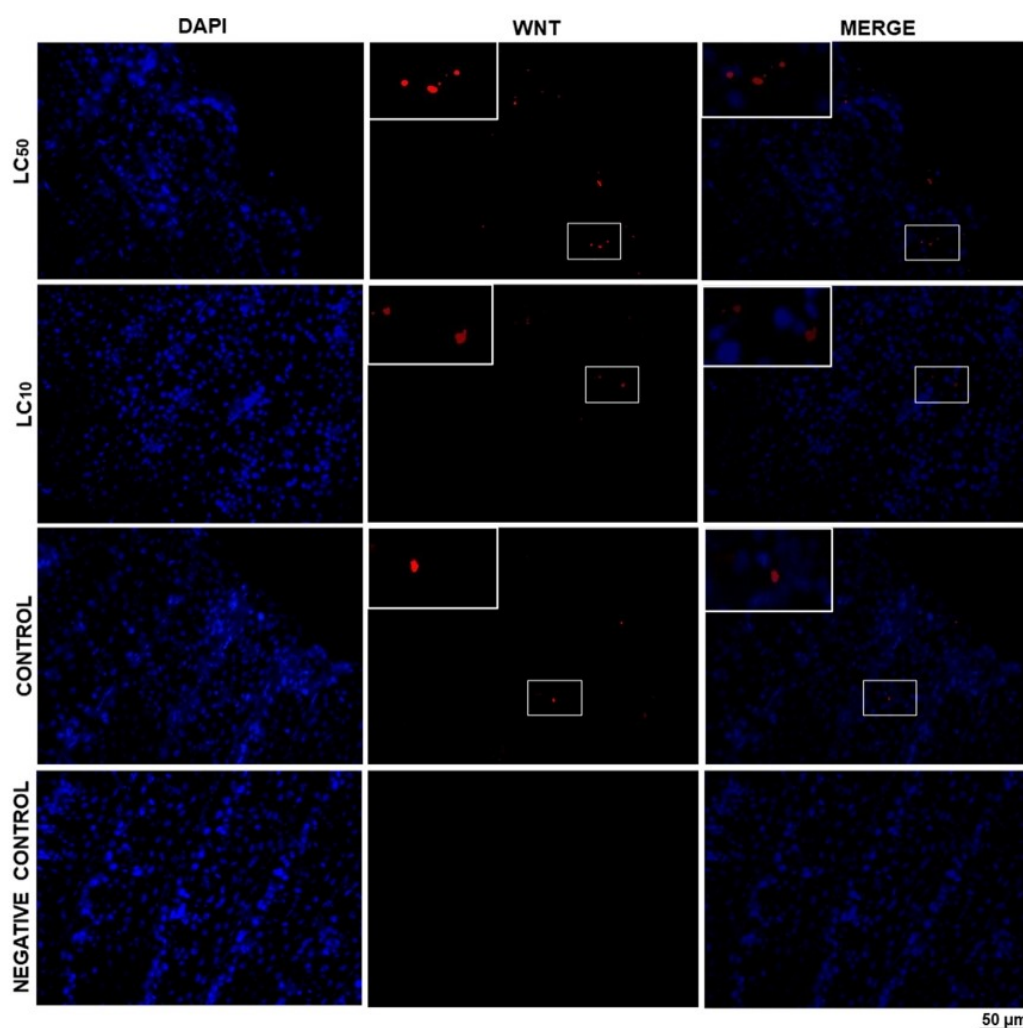


**Fig. 7.** Immunostaining of WNT positive cells in the midgut of *Partamona helleri* workers treated with LC<sub>50</sub> and LC<sub>10</sub> of the mix of herbicides (Mesotrione + Atrazine) or 50% sucrose solution (control). The negative control (without the primary antibody) was done with midgut of bees treated with LC<sub>50</sub>. Red: WNT positive cells. Blue (DAPI): cell nuclei.

we hypothesise that the increase in the number of cells positive for WNT or NOTCH (and slightly for MAPK) is related to the organ attempting to maintain homeostasis by increasing stem cell differentiation to compensate for cells that have been harmed after the ingestion of the mix of herbicides.

## 5. Conclusion

In conclusion, our findings demonstrate that oral exposure to the mix of herbicides decreases survival, reduces food consumption, and affects the walking and meandering behaviours of adult workers of *P. helleri*. The exposure also caused damage to the epithelium and MP of the midgut and changed the number of cells positive for proteins related to cell signalling pathways related to the proliferation and differentiation of midgut stem cells.

Although the conditions tested in the present study were in the laboratory, this study showed the potential toxicological effects of the mix of herbicides in beneficial insects, including a pollinator bee. Future studies are needed to estimate the risk imposed by the mix of herbicides in the field to pollinators and also to assess its effect on synergies with other

agrochemicals. These studies will also help to make decisions regarding the use of the mix of herbicides to mitigate its damage to pollinators.

## CRediT authorship contribution statement

**Renan dos Santos Araújo:** Conceptualization; Investigation; Methodology; Visualization; Writing - original draft. **Rodrigo Cupertino Bernardes:** Conceptualization; Investigation; Methodology; Software; Visualization; Making figures. **Gustavo Ferreira Martins:** Conceptualization; Funding acquisition; Project administration; Supervision; Writing - review & editing.

Supplementary data to this article can be found online at <https://doi.org/10.1016/j.scitotenv.2020.142980>.

## Declaration of competing interest

The authors declare that they have no known competing financial interests or personal relationships that could have appeared to influence the work reported in this paper.

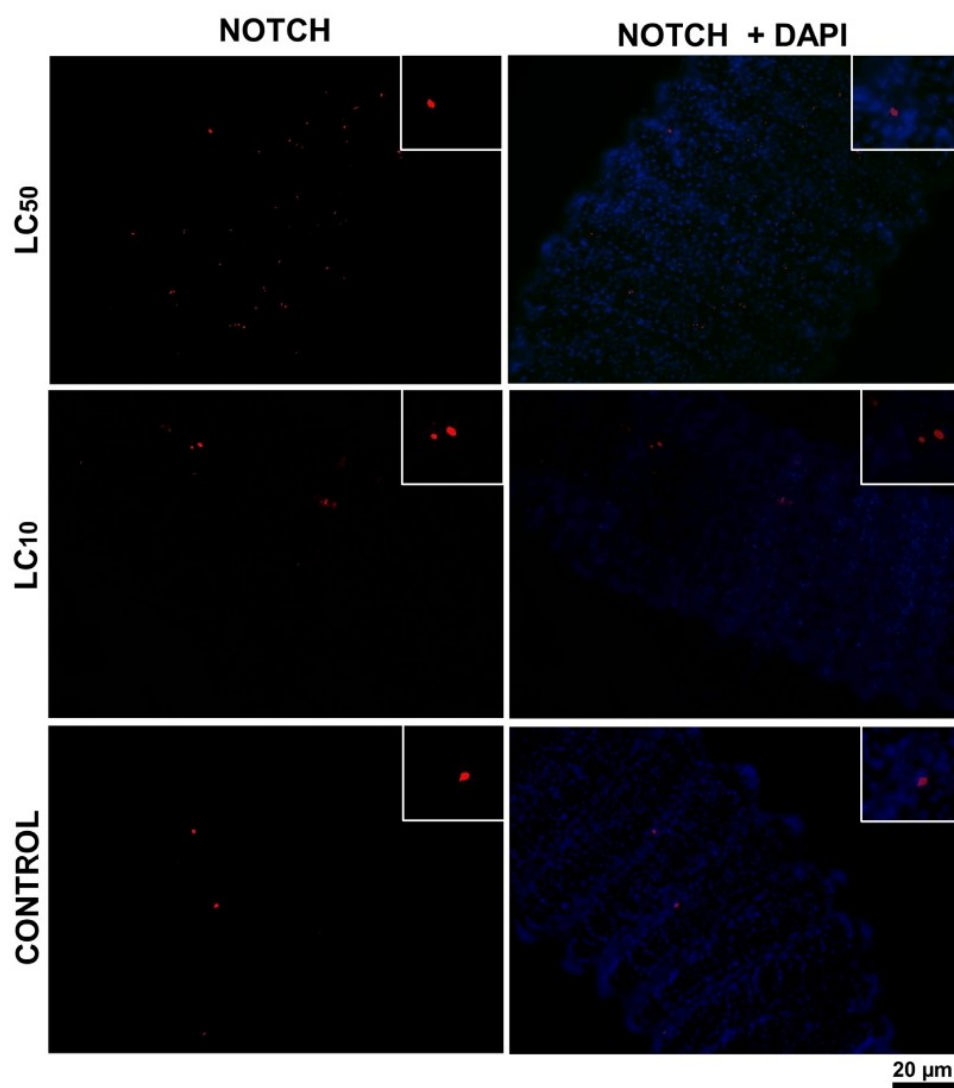


**Fig. 8.** Immunostaining of NOTCH positive cells (red) in workers treated with the LC<sub>50</sub> and LC<sub>10</sub> of the mix of herbicides (Mesotrione + Atrazine) or with 50% sucrose solution (control). Cell nuclei are stained with DAPI (blue).

## Acknowledgements

We thank the Conselho Nacional de Desenvolvimento Científico e Tecnológico (CNPq, 301725/2019-5), Fundação CAPES (Finance code 001) and Fundação de Amparo à Pesquisa do Estado de Minas Gerais (FAPEMIG, CBB-APQ-00247-14) for financial support.

## References

- Albuquerque, F.P., de Oliveira, J.L., Moschini-Carlos, V., Fraceto, L.F., 2020. An overview of the potential impacts of atrazine in aquatic environments: perspectives for tailored solutions based on nanotechnology. *Sci. Total Environ.* 700, 134868.
- Amcheslavsky, A., Song, W., Li, Q., Nie, Y., Bragatto, I., Ferrandon, D., Perrimon, N., Ip, Y.T., 2014. Enterendocrine cells support intestinal stem-cell-mediated homeostasis in *Drosophila*. *Cell Rep.* 9, 32–39.
- Anderson, M.J., 2014. Permutational multivariate analysis of variance (PERMANOVA). *Wiley Statsref: Statistics Reference Online*, pp. 1–15.
- Araújo, R.S., Lopes, M.P., Barbosa, W.F., Gonçalves, W.G., Fernandes, K.M., Martins, G.F., Tavares, M.G., 2019a. Spinosad-mediated effects on survival, overall group activity and the midgut of workers of *Partamona helleri* (Hymenoptera: Apidae). *Ecotoxicol. Environ. Saf.* 175, 148–154.
- Araújo, R.S., Bernardes, R.C., Fernandes, K.M., Lima, M.A.P., Martins, G.F., Tavares, M.G., 2019b. Spinosad-mediated effects in the post-embryonic development of *Partamona helleri* (Hymenoptera: Apidae: Meliponini). *Environ. Pollut.* 253, 11–18.
- Azmi, W.A., Wan Sembok, W.Z., Yusuf, N., Mohd. Hatta, M.F., Salleh, A.F., Hamzah, M.A.H., Ramli, S.N., 2019. Effects of pollination by the indo-Malaya stingless bee (Hymenoptera: Apidae) on the quality of greenhouse-produced rockmelon. *J. Econ. Entomol.* 112, 20–24.
- Barbosa, W.F., Tomé, H.V.V., Bernardes, R.C., Siqueira, M.A.L., Smagghe, G., Guedes, R.N.C., 2015. Biopesticide-induced behavioral and morphological alterations in the stingless bee *Melipona quadrifasciata*. *Environ. Toxicol. Chem.* 34, 2149–2158.
- Barchanska, H., Rusek, M., Szatkowska, A., 2012. New procedures for simultaneous determination of mesotrione and atrazine in water and soil. Comparison of the degradation processes of mesotrione and atrazine. *Environ. Monit. Assess.* 184, 321–334.
- Belsky, J., Joshi, N.K., 2020. Effects of fungicide and herbicide chemical exposure on *Apis* and non-*Apis* bees in agricultural landscape. *Frontiers in Environmental Science* 8, 1–9.
- Bernardes, R.C., Tomé, H.V., Barbosa, W.F., Guedes, R.N., Lima, M.A.P., 2017. Azadirachtin-induced antifeeding in Neotropical stingless bees. *Apidologie* 48, 275–285.
- Bernardes, R.C., Barbosa, W.F., Martins, G.F., Lima, M.A.P., 2018. The reduced-risk insecticide azadirachtin poses a toxicological hazard to stingless bee *Partamona helleri* (Friese, 1900) queens. *Chemosphere* 201, 550–556.
- Bernardes, R.C., Lima, M.A.O., Guedes, R.N.C., Martins, G.F., 2020. Ethoflow: computer vision and artificial intelligence-based software for automatic behavior analysis. *BioRxiv* <https://doi.org/10.1101/2020.07.23.218255>.

- Boily, M., Sarasin, B., DeBlois, C., Aras, P., Chagnon, M., 2013. Acetylcholinesterase in honey bees (*Apis mellifera*) exposed to neonicotinoids, atrazine and glyphosate: laboratory and field experiments. *Environ. Sci. Pollut. Res.* 20, 5603–5614.
- Botina, L.L., Bernardes, R.C., Barbosa, W.F., Lima, M.A.P., Guedes, R.N., Martins, G.F., 2020. Toxicological assessments of agrochemical effects on stingless bees (Apidae, Meliponini). *MethodsX* 7, 100906.
- Brook, W.J., Cohen, S., 1996. Antagonistic interactions between wingless and decapentaplegic responsible for dorsal-ventral pattern in the *Drosophila* leg. *Science* 273, 1373–1377.
- Campbell, G., Goring, H., Lin, T., Spana, E., Andersson, S., Doe, C.Q., Tomlinson, A., 1994. RK2, a glial-specific homeodomain protein required for embryonic nerve cord condensation and viability in *Drosophila*. *Development* 120, 2957–2966.
- Carles, L., Joly, M., Joly, P., 2017. Mesotrione herbicide: efficiency, effects, and fate in the environment after 15 years of agricultural use. *CLEAN—Soil, Air, Water* 45, 1700011.
- Cameiro, L.S., Martinez, L.C., Gonçalves, W.G., Santana, L.M., Serrão, J.E., 2020. The fungicide iprodione affects midgut cells of non-target honey bee *Apis mellifera* workers. *Ecotoxicol. Environ. Saf.* 189, 109991.
- Cheng, B., Jiang, F., Su, M., Zhou, L., Zhang, H., Cao, Z., Liao, X., Xiong, G., Xiao, J., Liu, F., Lu, H., 2020. Effects of lincomycin hydrochloride on the neurotoxicity of zebrafish. *Ecotoxicol. Environ. Saf.* 201, 110725.
- Christie, A.E., 2020. Assessment of midgut enteroendocrine peptide complement in the honey bee, *Apis mellifera*. *Insect Biochem. Mol. Biol.* 116, 103257.
- Crawley, M.J., 2012. *The R Book*. John Wiley & Sons.
- Cruz Landim, C., 2009. Abelhas: morfologia e função de sistemas. SciELO-Ed, UNESP.
- Delkash-Roudsari, S., Chicas-Mosier, A.M., Goldansaz, S.H., Talebi-Jahromi, K., Ashouri, A., Abramson, C.I., 2020. Assessment of lethal and sublethal effects of imidacloprid, ethion, and glyphosate on aversive conditioning, motility, and lifespan in honey bees (*Apis mellifera* L.). *Ecotoxicol. Environ. Saf.* 204, 111108.
- Desneux, N., Decourtye, A., Delpuech, J.M., 2007. The sublethal effects of pesticides on beneficial arthropods. *Annu. Rev. Entomol.* 52, 81–106.
- Di Cara, F., Bülow, M.H., Simmonds, A.J., Rachubinski, R.A., 2018. Dysfunctional peroxisomes compromise gut structure and host defense by increased cell death and tor-dependent autophagy. *Mol. Biol. Cell* 29, 2766–2783.
- Dumas, E., Giraudo, M., Goujon, E., Halma, M., Khili, E., Stauffert, M., Batisson, I., Besse-Hoggan, P., Bohatier, J., Bouchard, P., Celle-Jeanton, H., Gomes, M., Delbac, F., Forano, C., Goupil, P., Hussion, P., Ledoigt, G., Mallet, C., Mousty, C., Prévot, V., Richard, C., Sarraute, S., 2017. Fate and ecotoxicological impact of new generation herbicides from the triketone family: an overview to assess the environmental risks. *J. Hazard. Mater.* 325, 136–156.
- Ejomah, A.J., Uyi, O.O., Ekaye, S.O., 2020. Exposure of the African mound building termite, *Macrotermes bellicosus* workers to commercially formulated 2, 4-D and atrazine caused high mortality and impaired locomotor response. *PLoS One* 15, e0230664.
- Farland, J., Burnside, O., LeBaron, H.M., 2008. *The Triazine Herbicides*. Elsevier Science.
- Fernandes, A.F.T., Wang, P., Staley, C., Moretto, J.A.S., Altarugio, L.M., Campanharo, S.C., Stehling, E.G., Sadowsky, M.J., 2020. Impact of atrazine exposure on the microbial community structure in a Brazilian tropical latosol soil. *Microbes Environ.* 35, ME19143.
- Godfrey, J.A., Rypstra, A.L., 2018. Impact of an atrazine-based herbicide on an agrobiont wolf spider. *Chemosphere* 201, 459–465.
- Heard, T.A., 1999. The role of stingless bees in crop pollination. *Annu. Rev. Entomol.* 44, 183–206.
- Hegedus, D., Erlandson, M., Gillott, C., Toprak, U., 2009. New insights into peritrophic matrix synthesis, architecture, and function. *Annu. Rev. Entomol.* 54, 285e302.
- Helmer, S.H., Kerbaol, A., Aras, P., Jumarie, C., Boily, M., 2015. Effects of realistic doses of atrazine, metolachlor, and glyphosate on lipid peroxidation and diet-derived antioxidants in caged honey bees (*Apis mellifera*). *Environ. Sci. Pollut. Res.* 22, 8010–8021.
- Hrncir, M., Jarau, S., Barth, F.G., 2016. Stingless bees (Meliponini): senses and behavior. *J. Comp. Physiol. A* 597–601.
- Kondoh, K., Torii, S., Nishida, E., 2005. Control of MAP kinase signaling to the nucleus. *Chromosoma* 114, 86–91.
- Kraehmer, H., Laber, B., Rosinger, C., Schulz, A., 2014a. Herbicides as weed control agents: state of the art: I. Weed control research and safer technology: the path to modern agriculture. *Plant Physiol.* 166, 1119–1131.
- Kraehmer, H., Van Almsick, A., Beffa, R., Dietrich, H., Eckes, P., Hacker, E., Hain, R., Strek, H., Stuebler, H., Wills, L., 2014b. Herbicides as weed control agents: state of the art: II. Recent achievements. *Plant Physiol.* 166, 1132–1148.
- Kuwamura, M., Maeda, K., Adachi-Yamada, T., 2010. Mathematical modelling and experiments for the proliferation and differentiation of *Drosophila* intestinal stem cells I. *J. Biol. Dyn.* 4, 248–257.
- Kuwamura, M., Maeda, K., Adachi-Yamada, T., 2012. Mathematical modelling and experiments for the proliferation and differentiation of *Drosophila* intestinal stem cells II. *J. Biol. Dyn.* 6, 267–276.
- Le Goff, G., Hilliou, F., Siegfried, B.D., Boundy, S., Wajnberg, E., Sofer, L., Audant, P., Ffrench-Constant, R., Feyereisen, R., 2006. Xenobiotic response in *Drosophila melanogaster*: sex dependence of P450 and GST gene induction. *Insect Biochem. Mol. Biol.* 36, 674–682.
- Lima, M.A.P., Martins, G.F., Oliveira, E.E., Guedes, R.N.C., 2016. Agrochemical-induced stress in stingless bees: peculiarities, underlying basis, and challenges. *J. Comp. Physiol. A* 202, 733–747.
- Lopes, M.P., Fernandes, K.M., Tome, H.V.V., Gonçalves, W.G., Miranda, F.R., Serrão, J.E., Martins, G.F., 2018. Spinosad-mediated effects on the walking abilities, midgut, and Malpighian tubules of Africanized honey bee workers. *Pest Manag. Sci.* 74, 1311–1318.
- Lushchak, V.I., Matviishyn, T.M., Husak, V.V., Storey, J.M., Storey, K.B., 2018. Pesticide toxicity: a mechanistic approach. *EXCLI J.* 17, 1101–1136.
- Machado, T., Viana, B.F., da Silva, C.I., Boscolo, D., 2020. How landscape composition affects pollen collection by stingless bees? *Landsc. Ecol.* 35, 747–759.
- Marcus, S.R., Fiumera, A.C., 2016. Atrazine exposure affects longevity, development time and body size in *Drosophila melanogaster*. *J. Insect Physiol.* 91, 18–25.
- Marques, R.D., Lima, M.A.P., Bernardes, R.C., 2020. A spinosad-based formulation reduces the survival and alters the behavior of the stingless bee *Plebeia lucii*. *Neotropical Entomology* 1–8.
- Martins, G.F., Neves, C.A., Campos, L.A.O., Serrão, J.E., 2006. The regenerative cells during the metamorphosis in the midgut of bees. *Micron* 37, 161–168.
- Matte, W.D., Oliveira Jr., R.S., Machado, F.G., Constant, J., Biffe, D.F., Gutierrez, F.D.S.D., Silva, J.R.V., 2018. Efficacy of [Atrazine + Mesotrione] in control of weed in corn. *Revista Brasileira de Herbicidas* 17, 1–15.
- McCallum, M.L., Matlock, M., Treas, J., Safi, B., Sanson, W., McCallum, J.L., 2013. Endocrine disruption of sexual selection by an estrogenic herbicide in the mealworm beetle (*Tenebrio molitor*). *Ecotoxicology* 22, 1461–1466.
- Micchelli, C.A., Perrimon, N., 2006. Evidence that stem cells reside in the adult *Drosophila* midgut epithelium. *Nature* 439, 475–479.
- Ministério da Agricultura, Pecuária e Abastecimento [MAPA], 2020. Agrofit. Brasília, DF, Brazil: Coordenação Geral de Agrotóxicos e Afins/DFIA/DAS. [http://agrofit.agricultura.gov.br/agrofit\\_cons/principal\\_agrofit\\_cons](http://agrofit.agricultura.gov.br/agrofit_cons/principal_agrofit_cons).
- OECD, 2017. Test n°. 245: Honey bee (*Apis mellifera* L.), chronic oral toxicity test (10-day feeding). OECD Guideline for the Testing of Chemicals, p. 245.
- Oliveira, R.A., Roat, T.C., Carvalho, S.M., Malaspina, O., 2013. Side-effects of thiamethoxam on the brain and midgut of the africanized honeybee *Apis mellifera* (Hymenoptera: Apidae). *Environ. Toxicol.* 29, 1122–1133.
- Papaefthimiou, C., Zafeiroidou, G., Topoglidi, A., Chaleplis, G., Zografou, S., Theophilidis, G., 2003. Triazines facilitate neurotransmitter release of synaptic terminals located in hearts of frog (*Rana ridibunda*) and honeybee (*Apis mellifera*) and in the ventral nerve cord of a beetle (*Tenebrio molitor*). *Comparative Biochemistry and Physiology Part C: Toxicology & Pharmacology* 135, 315–330.
- Peterson, D.E., Shoup, D.E., Thompson, C.R., Olson, B.L., 2015. *Herbicide Mode of Action*. Cooperative Extension Service. Kansas State University, Kansas.
- R Core Team, 2020. R: A Language and Environment for Statistical Computing. R foundation for statistical computing, Vienna, Austria <https://www.R-project.org/>.
- Rortais, A., Arnold, G., Dorne, J.L., More, S.J., Sperandio, G., Streissl, F., Szentes, C., Verdonck, F., 2017. Risk assessment of pesticides and other stressors in bees: principles, data gaps and perspectives from the European Food Safety Authority. *Sci. Total Environ.* 587, 524–537.
- Schmidt-Jeffris, R.A., Cutulle, M.A., 2019. Non-target effects of herbicides on *Tetranychus urticae* and its predator, *Phytoseiulus persimilis*: implications for biological control. *Pest Manag. Sci.* 75, 3226–3234.
- Seide, V.E., Bernardes, R.C., Pereira, E.J.G., Lima, M.A.P., 2018. Glyphosate is lethal and cry toxins alter the development of the stingless bee *Melipona quadrifasciata*. *Environ. Pollut.* 243, 1854–1860.
- Syngenta, 2020. Disponível em: <https://portalsyngenta.com.br/produtos/calaris> Accessed data: 28 June 2020.
- Thornton, B.J., Elthon, T.E., Cerny, R.L., Siegfried, B.D., 2010. Proteomic analysis of atrazine exposure in *Drosophila melanogaster* (Diptera: Drosophilidae). *Chemosphere* 81, 235–241.
- Tomé, H.V.V., Martins, G.F., Lima, M.A.P., Campos, L.A.O., Guedes, R.N.C., 2012. Imidacloprid-induced impairment of mushroom bodies and behavior of the native stingless bee *Melipona quadrifasciata* anthidioides. *PLoS One* 7, e38406.
- Tomé, H.V.V., Barbosa, W.F., Corrêa, A.S., Gontijo, L.M., Martins, G.F., Guedes, R.N.C., 2015. Reduced-risk insecticides in Neotropical stingless bee species: impact on survival and activity. *Ann. Appl. Biol.* 167, 186–196.
- Tomé, H.V., Ramos, G.S., Araújo, M.F., Santana, W.C., Santos, G.R., Guedes, R.N.C., Oliveira, E.E., 2017. Agrochemical synergism imposes higher risk to Neotropical bees than to honeybees. *R. Soc. Open Sci.* 4, 2–11.
- Tong, S.M., Feng, M.G., 2018. Insights into regulatory roles of MAPK-cascaded pathways in multiple stress responses and life cycles of insect and nematode mycopathogens. *Appl. Microbiol. Biotechnol.* 103, 577–587.
- Tong, L., Nieh, J.C., Tosi, S., 2019. Combined nutritional stress and a new systemic pesticide (flupyradifurone, Sivanto®) reduce bee survival, food consumption, flight success, and thermoregulation. *Chemosphere* 237, 124408.
- Tosi, S., Nieh, J.C., Sgolastra, F., Cabbri, R., Medrzycki, P., 2017. Neonicotinoid pesticides and nutritional stress synergistically reduce survival in honey bees. *Proc. R. Soc. B Biol. Sci.* 284, 20171711.
- Vázquez, D.E., Latorre-Estivalis, J.M., Ons, S., Farina, W.M., 2020. Chronic exposure to glyphosate induces transcriptional changes in honey bee larva: a toxicogenomic study. *Environ. Pollut.* 261, 1–8.
- Vogel, A., Jocke, H., Sirot, L.K., Fiumera, A.C., 2015. Effects of atrazine exposure on male reproductive performance in *Drosophila melanogaster*. *J. Insect Physiol.* 72, 14–21.
- Wang, H., Liu, W., Zhao, K., Yu, H., Zhang, J., Wang, J., 2018. Evaluation of weed control efficacy and crop safety of the new HPPD-inhibiting herbicide-QYR301. *Sci. Rep.* 8, 1–11.
- Zeng, X., Hou, S.X., 2015. Enteroendocrine cells are generated from stem cells through a distinct progenitor in the adult *Drosophila* posterior midgut. *Development* 142, 644–653.

## CONCLUSIONS

- Ethoflow is an open-source desktop software with a graphical user interface, making it easier for the general public due to non-demand for programming. Additionally, Ethoflow is suitable for multivariate kinematic evaluations, behavioral assessments in heterogeneous environments, tracking individuals in groups maintaining their identities, and can be trained to learn specific animal behavior. Finally, Ethoflow is efficient in detecting bees in heterogeneous environments and performing different behaviors under no treatment or treated with pesticides with satisfactory processing speed and accuracy.

- The collective behavior of foragers of *M. quadrifasciata* exposed to glyphosate and imidacloprid was monitored automatically with Ethoflow. Integrating multivariate behavioral data with AI algorithms, it was obtained up to 91% accuracy for predicting agrochemical contamination in bees. Moreover, a multivariate assessment of the *in situ* detection of different proteins that play a role in the immune response, cell proliferation, and differentiation in midgut revealed that the agrochemicals differentially impact the midgut, depending on the modes of action of the agrochemicals. This effort provides a broad assessment of the adverse sublethal effects of glyphosate or imidacloprid on the pollinators. The method proposed can be widely applied for other bees, pointing to the field application of AI to predict the environmental factors influencing bees' health.

- The oral exposure to  $\text{CuSO}_4$  lead sublethal effects in foragers of *P. helleri*. The sublethal effects caused by this agrochemical included disturbances in the walking behavior, in the structure of the midgut epithelium, and in the PM organization. Additionally, the ingestion of  $\text{CuSO}_4$  lead oxidative stress and altered the immunofluorescence detection of proteins that play a role in the immune response, cell proliferation, and differentiation in the midgut. Accordingly,  $\text{CuSO}_4$  lead some potential toxicological risks for pollinating insects, such as *P. helleri*.

- The  $\text{LC}_{50}$  and  $\text{LC}_{10}$  were estimated for acute oral exposure to the mix of herbicides mesotrione and atrazine in forages of *P. helleri*. The mix of herbicides interfered in the food consumption and behavioral parameters of bees. The exposure also caused damage to the epithelium and PM and changed the pattern of cells positive for proteins related to the proliferation and differentiation of midgut stem cells.

- This work presented and validated the AI-based system Ethoflow. This software provides a useful tool for technical-scientific applications in the animal behavior field and in toxicological assessments of non-target organisms for modeling the multiple factors affecting

bees' health, including the adverse effects of agrochemicals. With Ethoflow it is possible to obtain multivariate behavioral data to train AI algorithms that predict the contamination by agrochemicals with high accuracy. Ethoflow also enabled holistic assessments, including sublethal effects of different agrochemicals on the behavior and physiology of bees.